DISSIPATION IN THE HELIUM II FILM

ABSTRACT

The theories that have been presented to explain the properties of liquid helium are reviewed. The existence of vortex lines and their importance to the dissipation in helium II are emphasised leading to a summary of the theories on dissipation in helium II. Attention is paid to the thermal fluctuation theories and to the resulting radical shift of emphasis on the idea of a critical superfluid velocity. The experimental results of measurements in narrow channels are abstracted and it is shown that support for the theories on vortex line equilibrium has been found and that the ideas from the thermal fluctuation theories can be validated. The properties of the helium II film are summarized; observed changes in flow rates, inertial oscillations occurring via film flow and the application of dissipation theories to film flow are discussed.

The experimental system is described. The film flow monitored was initiated through the initial run-in to equilibrium and through changing the chemical potential difference across the experimental beaker by applying a time-dependent voltage across one of the two capacitors that formed the liquid helium reservoirs. A detailed analysis of the accuracy of the experimental results is given.

The measured inertial oscillations were found to be in agreement with theoretical predictions. The flow rates were dominated by flow steps. No pattern in these steps was evident; there was a peak in their distribution at a superfluid velocity of ~ 25 cm sec^{-1}, and no evidence for either a critical superfluid velocity or forbidden flow rates. No evidence was found to support dissipative functions of the forms $\frac{dv}{dt} \propto f \exp(-\frac{v_b}{v})$ or $\frac{dv}{dt} \propto (v - v_o)^{3/2}$. Restricting the data to those when the velocity was a monotonic function of the driving force, supported Langer and Reppy's proposal that vortex lines parallel to the free surface are the dissipative mechanism in helium II film flow.

It is suggested that the very small volume of the annular cylinder formed by the helium film in the region of the beaker where dissipation was dominant may account for the difference between these results and those reported by other researchers.

DISSIPATION IN THE HELIUM II FILM

A thesis

presented by

Daniel B. Miller, BSc

to the

University of St Andrews

in application for the Degree of

Master of Science

DECLARATION

I hereby certify that this thesis has been composed by me, and is a record of work done by me, and has not previously been presented for a Higher Degree.

The research was carried out in the School of Physical Sciences in the University of St. Andrews, under the supervision of Professor J.F. Allen, FRS.

Daniel B. Miller

CERTIFICATE

I certify that Daniel B. Miller, BSc, has spent nine terms at research work in the School of Physical Sciences in the University of St Andrews under my direction, that he has fulfilled the conditions of the Resolution of the University Court, 1974, No 2, and that he is qualified to submit the accompanying thesis in application for the Degree of Master of Science.

Research Supervisor

PERSONAL PREFACE

After three years as an undergraduate at the University of Exeter, I graduated in 1973 with a First Class Combined Honours Bachelor of Science Degree in Physics and Mathematics.

In October 1973 I enrolled under the Resolution of the University Court, 1967, No 1, as a candidate for a PhD.

From October 1974 to September 1976 I was awarded a University Scholarship to continue my research in the School of Physical Sciences at the University of St Andrews, under the supervision of Professor J F Allen.

ACKNOWLEDGEMENTS

I would like to thank Professor J.F. Allen for his supervision of this work and for his comments on it. Mr. J.G.M. Armitage has been very helpful, particularly in the discussions which led to the concepts used in the method of approach to the experimental work and in the constructive criticism on the presentation of the results. Mr. J. McNab gave me much sound advice on machinery while I was building the capacitors. Parts of the cryostat were built by the staff of Mr. R. McGraw under his direction, and the glass beaker was made by Mr. F. Akerboom. Both Mr. R. Mitchell and Mr. T. Marshall were always accommodating in keeping me supplied with liquid helium for my experiments. I would also like the thank the typist who put so much care into producing this thesis.

CONTENTS

LIST OF FIGURES AND TABLES

CHAPTER I

INTRODUCTION

Helium was the last of the so-called "permanent" gases to be liquefied. This was achieved by Kammerlingh Onnes in 1908. An investigation of the state properties of liquid helium was expected to yield routine results demonstrating the validity of the classical theory of matter down to the lowest attainable temperatures: the helium atom was predicted to behave like the hard sphere of the classical kinetic theory. The Dutch school under Kammerlingh Onnes began to measure the properties of helium and were surprised to discover departures from the predicted behaviour. In 1911 measurements showed that as the temperature was lowered, the liquid density passed through a sharp maximum at 2.2K. Further experiments confirmed this behaviour, and further anomalies near 2.2K were noted, for example, discontinuities in the expansion coefficient and in the specific heat. The variation of the dielectric constant with temperature was so different above and below 2.2K, that Keesom and Wolfke divided liquid helium into two phases, labelling the higher temperature region helium I and the lower temperature region helium II (Wolfke & Keesom, 1928). The kinetic properties of helium I were found to be readily explicable in terms of classical theory, while helium II exhibited unique properties which entranced experimenters in the 1930's and continue to fascinate workers in the field of liquid helium.

The phase diagram for helium is illustrated in Figure I.i. The helium atom is the smallest among the group of inert elements. Consequently, the attractive forces between the atoms are very weak. The critical point (5.2K, 2.26 atmospheres' pressure) and the normal boiling point are lower than for other substances. It can also be seen that there is no triple point for helium and that helium under its own vapour pressure remains liquid down to 0 K. As classical theory expects all gases to solidify by 0 K this is indicative of the zero-point energy working to oppose the attractive van der Waals' forces. The zero-point energy is a quantum effect for, by quantum mechanics, any body with kinetic energy trapped within a box (such as an helium atom confined by the potential cage of its neighbours) will have an energy of at least $h^2/8mL^2$ where L is the inter-atomic spacing. Because the helium atom has such a small mass, the contribution of the zero-point energy is relatively large, with the result that the molar volume for liquid helium is three times larger than that calculated solely form the van der Waals' forces.

The transition temperature between the two phases is known as the lambda - point, named after the characteristic shape of the specific heat curve of liquid helium as it goes from helium I to helium II. The most obvious manifestation of the transition is the change in the appearance of the liquid from the agitated, bubbling liquid of helium I to the suddenly quiescent liquid of helium II. This is due to the remarkably high thermal conductivity of helium II, making it impossible to set up a temperature gradient which would allow boiling to

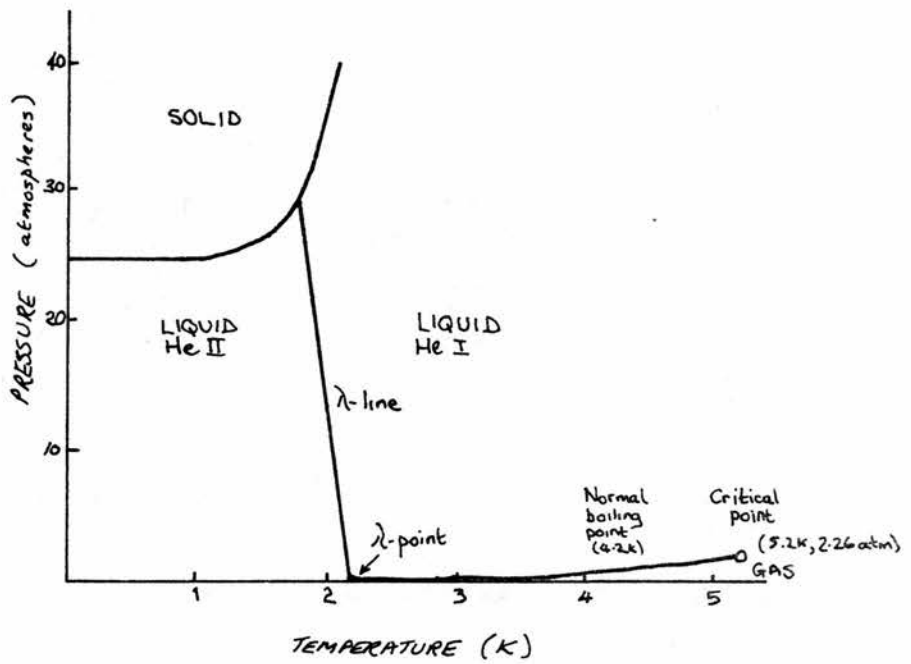

FIGURE I.1 THE PHASE DIAGRAM OF HELIUM-4

take place and so all evaporation occurs from the surface of the liquid. Though the exact nature of the transition is still unresolved, measurements of thermodynamic quantities indicate that the transition is at least of the second order according to the Pippard classification (where the latent heat is continuous and there are discontinuities in the specific heat and the expansion coefficient) (Wilks, 1967 , chapter 11; Keller, 1969a, chapter 7; Pippard, 1960 ; Kadonoff et al, 1967).

Some of the unusual kinetic properties of helium II were discovered in the late 1930's. The most remarkable is the vanishingly small viscosity of helium II which led to its being designated a "superfluid". This was discovered independently in 1938 by Kapitza and by Allen & Misener measuring the rate of flow through very narrow channels (Kapitza, 1938 ; Allen & Misener, 1938 ; Allen & Misener, 1939). However, measurements of the viscosity by two other standard methods, the damping of an oscillating disc and the drag on a rotating cylinder yielded results more in accord with those expected of a classical gas (Keesom & Macwood, 1938 ; Woods & Hollis Hallet, 1963). Another property of helium II known as the fountain effect was also discovered in 1938 (Allen & Jones, 1938). If a vessel is connected to a bath of liquid helium II by a very narrow channel or "superleak" (which allows the passage of helium II, but through which helium I cannot flow because of its viscosity), then increasing the temperature of the helium II within the vessel with respect to the bath will cause the level inside the vessel to rise.

Measurements of this thermomechanical effect showed that at any temperature below 2.2K, the difference in temperature was proportional to the difference in pressure as deduced from the change in height of the level of liquid in the vessel. The reverse effect, the mechanothermal effect, whereby flow out of a vessel via a superleak resulted in an increase in temperature within the vessel was discovered the following year (Daunt & Mendelssohn, 1939a).

It was also in the late 1930's that the first attempts at establishing a theory for liquid helium were made. F. London pointed out in 1938 that, since the helium atoms were bosons, the λ-point transition might be related to the phenomenon of Bose-Einstein condensation (London, F, 1938a; 1938b; 1939). If Bose-Einstein statistics are applied to an ideal gas in order to evaluate the average number of atoms per unit volume having a particular energy (or being in a particular momentum state), then it is found that the total number of atoms per unit volume, N, can be expressed as the sum of two terms, one of which gives the average occupation of the zero momentum state, n_0 . If the temperature drops below a value T_c (= 3.14K), then a finite fraction of the atoms will occupy the ground state of zero momentum i.e. there is a sudden condensation of atoms into the ground state at temperatures below T_c with the fraction in the ground state given by

$$\frac{n_o}{N} = 1 - \left(\frac{T}{T_c}\right)^{3/2} .$$

The treatment of liquid helium as a gas has some justification, for the molar volume of liquid helium is larger than is usual for most liquids and the potential field in which the atoms move hardly changes until the atom approaches within one atomic diameter of a neighbouring atom. Moreover, the temperature dependence of the viscosity of helium I resembles that of a gas, not a liquid. The model of a Bose-Einstein gas does have some features which are in qualitative agreement with the experimental results for liquid helium, and considerable attention has been paid to building a better model for liquid helium using interacting bosons (Josephson, 1972 , Hohenberg & Martin, 1965). The aspects which are difficult to account for, even by allowing for some distortion of the condensation phenomenon by the interatomic forces between the helium atoms, are the temperature dependence of the specific heat and the thermodynamically third-order transition that accompanies Bose-Einstein condensation.

The work of London inspired Tisza to develop a "two-fluid" model of liquid helium (Tisza, 1938 ; 1940 ; 1947 ; 1949). The abruptness of the Bose-Einstein condensation has the consequence that the thermodynamic properties describing the Bose system depend on whether or not the system is below the transition temperature T_c. In a sense, Bose-Einstein condensation represents an equilbrium of two phases, one phase containing atoms in the ground state, the other phase containing all the other atoms. Tisza's procedure is to make assumptions concerning liquid helium expressing characteristics of both a liquid and a gas and then to proceed along quasi-

thermodynamical lines. His first assumption was that at zero temperature the state of the system is liquid and not solid. The possible excitations are phonons and "shear modes" (corresponding to a rearrangement of atoms at constant density). He postulated that these excitations behave like ideal gases and divided the total density into two parts ρ_n and ρ_s, the "normal" density and the "superfluid"density. He finally postulated the existence of a temperature, T_o, (identified with the λ-point) such that ρ_n/ρ would be zero at zero temperature, unity at T_o and increase monotonically between $T = 0$ and $T = T_o$. Since it was possible for the excitations to acquire a relative velocity with respect to the system, Tisza was able to express the total mass current density by

$$j = \rho_n \underline{v}_n + \rho_s \underline{v}_s ,$$

where

$$\rho = \rho_n + \rho_s .$$

Tisza was able to show that the entropy of the system was carried solely by the normal part and derived the expression for the fountain effect which had been given earlier by H. London (1939):

$$\Delta P = \rho s \Delta T .$$

Using this two-fluid model it is easy to understand the apparently contradictory values obtained for the viscosity of helium II. In the oscillating disc experiment, $\rho\eta$ is the quantity that is measured. It is obviously necessary to

specify correctly the density which contributes to the inertia acting on the disc. Since only the normal fluid is dragged round by the disc, ρ_n should be used in calculations of the viscosity, and not the total density ρ. This was most clearly demonstrated by the experiments of Andronikashvili (1946). However, when the flow is through very narrow channels, the viscosity of the normal fluid prevents it from participating in the flow.

The two-fluid model enables a simple picture of two interpenetrating fluids to be used in describing some of the unique properties of liquid helium II. This concept of the two-fluid model has remained so useful as to become an integral part of the language of liquid helium. However, the Tisza model was unable to account for all properties of helium II (for example, the prediction of second sound, a temperature wave, rather than a temperature diffusion, does not have the correct temperature dependence), and it was desirable to base the theory of liquid helium on firmer and more fundamental postulates.

CHAPTER II

MICROSCOPIC THEORIES OF LIQUID HELIUM

i. Landau's Two-Fluid Model

In 1941 Landau derived a microscopic theory for liquid helium, using a process he called the "quantization of hydrodynamics" (Landau, 1941 ; 1947 ; 1949). Landau felt that any attempt to consider the motions of individual atoms in a strongly interacting system (as was done by Tisza in utilizing the Bose-Einstein condensation of an ideal gas in his phenomenological theory of liquid helium) ran contrary to the principles of quantum mechanics. Landau was able to construct an excitation spectrum for the whole system, rather than summing the spectra of the atoms constituting the system, and from this predicted the thermodynamic properties of liquid helium.

Landau's starting point was to change the classical parameters describing a liquid, such as the density and the mass current at any point, into quantum mechanical operators. The commutation relations between the various operators, when applied to macroscopic motion, yield the classical continuity equations. A comparison between the commutation rules for the angular momentum operator in quantum mechanics and those derived for the operator $\nabla \wedge \underline{v}$, where $\underline{v}$ is the velocity at any point, suggest that the transition between states of $\nabla \wedge \underline{v} = 0$ (potential motion) and states of $\nabla \wedge \underline{v} \neq 0$ (vortex motion) is

not continuous. This implies that there will be a gap (denoted by Δ) in the energy spectrum between the lowest energy levels of potential and of vortex motion.

For any slightly excited macroscopic system, a concept of elementary excitations can be introduced. These describe the collective motions of the particles. The excitations corresponding to potential motion in liquid helium are phonons having an energy-momentum relationship defined through

$$\epsilon = c\,p \quad ,$$

where c is the velocity of sound. The excitations corresponding to vortex motion were called rotons by Landau. For small momenta the energy of the roton was modified by Landau in a later paper in order to conform to experimental results:

$$\epsilon = \Delta + \frac{(p - p_o)^2}{\mu}$$

where μ is the effective mass of the roton, and quantities Δ, p_o and μ are empirically determined. The excitation spectrum for liquid helium for low momenta was then continuous. After an initial linear part (phonon spectrum), $\epsilon(p)$ passed through a maximum, went through a minimum located by p_o (the roton minimum), and then increased again.

Though the excitation spectrum implies that the distinction between phonons and rotons is artificial, if the number of excitations per unit volume is not too large, they can be regarded as a mixture of two ideal gases, a phonon gas obeying Bose statistics and a roton gas obeying Maxwell-Boltzman

statistics (since the energy of a roton is at least $\Delta >> k_B T$). It now becomes a straightforward problem in statistical mechanics to calculate the thermodynamic properties of liquid helium. For example, the specific heat contribution from phonons is proportional to T^3, in accord with experimental results for liquid helium below 1K.

Landau then went on to consider liquid helium at absolute zero and showed how the phenomenon of superfluidity could be a consequence of the proposed energy spectrum. Any ordinary liquid flowing through a capillary slows down due to frictional forces originating at the walls of the capillary and from within the liquid itself. Liquid helium at 0 K would flow as a perfect fluid until the velocity of flow was such that an elementary excitation could be created. The energy required for this excitation would come from the kinetic energy of the flow, and thus the entire fluid would slow down. The change in energy of the liquid would be $\epsilon + \underline{p}.\underline{V}$ where $\underline{V}$ is the velocity of flow required to create and excitation of energy ϵ and momentum $\underline{p}$. This implies that the minimum velocity needed to create an excitation is given by

$$V_o = |\epsilon/\underline{p}| \quad .$$

This has the approximate values of 2×10^4 cm sec^{-1} for phonons and 6×10^3 cm sec^{-1} for rotons. Thus, if the velocity of flow $\underline{V}$ is not too large ($< V_o$), neither rotons nor phonons can be excited and the flow of the liquid would not slow down, disclosing the phenomenon of superfluidity. (Since

throughout the argument, no use was made of helium being at 0 K, this argument implied that at slightly higher temperatures, when the excitations can be considered as a gas of rotons and phonons, no new excitations can be created at low velocitis of flow).

Consideration of the properties of a liquid with the above characteristics inside a rotating vessel led Landau to the conclusion that only part of the liquid rotates with the walls of the containing vessel. It thus becomes possible to regard liquid helium as if it were a mixture of two fluids, one of which is superfluid having no entropy (thus the flow of helium II in which only the superfluid takes place is thermodynamically reversible) and the other (the excitation gas) which behaves as a normal fluid. Landau introduced the density of the normal fluid, ρ_n, and thereby defined the superfluid density, ρ_s, as $\rho - \rho_n$, where ρ is the total density. Calculations of ρ_n/ρ from the proposed energy spectrum are in good agreement with experimental values, as are values of the entropy determined by the statistical distribution of phonons and rotons.

Landau goes on to the hydrodynamic equations for helium II, describing the motion through the use of two velocity fields $\underline{v}_n$ and $\underline{v}_s$, where the subscripts refer to the normal fluid and the superfluid (Landau & Lifshitz, 1959). He utilized the potential flow characteristics of the superfluid ($\nabla \wedge \underline{v}_s = 0$), the conservation laws of energy momentum, mass and entropy, and the principle of Galilean relativity to obtain the equations of

motion. When terms quadratic in the velocity and viscous effects can be ignored, the linearized equations are:

$$\rho = \rho_n + \rho_s$$

$$j = v_n \rho_n + v_s \rho_s$$

$$\frac{\partial(\rho s)}{\partial t} = -\nabla(\rho s v_n)$$

$$\frac{\partial j}{\partial t} = -\nabla P$$

$$\frac{\partial v_s}{\partial t} = -\nabla \mu = s\nabla T - \frac{1}{\rho}\nabla P \quad .$$

where μ is the chemical potential and P the pressure.

These two-fluid equations of motion have proved to be remarkably successful in describing the properties of helium, particularly at lower temperatures. For example, they were used by Landau to predict the form of a temperature wave (rather than a diffusion process) called second sound. This was experimentally confirmed by Peshkov in 1944 (Peshkov, 1944). At higher temperatures, the excitations can no longer be treated as independent ideal gases, though with the addition of interaction terms to the phonon-roton model, the transport properties of helium II have been well accounted for (Khalatnikov, 1965).

There are, however, two major shortcomings to the Landau model of liquid helium. The theory is unable to give an adequate description of the λ - transition; the other difficulty concerns the interpretation of the veolcity of flow needed to create excitations. If this is interpreted as a limiting condition of the maximum flow rates possible experimentally,

then the Landau criterion predicts values orders of magnitude larger than normal experimental values (under particular conditions, values close to the Landau value have been reported (Phillips & McClintock, 1974 ; Allum et al, 1977)).

ii. The Feynman Wavefunction and the Vortex Line

Feynman's treatment of liquid helium gave a partial answer to both these problems. His approach to studying the thermodynamic properties of liquid helium was through a computation of the partition function for the system. He developed a method enabling him to express the partition function as an integral over possible trajectories of the atoms of the system (Feynman, 1948). He then neglected those trajectories which, from physical arguments, seemed unlikely and found that the simplified partition function had features very similar to those of an ideal Bose gas (Feynman, 1953a). In other words, starting from a description of a system of interacting atoms, he was able to show that the inclusion of large interatomic forces did not alter the central features of Bose-Einstein condensation and that thereby, the transition from helium I to helium II was essentially the same process as the condensation phenomenon in an ideal Bose-Einstein gas.

Having obtained a suitable partition function, Feynman was able, by using physical arguments, to show why the only low-lying excited states should be phonons (Feynman, 1953b).

By extending the argument to higher energy excitations, Feynman obtained a wave function of the form

$$\psi = \phi_0 \sum_i e^{i\underline{k}\cdot\underline{r}_i} ,$$

where ϕ_0 is the ground state wave function and $\underline{r}_i$ is the position vector of the i^{th} atom (Feynman, 1954). This yields an energy spectrum

$$E(k) = \hbar^2 k^2 / 2mS(k) ,$$

where S(k) is the structure factor of the liquid. This spectrum has the same form as that Landau obtained. For small $\underline{k}$ the spectrum is a phonon spectrum, while the maximum in S(k) at $k = 2\pi/a$ (the nearest neighbour wavelength) corresponds to Landau's roton minimum. This puts the Landau spectrum on a far firmer microscopic basis, since the solution Feynman derived comes about by considering the collective motion of the atoms constituting the system, and a complete solution to the theory of liquid helium can, according to theorists, only be possible through the solution of the exact Schroedinger equation for the system.

Feynman next considered the situation at low temperatures when the fluid was in motion. He obtained a wavefunction of the form

$$\psi = \phi_0 \exp\left\{ i \sum_i s(\underline{r}_i) \right\} ,$$

where $s(\underline{r})$ is a function of position. The velocity at any point is then given by

$$\underline{v}_s(\underline{r}) = \frac{\hbar}{m} \nabla s(\underline{r}) ,$$

yielding

$$\nabla \wedge \underline{v}_s = 0 \quad .$$

For a singly-connected region, there can be no circulation; however, in a multiply-connected region circulation is possible. Onsager had suggested that the circulation in superfluid helium might be quantized in units of h/m (Onsager, 1949). This was developed independently by Feynman (1955), for the circulation, κ , is defined as

$$\kappa = \oint \underline{v}_s \cdot d\underline{\ell} = \oint \frac{\hbar}{m} \nabla S \cdot d\underline{\ell}$$

$$= n h/m \qquad \text{where n is an integer.}$$

(The wavefunction ψ can be shown to violate current conservation. To account for this, Feynman and Cohen constructed another wavefunction which is very similar to that of Landau (Feynman & Cohen, 1956):

$$\psi = \phi_0 \sum_i \exp(i \underline{k} \cdot \underline{r}_i) \left[1 + i \sum_{i \neq j}' \frac{A}{r_{ij}^3} \underline{k} \cdot \underline{r}_{ij} \right] .$$

This describes the roton state as a microscopic vortex ring of a diameter comparable to the atomic spacing).

The possible existence of quantum vortices in the superfluid helium suggests a solution to the difficulty of the high critical velocity required by Landau's theory of liquid helium. Though turbulence will begin at any velocity in a classical fluid, in a quantum fluid the velocity must be such that the kinetic energy from the flow is sufficient to produce a quantum of vorticity. If, instead of the momentum used in the

Landau excitation spectrum, the impulse needed to create a vortex ring with a core size of the atomic spacing, a, were used, then,

$$p = \tfrac{1}{4} \pi \rho \kappa d^2 \quad ,$$

$$\epsilon = \tfrac{1}{4} \rho \kappa^2 d \left(\ln 4d/a - \tfrac{7}{4} \right) \quad ,$$

and

$$v = \epsilon / p = \frac{\kappa}{\pi d} \left(\ln 4d/a - \tfrac{1}{4} \right) \quad ,$$

where d is the channel width. (These expressions, which are for a free classical vortex ring [Lamb, 1932], are modified when the effect of the walls are taken into account [Fineman & Chase, 1963 ; Gopal, 1963]). The values of the velocity obtained in this manner are still far higher than the values deduced from experiments, but the expression is satisfactory in other ways since the velocity increases with decreasing channel width and the product vd is a slowly increasing function of d, in accord with experimental results.

Evidence for the existence of quantized vortex lines was first obtained by Vinen, studying a vibrating wire in rotating helium (Vinen, 1961b). The model of an array of vortex lines suggested by Feynman was shown to be essentially correct by Hall and Vinen (1956), and an array of vortex lines has been photographed (Williams & Packard, 1974b). These experiments have all been carried out in rotating vessels of superfluid helium, and since Rayfield and Reif have demonstrated the validity of vorticity in flow experiments (Rayfield & Reif, 1963 ; 1964), work on the behaviour of vortex lines in rotating systems both theoretically and experimentally, has

led to a greater understanding of the superfluid vortex line (Hall, 1960 ; Vinen, 1961a; Andronikashvili & Mamaladze, 1966 ; Pitaevskii, 1961 ; Fetter, 1965 ; 1967).

iii. Microscopic Models

Though Feynman's description shows how some of the difficulties associated with Landau's two-fluid model (the transition, the scarcity of low-lying excitation states, and the problem of the limiting flow velocity) may be overcome, his arguments were based on physical intuition. The limiting flow velocity will be discussed in the next chapter. The remainder of this chapter will give a brief survey of the evolution of the derivation of a wavefunction for liquid helium from first principles and the inclusion of vortices within such a system.

In 1947 Bogoliubov produced a theory of superfluidity by considering the behaviour of a weakly interacting Bose gas (Bogoliubov, 1947), utilizing the many-body language of second quantization. He assumed that the ground state of the system was macroscopically occupied (this means that the creation and annihilation operators are both approximately equal to the square root of the number of particles in the ground state) and that the interatomic interaction was weak (and so all orders higher than the second, of non-zero momentum states can be neglected). This resulted in an Hamiltonian for the system consisting of a contribution from

the zero-momentum state and a perturbation term arising from all the other momentum states. Diagonalizing the Hamiltonian showed the total energy of the interacting gas to consist of the energy of quasi-particles (excitations) with wave number k ($k \neq 0$), and transformed the original operators into operators for the quasi-particles. The ground state condensate was shown to move with arbitrary small velocity, under certain conditions, without any friction with respect to elementary excitations, thus fulfilling Landau's criterion for superfluidity. Though the excitations at long wavelengths are phonons, and, for large k, resemble free-particles, the energy spectrum Bogoliubov postulated is without any "roton" minimum.

In 1956 Penrose and Onsager generalized the definition of Bose-Einstein condensation to make it applicable to any Bose system (Penrose & Onsager, 1956). Physically, their definition meant that whenever a finite fraction of particles occupied one quantum state, Bose-Einstein condensation was present. To determine whether a particular system satisfied their criterion, Penrose and Onsager evaluated the density matrix for the system. Following Bogoliubov, they divided the matrix into two parts, one part being the zero-momentum contribution, the other arising from contributions from all the other states:

$$\rho(\underline{r},\underline{r}') = n_0 + \tilde{\rho}(\underline{r},\underline{r}') \quad .$$

The average value of $\tilde{\rho}$ tended to zero as $\underline{r}-\underline{r}_0$ tended to

infinity, showing that the momentum correlation for $\tilde{\rho}$ is short range. Penrose and Onsager showed that the eigenvalues for $\tilde{\rho}$ form the occupation numbers for the momentum states, and they were able thereby to calculate the condensation condition.

To consider liquid helium at 0 K, Penrose and Onsager constructed a wavefunction which describes the liquid as a system of hard spheres with two-body interactions. Assuming that no long-range configurational order exists in the liquid, they showed that condensation does occur in such a system, with a condensate fraction of about 8%. By extending their treatment, they showed that condensation should occur at finite temperatures, below the transition temperature. Thus, though Penrose and Onsager did not present a proof of Bose-Einstein condensation in liquid helium II, they gave convincing arguments for its existence.

Lee, Yang and Huang have calculated the ground state energy and other properties of the system, using a hard-sphere model for liquid helium (Huang & Yang, 1957 ; Huang et al, 1957 ; Lee & Yang, 1957 ; Lee et al, 1957 ; Lee & Yang, 1958 ; 1959 ; 1959 ; 1960). The advantage of their approach over a perturbation method based on Bogoliubov's treatment (as was used by Hugenholtz and Pines (1959), for example), is that the calculations can be simplified and readily extended to the finite temperature region. Lee, Yang and Huang's results showed agreement with experiments in the values of first sound and in the behaviour of the specific heat.

Variational techniques have also been applied to helium assuming a Lennard-Jones potential for the system (McMillan, 1965 ; Kalos et al, 1974). This involves finding an exact solution for the Schodinger equation by a Monte Carlo technique, using the hard-sphere model with a Lennard-Jones potential as a perturbative correction. This technique produced accurate simulations of ^{4}He at 0 K, but cannot be used at finite temperatures (Chester, 1975). Both the exact and the variational methods give the fraction of particles in the ground state at 0 K as 10% (Kalos et al, 1974).

Josephson has applied variational principles to obtain a microscopic theory of a Bose liquid (Josephson, 1972). He assumed that all quantities varied slowly in space and time and ignored all singularities except those associated with phonons. He showed that the density and current density computed for this system are the same as those predicted by the phenomenological theory of liquid helium (Khalatnikov, 1965).

Most microscopic theories assume that Bose-Einstein condensation occurs in the system under consideration. Through this, a definition of the superfluid velocity field can be derived (Chester, 1975 , page 23). What is more difficult, is to derive an equation of motion for the superfluid components using only microscopic theory. Though some progress has been made in this direction, an unambiguous connection between Bose-Einstein condensation and superfluidity has yet to be established (Josephson, 1972 ; Hohenberg & Martin, 1965).

iv. The Inhomogeneous System

The wavefunction for liquid helium, ψ , is usually written as

$$\psi = \phi_o \exp\left[i \sum_j s(\underline{r}_j) \right]$$

from which it is possible to derive a definition of the superfluid velocity (see section ii):

$$\underline{v}_s(\underline{r}) = \hbar/m \, \nabla s(\underline{r}) \quad .$$

The wavefunction ψ remains valid provided that the velocity of flow varies sufficiently slowly with position: the ground state wavefunction, ϕ_o, must remain unaffected by the flow. The characteristic scale, ξ_c, below which these conditions break down, is known as the coherence length of the condensate wavefunction.

In 1958 Beliaev applied a perturbation theory to Bogoliubov's treatment using the quantum field theory technique of Green's functions (Beliaev, 1958b). He obtained a matrix element for n_o

$$n_o = \langle \psi^\dagger(\underline{r}) \psi(\underline{r}') \rangle \quad ,$$

where one state has an additional particle in the condensate. He concluded that $\langle\psi\rangle$ could be written as a product of an amplitude and a time-dependent phase

$$\langle \psi(\underline{r}) \rangle = n_o^{1/2} \exp(-i\mu t/\hbar) \quad ,$$

The quantity $\langle\psi(\underline{r})\rangle$ has become known as the superfluid order

parameter. μ is the chemical potential per particle representing the change in energy of the ground state through the addition of a single particle to the condensate.

Close to the λ-point, this quasi-microscopic approach to superfluid helium is invalid. Ginzburg and Pitaevskii applied the phenomenological theory of phase transition to obtain an equation analogous to the Ginzburg-Landau equation in superconductivity (Ginzburg & Pitaevskii, 1958). They assumed that the phase transition for liquid helium was of second order (which is not strictly correct for liquid helium). The thermodynamic potential of the system was expanded in terms of some order parameter, which, in equilibrium, is zero on one side of the transition and its value on the other side is determined by minimizing the thermodynamic potential with respect to this parameter. Since $\rho_s = 0$ for helium I, the order parameter must be connected with the superfluid density.

Ginzburg and Pitaevskii assumed an order parameter, Ψ , similar to that obtained by Beliaev,

$$\Psi = a e^{i\phi} \quad ,$$

such that

$$\rho_s = m |\Psi|^2 \quad \text{and} \quad \underline{v}_s = \hbar/m \nabla\phi \quad .$$

They then obtained an equation for the variation of Ψ which, if the thermodynamic potential is expanded in powers of $|\Psi|^2$, is of the form

$$-\frac{\hbar^2}{2m}\nabla^2\Psi - \alpha\Psi + \beta|\Psi|^2\Psi = 0 \quad .$$

This equation has associated with it a coherence length, ξ_{Gc},

$$\xi_{Gc} = \hbar/(2m\alpha)^{1/2}$$
$$\simeq \frac{4\times10^{-10}}{(T_\lambda - T)^{1/2}} \quad m \quad .$$

If the order parameter for a vortex filament is expressed as

$$\Psi(r,\varphi) = \Phi(r)e^{in\varphi} \quad ,$$

then this method can be used to show that vortices with $n>1$ are unfavourable.

A more direct method for including vortices was used by Pitaevskii to generalize the Bogoliubov method to a non-uniform situation (Pitaevskii, 1961). The wavefunction is expressed as a matrix element in terms of annihilation and creation operators. Pitaevskii assumed the particles to have a repulsive point-interaction of a strength V_o; and since for a stationary state $\Psi \propto \exp i\omega t$, obtained

$$-\frac{\hbar^2}{2m}\nabla^2\Psi - \omega_o\Psi + V_o(\Psi^\dagger\Psi)\Psi = 0 \quad ,$$

which is of the same form as the Ginzburg and Pitaevskii equation with a coherence length

$$\xi_{Gc} = \hbar(V_o n_o m)^{1/2} \quad .$$

This technique allows for the existence of inhomogeneities within the system, but does not affect the macroscopic equations of motion. For example, writing $\Psi = ae^{is}$ and $v_s = \hbar/m\,\nabla s$, solving for the real and imaginary parts of

Ψ from Pitaevskii's equation yields the mass continuity equation for $\underline{V}_s$:

$$\rho \frac{\partial \underline{v}_s}{\partial t} + \rho \nabla \left(\tfrac{1}{2} v_s^2 \right) = -\nabla \left(V_0 \frac{a^2}{m} - \frac{1}{2m^2} \nabla \left(\frac{\nabla^2 a}{a} \right) \right) .$$

If the last term is neglected i.e. if the variation of Ψ is over lengths large compared with ξ_c, then it reduces to the usual macroscopic equation for the superfluid flow:

$$\frac{\partial \underline{v}_s}{\partial t} = -\nabla \left(\mu + \frac{1}{2} v_s^2 \right) .$$

CHAPTER III

THEORIES OF DISSIPATION IN HELIUM II

In the theory of superfluidity developed by Landau it was shown that below a certain velocity of flow, thermal excitations could not be created in helium II, and thus for all values of flow velocity below this velocity the flow should be frictionless. Values of the flow velocities obtained through experiments show that the maximum value is several orders of magnitude lower than that predicted by the Landau model. The concept of a vortex line as a sort of excitation of lower energy than thermal excitations provided a means of reducing this discrepancy. As shown in Chapter II, the predictions of the limiting velocity as a function of parameters such as the channel width, were qualitatively correct. There still remained the problems of how a vortex line was initiated in helium II, and, since the vortex line was part of the superfluid, not the normal fluid, how to account quantitatively for the observed values of flow velocities (Vinen, 1961a).

In 1965 Iordanskii suggested that vorticity might be produced in the superfluid by thermal fluctuations (Iordanskii, 1965). His starting point was the suggestion that any state satisfying the Landau criterion, $|v_n - v_s| < |\epsilon(p)/p|_{min}$, in which there is relative motion between the normal and superfluid components of velocity is only metastable, and

would tend towards a state in which there was no relative motion of velocity components. He assumed that the approach to equilibrium was through the formation (through thermal fluctuations) of vortex filaments in the superfluid and the consequent reduction in the relative velocity between v_n and v_s. The shortest length of vortex line that is continuous or which ends on a boundary is a vortex ring.

The energy, A, of a vortex ring of radius R is found by utilizing the Galilean transformation

$$A = \epsilon(R) + \underline{p}(R) \cdot \underline{v}_s$$

where ϵ and p are the energy and momentum of a classical vortex ring in a fluid at rest. The size of the ring depends on the balance of forces acting on the vortex filament. There is a critical size of vortex ring, determined by $\partial A/\partial R\big|_{R_c} = 0$. Below this the vortex ring exchanges energy reversibly with fluid, growing or diminishing in size. However, above this size, the further growth of a vortex ring is energetically favourable, extracting energy from the fluid and thereby slowing down the flow of the fluid. The vortex rings can attain a critical size by means of random repeated expansions as a result of fluctuations related to the presence of excitations in the fluid. This notion of a vortex ring randomly colliding with an excitation gas is a similar concept to that used in considering Brownian motion, and Iordanskii obtained a Fokker-Plank equation for the number of vortex rings in a particular state.

Manipulation of this Fokker-Plank equation showed that the number of vortex rings of radius R is proportional to $\exp(-B/k_B T)$. His calculations showed that there was an appreciable formation of vortex rings when the superfluid velocity was greater than 60 cm sec^{-1}, and fell off sharply to unobservable values at velocities below 40 cm sec^{-1}.

In 1966 a different approach was taken by Anderson in determining the relationship of vorticity and the forces applied to a superfluid (Anderson, 1966). He considered the wavefunction

$$\psi(\underline{r},t) = f(\underline{r},t) \exp i\phi(\underline{r},t)$$

and noted that the phase ϕ was responsible for the superfluid properties since it was ϕ which responded to external forces. (In this respect, Anderson returned to the Beliaev treatment of the wavefunction, where the condensate wavefunction was expressed as a product of an amplitude and an explicit time-dependent part determined by the chemical potential (Beliaev, 1958),

$$\hbar\, \partial\phi/\partial t = \partial E/\partial N = \mu \quad .)$$

If the system is in a steady state, ϕ and hence μ must also be constant. Conversely, if a potential difference $\mu_1 - \mu_2$ exists between two elements then $\phi_1 - \phi_2$ must change in time. Taking the gradient of the above equation:

$$\frac{d}{dt}(\hbar \nabla\phi) = \nabla\mu = F$$

where F is the total force on the particles. Since $\hbar\nabla\phi = p_s = mv_s$, this reduces to

$$\frac{d}{dt}(mv_s) = \nabla\mu \quad ,$$

which states simply that the superfluid may be accelerated by external forces without any frictional damping.

There is however, another way whereby the phase difference can change in time. The integral of $\nabla\phi$ round a vortex line differs by 2π from the integral of $\nabla\phi$ passing through a vortex, and so if a vortex crosses a line joining points of different phase, then the phase difference between these points will change by 2π and there will be what Anderson called a "phase slippage" between the points. If vortices crossed the line at some average rate $\langle dn/dt \rangle$,

$$2\pi \langle dn/dt \rangle = d/dt \langle \phi_1 - \phi_2 \rangle$$

or $$\hbar \frac{d}{dt} \langle \phi_1 - \phi_2 \rangle = \langle \mu_1 - \mu_2 \rangle .$$

This suggests that whenever there is a potential difference there will also be a transport of vorticity (a phase slippage). Since the phase must change by multiples of 2π, it becomes possible to define a "critical" velocity at which vortices are created and transported ($\langle \mu_1 - \mu_2 \rangle = 2\pi\hbar \langle \frac{dn}{dt} \rangle$) and below which the superfluid is simply accelerated ($\mu = \frac{d}{dt} mv_s$).

The work of Anderson was generalized by Huggins in 1970 (Huggins, 1970a). He showed that it was possible to divide the velocity field into two parts: a potential field and a

vortex velocity field. In this way he was able to demonstrate clearly that when a force did work on the potential flow, the only way the potential could lose the energy it thereby gained, was by having vortices cross the potential current. As was stressed by Campbell, vortex growth in itself cannot be considered a dissipative process: rather, it is a redistribution of kinetic flow energy and as such is irreversible (Campbell, 1972a). Though the decay of a vortex (and its attendant energy loss) consists of a term proportional to the stream velocity and a term representing the initial energy of the vortex, when the phase condition is applied, the stream energy exactly balances the former term, and thereby energy for the creation of vortices cannot be obtained from the flowing stream (Campbell, 1970). This limits the energy for the creation of vortices to that obtained by fluctuations. Thus any theory of critical velocities or of the creation of vortices must pay cognisance to the phase coherence which can be said to characterize a superfluid (Schwartz, 1975).

Similar ideas to those of Iordanskii were developed independently by Langer and Fisher by analogy with the supersaturated vapour. Their work was stimulated by the observation of Clow and Reppy that an intrinsic critical superfluid velocity independent of the geometry of the container, existed near the λ-point (Clow and Reppy, 1967). Langer and Fisher asserted (as Iordanskii did) that non-zero superflow must be only metastable and, as with a supersaturated vapour, for any given metastable phase there would be a finite

probability for nucleation of the stable phase (Langer & Fisher, 1967). The probability for nucleation depends on the superflow velocity: the probability rate for nucleation to the stable phase would be too small to be observed for a sufficiently small superfluid velocity, and a "critical" velocity would occur when the rate of nucleation became appreciable.

Langer and Fisher assumed that the relevant states of the system could be described using a continuous order parameter, $\psi(\underline{r})$. The probability that the system would be found in state $\psi(\underline{r})$ was then proportional to $\exp\left[-F\{\psi(\underline{r})\}/k_B T\right]$ where F is a free-energy function. Any metastable (or stable) state corresponded to a minimum in F. Since F was continuous, for the system to reach a metastable state of lower free energy it had to overcome an energy barrier, the height of which determined the rate at which ψ decays from one state to the other. (This has been described in terms of the saddle point of F by Langer (1967). The saddle point criterion is that a metastable state must be a stationary point of F i.e.

$$\left| \frac{d F\{\psi\}}{d \psi} \right|_{\psi=\psi_c} = 0 \ ,$$

where ψ_c is the saddle point. This is a generalized Ginzburg-Landau equation, which can also describe the hydrodynamics of a superfluid in which quantized vorticity can occur).

Langer and Fisher then argued that the localized fluctuation which would take the system from one metastable state to another must be a vortex ring. Not only was the

generalized Ginzburg-Landau equation consistent with observations on vortex rings (Rayfield & Reif, 1964), but, as Anderson had shown, a vortex ring has the right phase properties to allow a transition from a state $\psi_k(\underline{r}) = Ae^{i\underline{k}\cdot\underline{r}}$ corresponding to a uniform superfluid velocity $\underline{v}_s = \hbar/m|\underline{k}|$ to a state of one wavelength less $\underline{v}_s = (k - 2\pi/L)\hbar/m$. If there was a vortex ring of unit vorticity, the change of phase passing through the centre of the ring would be 2π less than the phase change along any path passing around the ring. The free energy would be lowered if the ring expanded and if the ring were subsequently annihilated at the walls of the container, the order parameter ψ would lose one wavelength across the whole system.

Langer and Fisher then went on to consider the nucleation rate. For a ring moving in a rest frame, the energy in the moving frame is

$$E = E_o - p_o v_s \quad ,$$

where E_o and p_o are the energy and momentum of a classical vortex ring of radius R. This has a maximum E_c at $R = R_c$ determined by

$$\left.\frac{dE_o}{dR}\right|_{R=R_c} - v_s \left.\frac{dp_o}{dR}\right|_{R=R_c} = 0 \; .$$

Now, since rings with $R > R_c$ lower their free energy by expanding and rings with $R < R_c$ tend to collapse, the free energy barrier, ΔF , must be E , i.e.

$$\Delta F \propto \rho_s(T)/v_s(T) \; .$$

The "critical" velocity is then determined from the expression for the nucleation rate per unit volume

$$f = f_0 \exp(-\Delta F / k_B T) ,$$

where f_0 is some characteristic rate for microscopic processes. If f exceeds some minimum observable frequency (say, $0.1 cm^{-3}\ sec^{-1}$) the superfluid velocity exceeds the critical velocity determined from the last two equations.

These ideas were expressed in a more useful form by Langer and Reppy (Langer & Reppy, 1970). They assumed an activation energy $E_a(v_s, T)$ for the required fluctuation existed, and that E_a was independent of the shape and size of the container. If A is the cross-section and L is the periodic length of a container, then the rate at which fluctuation would occur would be

$$R = A L f_0 \exp(-E_a / k_B T) .$$

Since a fluctuation carried the system over to a neighbouring state, they assumed a velocity change $\Delta v_s = -h/mL = -\kappa/L$ implying

$$\frac{dv_s}{dt} = R \Delta v_s = -\kappa A f_0 \exp(-E_a / k_B T) .$$

This allowed the critical velocity to be defined either as that velocity below which dv_s/dt is too small to be experimentally observed or that velocity above which dv_s/dt is so large that the metastable state cannot persist for observable times.

This statement represented a radical shift of emphasis on the idea of a "critical" velocity, for the Iordanskii-Langer-Fisher idea suggested that flow without dissipation is not possible and that instead of a "critical" velocity, there is a limiting velocity governed by the exponential $E_a(v_s, T)/k_B T$. The term critical velocity will henceforth be used to denote that velocity above which further acceleration is experimentally indetectable.

An estimate of critical velocity, v_c , can be obtained by estimating an observable value of $dv_s/dt = \Phi_o$ (of the order of 1 cm sec^{-2}) where

$$\Phi_o = \kappa A f_o \exp\left[-E_a(v_c)/k_B T\right] .$$

The authors assumed that E_a was a decreasing function of both v_s and T and therefore dv_s/dt was a rapidly decreasing function of v_s and T; i.e. E_a is such that no decay or no metastable state can be detected. That suggested that E_a need only be known when v_s was near v_c and enabled E_a to be expanded as a function of $(v_s - v_c)$. For long times,

$$v_s \simeq v_c - \frac{1}{\alpha} \ln(\alpha \Phi_o t),$$

where

$$\alpha = -\frac{1}{k_B T}\left(\frac{\partial E_a}{\partial v_s}\right)_{v_c} .$$

This result has been experimentally confirmed near T_λ (Kukich et al, 1968a; 1968b).

Since the publication of the papers of Iordanskii and Langer & Fisher, numerous experiments have been carried out to test the concept of the fluctuation model as a basis of dissipation in superfluid flow. Though the exact form of the dissipation is not that suggested by Langer and Fisher, experiment does seem to have validated the major ideas. These experiments will be discussed in the following chapters.

CHAPTER IV

CRITICAL VELOCITIES IN CHANNELS AND PORES

The pioneering work for the flow of liquid helium through narrow channels and through porous media was undertaken by Allen and Misener in 1939 (Allen & Misener, 1939). They investigated the dependence of the applied pressure head on flow rate through capillaries and channels ranging from 1 mm to 10^{-4} mm and also through packed jeweller's rouge. They were also the first to observe the inertial oscillations which occur as the level difference between two containers coupled by a narrow channel decays to equilibrium. These oscillations were utilized by Atkins to measure the critical velocity of flow through the superfluid flim (Atkins, 1950) (see Chapter V) and were completely described by Robinson in 1951 (Robinson, 1951).

After the acceptance of the Tisza-Landau two-fluid model of helium II, workers measuring the flow through channels looked for deviations from the behaviour expected from the linearized Landau equations of motion given in Chapter II. Considerable care has had to be exercised in deciding the region where non-linear behaviour first begins, particularly in the case of wide channels ($\gtrsim 10^{-3}$ cm) where the turbulence of the normal fluid will give rise to non-linear effects (De Bruyn Ouboter et al, 1967 ; Keller, 1969b; Childers & Tough, 1973 ; 1974 ; 1976). Measurements of

critical velocities in channels are normally made under one of two experimental conditions: counterflow conditions or pressureflow conditions.

Counterflow experiments are restricted to channels sufficiently wide to allow the transport of the normal component of helium II. In these experiments heat is carried away from a heat source by the normal component, and, to conserve mass, the superfluid component must flow towards the heat source. If the heat current density is expressed as

$$W = \dot{Q}/\pi a^2 \quad ,$$

where $\dot{Q}$ is the heat supplied and a is the channel radius, then the magnitude of the superfluid velocity and of the relative velocity between the superfluid and the normal components can be deduced from the Landau hydrodynamic equations to be

$$v_s = \frac{W \rho_n}{\rho s T \rho_s}$$

and

$$v = v_n - v_s$$

$$= \frac{W}{\rho_s s T}$$

respectively. For large heat currents the pressure gradient can no longer be given simply in terms of the viscosity. An attempt was made by Gorter and Mellink to explain the ensuing non-linearity through a mutual-friction force describing the interaction between the normal and superfluid velocity components when

their relative velocity was large (Gorter & Mellink, 1949). In 1957/8 Vinen developed a theory for the balance between the growth and the decay of vortex lines, based both on a microscopic analysis of the interaction between the normal fluid and the superfluid vortex lines, and on physical dimensional arguments (Vinen, 1957 ; 1958 ; 1961a; 1963 ; 1966). This theory, slightly modified, has been used remarkably successfully in explaining experimental results (Childers & Tough, 1973 ; 1974 ; 1976).

From results of the attenuation of second sound in rotating helium (Hall & Vinen, 1956a), Vinen was able to derive the Gorter-Mellink mutual friction force by considering the forces acting on a vortex line due to the relative motion between the line and the normal fluid. He assumed that there existed a homogeneous tangled mass of vortex lines, the result of turbulence arising from the relative motion of the two fluids, and considered the equilibrium state of such a tangled mass. Characterizing the velocity by the length of vortex line per unit, L, and presuming that the generation of new vortex line (a process assumed to be homogeneous and independent of the channel boundaries) proceeds in a similar manner to that of the growth of a vortex ring, Vinen obtained the following term for the growth of a vortex line : -

$$\frac{dL}{dt} = \frac{1}{2} \chi_1 B \rho_n / \rho \, L^{3/2} v \, .$$

where χ_1 is the dimensionless constant, B is a dimensionless parameter describing the roton-vortex line scattering (like χ_1 of the order of unity), and v is the relative velocity.

The walls will interfere with the growth process: for a distance of $L^{-1/2}$ (the average spacing of the vortex lines) there will be no generation of vortices, and so the above term is modified by a factor $(1-\frac{\alpha}{d}L^{-1/2})$ where α is a dimensionless constant and d is the channel diameter. This generation term can be justified by dimensional analysis and by physical argument, and describes the build-up of turbulence through the relative motion of the two fluids: the normal fluid exerts a force on the vortex lines, causing them to move according to the Magnus effect. This movement, together with interactions between the lines, leads to a continuous stretching of the vortex lines.

The decay of vortex lines proceeds through the tendency of the lines to cluster together and, thereby, for lines of opposite sense to annihilate each other. Vinen derived a term for this in analogy to the empirical law for the decay of turbulence in classical fluids, as well as by dimensional argument:

$$\frac{dL}{dt} = -\chi_2 \frac{\kappa}{2\pi} L^2 ,$$

where κ is a quantum of circulation h/m. The basis of this term has been justified on microscopic grounds (Silton & Moss, 1972 ; Ashton & Northby, 1973). In equilbrium $dL/dt = 0$, and the equilibrium length is given through

$$\tfrac{1}{2}\chi_1 B \rho_n v \left(1-\frac{\alpha}{L_0^{1/2} d}\right) L_0^{3/2} = \chi_2 \rho \frac{\kappa}{2\pi} L_0^2 .$$

The critical velocity can then be determined:

$$v_c d = 4\kappa\rho\alpha\chi_2 / (\pi B \rho_n \chi_1) .$$

This theory did not attempt to explain how vorticity enters the flow (Vinen included an empirical term to describe this, but subsequent experimenters have not found any evidence to support this [Vinen, 1957 ; 1958 ; 1961 ; 1963 ; 1966 ; Brewer & Edwards, 1961]), but described the dynamic balance of a length of vortex line. As such, it accounted quantitatively for the experimental results of Childers and Tough (1973 ; 1974 ; 1976), and seems to be applicable, with a modification to the rate of growth of vortex line term, even under conditions where there may be turbulence in the normal fluid (Lander et al, 1976).

The other method often used to determine critical velocities in capillaries, is to use a pressure head to drive the fluid through the channel. This was the method used by Allen and Misener in their experiments (Allen & Misener, 1939). The Leiden School at the Kammerlingh Onnes Laboratory have thoroughly investigated flow through a capillary (van der Heijden et al, 1972a; 1972b; 1974 ; Olijhoek et al, 1974 ; van Alphen et al, 1969). They have studied thermal effects during the adiabatic flow of helium II, investigated the forces operating during helium II flow and measured the accompanying energy dissipation. Their data suggested that the introduction of the Gorter-Mellink mutual-friction term (Gorter & Mellink, 1949) into the hydrodynamic equations described the observed flow, though there appears to be an additional force acting on the superfluid alone which depends in a complex way on the relative velocity (van der Heijden et al, 1972a; 1972b; 1974 ; Olijhoek et al, 1974). They were able to formulate an empirical relationship between the critical velocity (in cm sec^{-1}) and the channel

diameter (in cm):

$$v_c \simeq d^{-1/4} \quad .$$

This appears to be valid for channels from 6 x 10^{-6} mm (Vycor glass) to 6 mm (van Alphen et al, 1969). It fitted the results of Keller and Hammel (1961a; 1960 ; 1961b).

The results of Kidder (1962 ; 1965) and Weaver (1972), however, suggested that

$$v_c \simeq d^{-1} \quad ,$$

in agreement with the Feynman idea that the critical velocity was determined by the rate of formation of vortex rings in a narrow channel (Feynman, 1955). Glaberson and Donnelly (1966) have extended Vinen's hypothesis (Vinen, 1961a) that short lengths of vortex line are always present in helium II and that these are attached to energetically favourable sites, forming nucleation centres for the production of new lengths of vortex line. They considered a length of vortex line pinned across the stream of flow, and looked at the forces acting on the line. They showed that, beyond a critical velocity (essentially that given by Feynman), the Magnus force bowing the line away from the wall of the channel was greater than the self-induced velocity of the line tending to keep the line stationary, and the line grew virtually unimpeded, absorbing energy from the flow of the fluid. If two elements of the line approached each other, a vortex ring could be "pinched-off" leaving the original line to produce more vortex rings. The results of Weaver (1972) show some support for this theory.

These results all supported the notion that vortex lines were intimately involved in limiting superfluid flow, and

considerable effort has been devoted to determining an exact expression for energy required to create a vortex line and to determining the resultant critical velocity of flow (Fineman & Chase, 1963 ; Fetter, 1965a; Amit & Gross, 1966 ; Peshkov, 1966 ; Craig, 1966). Donnelly and Roberts have developed a theory using the Fokker-Plank diffusion equation to describe the growth of the smallest vortex rings to their critical size (Donnelly & Roberts, 1971). Using the stochastic formalism of Brownian motion theory, they obtained an expression similar to that of Iordanskii (1965) for the number of vortex rings in equilbrium in helium II. Their analysis suggested that the vortex-mill model of Glaberson and Donnelly should be temperature dependent (Donnelly & Roberts, 1971). They assumed that the energy for the growth of the vortex ring comes form the flow of the superfluid, and this has been criticized by Campbell (1972a) who showed that the only valid model for the creation of vortices is the fluctuation model.

First evidence supporting the thermal fluctuation ideas came from observing the decay of persistent currents in a torus packed with filter paper (Kukich et al, 1968b). Stronger evidence came from Notarys in 1969. He considered driven flow through porous mica, having pore sizes from 2×10^{-6} to 2×10^{-5} cm diameter. Langer-Fisher theory predicts that the velocity of the superfluid will be proportional to ρ_s/T at a constant pressure and that the inverse of the temperature will be proportional to the natural logarithm of pressure at a constant temperature (Langer & Reppy, 1970). Both these relationships were shown to hold, though the values of the attempt

frequency, f_o, was found to be lower by a factor of 10^7, and the activation evergy, E_a, lower by a factor of about 22, than the values predicted by Langer-Fisher theory. The value of the activation evergy was found to be in agreement with the earlier value of Kukich et al (1968). Notary's experiment is, however, the only experiment which has demonstrated a temperature independent frequency, f_o; a strong temperature dependence was observed by Cannon et al (1972). This temperature dependence has also been observed in pinhole flow and in film flow (see Chapter V).

Hess has measured the critical flow velocity through pinhole orifices (10μm diameter), observing two distinct types of flow (Hess, 1971 ; 1972 ; 1973). The first type he called "extrinsic" in that the flow depended on the geometry, was direction dependent, was not generally reproducible day to day and could best be described in terms of the Feynman or the Glaberson-Donnelly ideas (Hess, 1973). The second he called "intrinsic" in that the flow could be described in terms of the Iordanskii-Langer-Fisher model. He too found that the velocity observed was lower than that predicted, and measured the slope of a logarithmic plot of the velocity against $\rho/\rho_s T$ to be 0.8 instead of the expected 1.0. He suggested that the lower velocity might be the result of cracks of protrusions of near-atomic dimensions on the orifice surface. (He has developed this idea further, showing that in the vicinity of dust particles nucleation of vortices could occur at velocities lower than that required for intrinsic dissipation, and that such particles could effectively control the critical velocity [Hess, 1972a]).

Hess discovered that by placing superleaks on either side of the pinhole, extrinsic dissipation was inhibited. Hulin et al have also observed two distinct velocity regimes while monitoring flow rates through pinholes, the fast velocity varying as $(\ell^3/\rho T)^{\frac{1}{2}}$, and the slower proportional to the square root of the pressure head (Hulin et al, 1972). Banton has additionally observed a third regime where the flow is proportional to the pressure head and has seen switching between the modes of flow (Banton, 1974). To test the idea that a pinned vortex would act as a nucleating centre (vortex-mill), Laroche et al have placed a thin wire in front of an orifice and demonstrated that the velocity through the orifice was dependent on the direction of flow (Laroche et al, 1974).

An attempt to unify the Feynman expression for the critical velocity with that of Iordanskii-Langer-Fisher has been made by Weaver, who took into account the effect of the surface roughness of the channel walls (Weaver, 1973 ; 1974). He was able to obtain an expression for the critical velocity which fitted the available data, but the accuracy of fit was made possible by arbitrarily adjusting the value of the roughness parameter.

All the work in channel flow has suggested that the production of vortex lines by some means could explain the observed flow velocities. Though a great deal is not readily explicable, such as the instabilities in the flowrates, two theories have been able to predict most of the results. As will be discussed in the next chapter, the success of the Feynman-Glaberson-Donnelly and the Iordanskii-Langer-Fisher ideas has prompted theorists dealing with film flow to consider

the film as a channel with one free surface.

CHAPTER V

PROPERTIES OF THE SATURATED HELIUM II FILM

In 1922 Kammerlingh Onnes noticed that when the levels of helium II in concentric beakers were different they fairly quickly reached a common equilibrium level and thereafter continued to rise and fall together (Kammerlingh Onnes, 1922). He attributed this effect to an evaporation and distillation mechanism. In 1936 Rollin postulated that any solid surface in contact with liquid helium was covered by a thin film of liquid helium and in order to explain an apparent anomaly in a heat flow experiment, suggested that the thermal conductivity of the film changed dramatically below the λ-point (Rollin, 1936). In 1938 Daunt and Mendelssohn began a series of experiments on the properties of the helium film. They measured the rate at which an empty beaker, on being partly immersed in a bath of liquid helium II, filled with liquid, and noted that if the beaker was then removed from the bath, it emptied, droplets of liquid forming on the bottom of the beaker and dripping back into the bath (Daunt & Mendelssohn, 1938a). It was also observed that a wick leading from the bath to the beaker rim increased the rate of flow. Measurements of heat flow led them to the conclusion that a change in the thermal properties of the film could not explain their results, but that flow was occurring via the film i.e. that

the film was mobile (Daunt & Mendelssohn, 1938b). (Experiments by Rollin and Simon between 1936 and 1939 supported this conclusion [Rollin & Simon, 1939]).

These results were soon interpreted in terms of the Tisza-Landau two-fluid model (Tisza, 1938 ; 1947 ; Landau, 1941 , 1946). The film was considered as a very narrow channel through which only superfluid could flow (the normal fluid flow being inhibited by viscosity). This idea was vindicated by the observation in 1939 of a thermomechanical effect in the film (Daunt & Mendelssohn, 1939a; 1950) analogous to the fountain effect discovered by Allen and Jones (1938). Since then a large number of experiments have been studied, the principle areas of interest being the determination of the thickness of the film and a characterization of the parameters affecting the rate of flow. Though the situation has been clarified, expecially with regard to the thickness of the helium film, many inconsistencies still remain.

(i) Thickness of the Static Film

The thickness of the static helium film was first estimated by Kikoin and Laserew in 1938 by measuring the volume of liquid required to cover a formerly dry surface (Kikoin & Laserew, 1938 ; 1939), and over the following ten years by other workers using similar methods (see review article by Jackson and Grimes [1958]). It was not until 1949 that the thickness of the film was reliably measured (Jackson & Burge, 1949) using an optical technique

whereby the thickness of the film was directly related to the change in polarization of plane-polarized light reflected off a surface covered by the helium film. They found that the thickness of the film, d, varied with the height of the film above the free surface according to

$$d \simeq k h^{-1/n} ,$$

where $k \simeq 3 \times 10^{-6} \text{cm}^{(1+1/n)}$ and is slightly temperature dependent and where n ranged from 3 to 4. A similar height dependence was observed by Atkins (1950a).

Simple theory suggests that the thickness of the film depends on the van der Waals' force due to the substrate. Fehl and Dillinger (1974) have shown that the film thickness increases with the roughness and this has also been noted by van Spronsen et al who observed hysterisis changes in the thickness of the film on a glass substrate (van Spronsen et al, 1975).

The theory of the thickness of the film derives from a treatment in which the thickness is determined by a balance of the gravitational and the van der Waals' forces. The potential energy of an atom in the film can then be given by

$$u = mgh - \alpha z^{-3}$$

where m is the atomic mass, h the height above the bulk liquid surface, z is the distance from the substrate and α is a constant dependent on the strength of the van der Waals' forces (Frankel, 1940 ; Schift, 1941 ; Dzyaloshinskii et al, 1961 ; Sabisky & Anderson, 1970 ; 1973). To this

expression Atkins has added a correction term to take into account the zero-point energy of the atoms (Atkins, 1953 ; 1954) and McClintock has estimated the effect of a curved substrate on the thickness of the film (McClintock, 1973).

The usual way of expressing the static film thickness is to write

$$d = kh^{-1/n}$$

where k for glass has values ranging from 3.0 to 4.3 x 10^{-6} (cgs units) and n ranges from 3.0 to 3.5 (von Spronsen et al, 1975 ; Hallock & Flint, 1974b; Campbell et al, 1976).

(ii) Thickness of the Moving Helium II Film

In 1956, Kontorovich, using the Landau equations of motion (Landau, 1959), predicted that a moving helium II film would be thinner than a static film by an amount $\Delta\delta$ given by

$$\Delta\delta = \frac{\rho_s \delta_0 v_s^2}{2\eta\rho g z}$$

where δ_0 is the thickness of the static helium film a height z above the bulk level (Kontorovich, 1956). Seven years later, Gribbon and Jackson, using the technique of reflecting polarized light through the helium film, found general agreement with this prediction (Gribbon & Jackson, 1963). However, in 1970, Keller (1970) found that his measurements showed $\Delta\delta$ was zero to within a few Angstrom. This result prompted several theories to explain under what circumstances thinning of the moving film would be observed, as well as experiments in different geometries and in different

temperature ranges. The majority of these confirmed the ideas of Kontorovich (Dutch & Pollack, 1971 ; van Spronsen et al, 1972 ; 1973 ; 1974 ; Graham & Vittoratos, 1974 ; Williams & Packard, 1974 ; Flint & Hallock, 1975), though the experiment of Telschow et al, having taken into consideration any other effect that might influence film thickness , concluded that unless the superfluid density was dependent on the velocity, no thinning occurred in the moving film (Telschow et al, 1975).

To explain Keller's experiment, alternative mechanisms which would compensate for the decrease in thickness were suggested (Huggins, 1970 ; Putterman & Rudnick, 1971 ; Goodstein & Saffman, 1971 ; de Bruyn Ouboter, 1973). Goodstein and Saffman have pointed out that if the thinning predicted by Kontorovich occurred, then there would be supercooled vapour in the region vacated by the film (Goodstein & Saffman, 1971). From this, Ouboter has suggested that recondensation from the gas would occur and that therefore the only circumstances under which Bernoulli thinning would be observable, would be if the gas could be isolated from the fluid (de Bruyn Ouboter, 1973). Support for this seemed to come not only from Keller's experiment but also from an experiment showing film thinning at temperatures below 1 K, where the effect of the helium vapour is small (Williams & Packard, 1974). However, film thinning has since been observed under conditions which would favour recondensation (Graham & Vittoratos, 1974). Goodstein and Saffman have tried to explain these conflicting

results, by reformulating their original theories (Goodstein & Saffman, 1975). In that paper, they have overcome some of the objections raised against their assumptions (Bergman, 1973) and stated that consideration of the system's time constants was necessary. The two constants of importance were τ_2, a relaxation time describing how long it takes for the helium gas to be replenished if condensation occurs and τ_3, a characteristic time for the depletion of gas due to condensation. They suggested that if $\tau_2 \simeq \tau_3$, then no thinning would occur and that only when $\tau_2 \gg \tau_3$ would thinning be observable.

This theory is not entirely satisfactory (it has been estimated that recondensation is a statistically improbable event [Graham & Vittoratos, 1974]) and the most acceptable theory is still that of Kontorovich, even though there are experiments which it cannot explain (Keller, 1970 ; Telschow et al, 1975 [In 1979, an experiment found agreement with Kontorovich thinning, in contrast to Telschow et al (Ekholm, 1979a)]).

The Kontorovich expression for the thinning of a moving helium film was derived from a Bernoulli equation for the superfluid when there is a steady flow. Wang and Petrac have pointed out that acceleration of the superfluid should produce a film thickness change independent of the Bernoulli thinning, provided that the third-sound wavelength (Atkins & Rudnick, 1970) is much greater than the characteristic experimental cell dimension. They have also demonstrated that such a change in film thickness (within an accuracy of

12%) (Wang & Petrac, 1975).

(iii) The Flow Rate

The general characteristics of the flow rate were elucidated in a series of experiments by Daunt and Mendelssohn in 1939 (1938a,b; 1939a,b,c; 1947). They examined the rate of flow as a function of pressure head (level difference), as a function of the length of the flow path and as a function of the geometrical dimensions of the beaker from which flow was taking place. They found that the flow rate was temperature dependent, was almost independent of the level difference, that it was independent of the length of the flow path, that it was proportional to the narrowest perimeter above the upper liquid level, across which flow took place and that it was almost independent of the substrate.

Since the rate of transfer was approximately constant the concept of a critical velocity of the moving superfluid film, v_c, was developed, whereby the film accelerated up to this velocity, but was prevented from undergoing any further acceleration by some mechanism (the idea of a critical velocity has been considerably modified, as discussed in Chapter III, although the terminology has remained). Assuming that the density of the superfluid component is the same in a saturated helium II film as it is in the bulk liquid, then the rate of transport of mass per unit length of perimeter over which the film flows is $\rho_s v_c \delta$ gm cm^{-1} sec^{-1} where δ is the thickness of the film. The "critical" rate of transfer, in terms of the volume of bulk liquid transferred to or from the inside of a vessel, α_c , is defined by

$$\sigma_c = \frac{\rho_s}{\rho} v_c \delta \quad cm^2 sec^{-1} .$$

The critical rate of transfer followed the ρ_s/ρ dependence on temperature, at least for temperatures above about 1 K (Daunt & Mendelssohn, 1939b,c; 1947 ; Webber et al, 1949 ; Fairbank & Lane, 1949). The variation of the flow rate below 1 K is less certain; some experiments suggested there was an increase in rate by 10 - 30% (Mendelssohn & White, 1950 ; Ambler & Kurti, 1952 ; Lesensley & Boorse, 1952 ; Herbet et al, 1957), though Waring (1955) showed a flat region below 0.6K and Crum's results suggested a decrease below 0.4K (Crum et al, 1974).

The dependence of the flow rate on impurities on the surface and on the substrate material used, has also been investigated. Film flows over many materials from metal to solidified argon have been observed and for the most part, the values obtained are consistent with the changes in thickness of the saturated film due to the differences in the van der Waals' forces between the helium film and the substrate (Mendelssohn & White, 1950 ; Boorse & Dash, 1950 ; Dash & Boorse, 1951 ; van den Berg, 1951 ; Chandrasekhar, 1952 ; Smith & Boorse, 1953a,b; 1955a; Milbrodt & Pollack, 1963 ; Esel'son et al , 1972 ; 1973 [but see also Wagner, 1973 ; Harris-Lowe et al, 1974]). Impurities on the surface and the finish of the surface also influenced the transfer rate possibly by increasing the flow path-length, or by affecting the film thickness or by providing sites for the nucleation of vortices (see Chapter IV) (Boorse & Dash, 1950 ; Dash &

Boorse, 1950 ; Bowers & Mendelssohn, 1950 ; van der Berg, 1951 ; Chandrasekhar & Mendelssohn, 1952 ; Smith & Boorse, 1953a,b; 1955a,b).

The dependence of the rate of flow on the height of the beaker rim above the bulk liquid level was first investigated by Daunt and Mendelssohn in 1939 (1939b,c; 1947). They observed almost no variation in the flow rate. However, in 1950 Atkins noted that there was a slight dependence (Atkins, 1950) and the role of film height in determining the flow rate was examined in detail five years later (Smith & Boorse, 1955b). The rate has been determined for heights up to 0.36 m (Sedden et al, 1965), and has been fitted to various functional forms (Allen & Armitage, 1966 ; Duthler & Pollack, 1970 ; 1971). More recently, it has been realized that the thickness of the film on a particular substrate was the governing factor in determining the flow rate as measured from the changes in level difference or from other driving forces, and the only satisfactory way of describing the flow rate is to integrate the film thickness along the whole flow path (see, for example, Campbell [1975]). Other factors have an influence on the rate of flow: vibration should be avoided (Allen, 1960 ; Seldon & Dillinger, 1965) and it has been shown that an electric field across the flow path will reduce the flow rate (Esel'son et al, 1974).

One difficulty with flow rate measurements is their non-reproducibility of the rates from day to day. Results have differed from experiment to experiment even when elaborate precautions have been taken to ensure a clean

experimental evniroment (Seki, 1962). The flow rate, as measured by pressure head techniques, seemed to depend on the past history of the beaker and on the method used to fill the beaker. Allen et al postulated the existence of two types of film, a "normal" film formed by superfluid flow over a formerly dry surface and a "thick" film giving rise to enhanced flow rates, formed by drainage after immersing the beaker (Selden & Dillinger, 1965 ; Allen & Matheson, 1965 ; Allen et al, 1965). More puzzling was the instability of the flow rates and a fine-structure preference for certaine values of the transfer rate (Selden et al, 1965). Harris-Lowe et al have detected transitions as small as 1.5% of the flow rate (Harris-Lowe et al, 1966 ; Turkington & Edwards, 1967 ; Harris-Lowe & Turkington, 1971 ; Turkington & Harris-Lowe, 1973). Such jumps have also been observed by Allen & Armitage (1966) and by Crum et al (1974), who both noted that transitions were predominantly to a lower rate of flow. These observations, which have also been noted in flow through orifices (Chapter IV), have no theoretical basis at present.

(iv) Oscillations of the Helium Film

If, in an experiment, two baths of liquid helium of differing chemical potentials are connected by a mobile helium film, liquid will move, via the film, towards a state of zero chemical potential difference. Because of the momentum of the flow, the liquid will overshoot, and oscillate about the equilibrium position. These oscillations were first observed by Allen and Misener in connection with

with flow through narrow channels, and was utilized by them in estimating the cross-sectional area of the channels (Allen & Misener, 1939). In 1950, Atkins used the oscillations to calculate the thickness of the helium film (Atkins, 1950a,b). Atkins derived an expression for the period of oscillation by equating the kinetic energy of the moving film to the potential energy liquid. In deriving the equation he stated the following assumptions:

- that the film density was the same as that of the bulk liquid;
- that only the superfluid component participated in the flow;
- that the film profile was constant;
- that the temperature throughout the system was constant;
- that viscous effects could be ignored;
- that the velocity of the film at a fixed weight and time was constant across the film thickness;
- that the hydrodynamics were those of an ideal fluid i.e. followed Euler's equation for an irrotational fluid:

$$\frac{\partial \underline{v}}{\partial t} + (\underline{v}.\nabla)\underline{v} = -\frac{1}{\rho}\nabla P \quad .$$

Under the above assumptions, he obtained the following expression for the period of oscillation:

$$\tau = 2\pi \left[\frac{\rho}{\rho_s} \frac{r}{g} \int_0^{\ell} \frac{dh}{\delta(h)} \right]^{1/2} \quad ,$$

where ℓ was the height of the rim of a beaker (of radius r) above the bath level and $\delta(h)$ was the film thickness. From his results, he concluded that the frequency was dependent

on temperature gradients across the beaker.

In 1951, Robinson presented a theoretical account of the oscillations, considering, in particular, the case of two containers, which were not in isothermal contact, linked by superfluid helium (Robinson, 1951). He showed that adiabatic oscillations could exit, and that these were of a higher frequency than isothermal oscillations. He also pointed out an aperiodic region where the containers were neither under approximately isothermal or approximately adiabatic conditions, and showed that both the changes in the oscillation frequency and the damping of the oscillations, were due to deviations from isothermal or adiabatic conditions.

Picus, in his experiments on film flow, was able to use Robinson's equations to show that the damping of the observed oscillations was due to a temperature difference of the order of 10^{-7}K between his beaker and the helium bath. (Picus, 1954). He also noted that the period of the initial oscillations was longer than that of the final oscillations and attributed this to a difference between the stationary and the moving film (Campbell [1976] pointed out that the frequency shift could also have been due to parallel-path flow).

Experimental evidence of adiabatic oscillations was not reported until two years later. Manchester and Brown found that the general behaviour of the oscillations agreed with Robinson's predictions and found that the temperature dependence of the frequency of the oscillations closely followed the theory. They had difficulty in

measuring the damping of the osicllations and could not obtain agreement with the damping expected from thermal linkage between the bath and the beaker (Manchester, 1955 ; Manchester & Brown, 1957).

In 1972, Allen et al (1972) and Hoffer et al (1972) reported on observations of inertial oscillations; both the frequency and temperature dependence of the decay of the oscillations followed Robinson's theory. In 1973, Hallock and Flint measured the small temperature oscillations that accompanied level oscillations. These were found to be in accord with the expected results, both in amplitude and in phase (Hallock & Flint, 1973b; 1974b). Van Spronsen et al found that although the damping of their oscillations could be explained by thermal conduction between their glass spiral and the helium bath, they could not preclude the existence of an additional damping mechanism at velocities near to the critical velocity (van Spronsen et al, 1974). Campbell et al have shown that the shape of the oscillations was distorted from the pure sinusoidal form predicted by Robinson because of changes in the thickness of the moving film (Campbell et al, 1976).

Campbell has derived equations for film flow between two reservoirs when more than one flow path was available. If the paths were of unequal length then circulating currents could be induced around the paths which would persist throughout the thermally damped oscillations. This would change the oscillation frequency and affect the film thickness as the persistent current enhanced or diminished

the changing flow arising from the level oscillations. He also suggested that parallel-path flow would be characterized by an anomalously large first half-cycle amplitude if one path length was much larger than another and that the decay of the earlier oscillations would decrease by a constant amount every half-cycle rather than by the constant percentage amount expected of a damped harmonic oscillator. Using these theories, Campbell was able to explain the frequency shifts and damping maxima observed by Hammel et al (1970) and was able to show that the sensitivity of film thickness to the direction of flow noted by Williams and Packard (1974) was the result of parallel-path film flow induced by an unsuspected leak (Campbell, 1975) (Hallock [1975] came independently to the same conclusion). Experimental confirmation of Campbell's theories was reported by Galkiewicz and Hallock who obtained quantitative agreement with the predicted behaviour of film flow in two parallel paths (Galkiewicz & Hallock, 1976). In 1977, Brooks and Hallock reported the observation of two distinct stable rates of decay, consistent with parallel-path flow (Brooks & Hallock, 1977). In their experiments, which were below 1 K, they could find no evidence for obvious parallel flow paths and concluded that the effective multiply-connected flow paths must have resulted from the helium film motion, possibly by trapped vorticity.

(v) Dissipation

The thermal damping characterized by the Robinson equations can be said to represent an extrinsic dissipation

as it is a function of the thermal and geometrical properties of the experimental system. Intrinsic dissipation of the type discussed in Chapters II and IV should manifest itself as a difference from the Robinson damping or should be deducable from non-oscillatory flim flow. In 1961, Allen suggested that if the motion of the film was brought about by an array of vortex lines, then scattering of the rotons by the vortex lines would give rise to a damping of oscillations, and that the logarithmic decrement would be proportional to $\exp(-\Delta/k_B T)$ where Δ was the roton gap energy (Allen, 1961). Though agreement with this was found (Glick & Werntz, 1969), Hallock and Flint have pointed out that the observed agreement can be understood from geometrical considerations (i.e. Robinson damping) and that Allen's prediction need not be utilized. Calvani et al, extending Feynman's suggestion (1954) of polarized excitations, proposed that the energy required to orient their momenta in the opposite direction to that of the local superfluid velocity in an accelerated superfluid would cause damping of the oscillations and that the damping coefficient, α, could be found from

$$\alpha = \frac{\omega}{2\pi} \ln\left(\ell/\ell_s\right) \quad ,$$

where ω is the observed frequency (Calvani et al, 1973). No support for this was found by Hallock and Flint (1974a,b).

The theory developed by Langer and Reppy that the flow was limited by the nucleation of vortices, suggested that $dv/dt \propto a_f \cdot \omega \cdot \kappa \cdot \exp(-E_a/k_B T)$. This form was modified to $dv/dt \propto a_f \cdot \omega \cdot \kappa \cdot v^c$ for film flow in which the medium

for dissipation was assumed to be antiparallel vortex lines perpendicular to the film, rather than the vortex rings considered in the original argument (Langer & Reppy, 1970). Agreement with the former dissipative form for film flow was first found by Liebenberg (1971a,b). Cannon et al, too, found general agreement, though, like Liebenberg, the magnitudes of and E differed considerably from the predicted values. Cannon et al expressed the superfluid equation by

$$\frac{\partial v}{\partial t} + \nabla\mu = -a_f \omega H e^{-v_b/v}$$

and were the first to observe a temperature dependence of the attempt frequency, ω (Cannon et al, 1972). Similar results have been found by other workers (Allen et al, 1972 ; Hoffer et al, 1972 ; Campbell et al, 1976). Campbell et al have compared four forms of the dissipative function (the two mentioned above, a form suggested by Donnelly and Roberts (1971) and a Taylor expansion of a functional exponent about a velocity v_o) and, while finding reasonable fit of all four functions to their data, concluded that the most accurate form of dissipative function was

$$\frac{dv}{dt} \propto -\omega(T)\, e^{-v_b(T)/v} .$$

The earliest support for the original work of Langer and Fisher (1967) came from the observations on the decay of persistent currents in narrow channels (Kukich et al, 1968 ; Notarys, 1969). Though not all workers were able to observe persistent current flow in helium films (see for

example, Wagner [1973]), many workers have reported on their existence (Verbeck et al, 1974 ; Galkiewicz & Hallock, 1974 ; van Spronsen, 1974). Only Ekholm and Hallock have discussed the decay of the persistent currents (1979). Their data revealed substantial deviations from the predicted decay rule.

In 1977, Harris-Lowe presented a theory on the dissipation in superfluid film flow, based on the successful application of Vinen's theories on growth and decay of vortex lines in narrow channels (Vinen, 1957a,b). His arguments for a new model were that the Iordanskii-Langer-Fisher theories were intended to apply at temperatures near to the λ -point, and that the attempts to extend them to include all temperatures, had not met with the same success. He built up a theory in a similar way to Vinen, and predicted that at velocities in excess of some critical velocity, v_c, the rate of dissipation would be given by

$$\dot{Q} = AN (v - v_c)^{3/2}$$

where A is a constant and N is the number of pinned vortex lines (Harris-Lowe, 1977). Experimental support for this theory was reported by Turkington and Harris-Lowe in an experiment where a heater produced a temperature difference between the beaker and the bath (Turkington & Harris-Lowe, 1977). The equation above was expressed in terms of the heater power and the measured exponent was 1.49 ± 0.02. However, no evidence of the $3/2$ power law was found by Armitage et al (1978), although they found that their

results below 1 K could not be explained by the Iordanskii-Langer-Fisher theories if the level difference was less than 50 μm and that below 20 mK, the dissipation had a term proportional to the superfluid velocity.

CHAPTER VI

THE APPARATUS

The experimental apparatus consisted of an inverted glass 'U'-tube whose ends terminated in cylindrical capacitors, serving both as liquid helium reservoirs and as the means of measuring the liquid helium level. This beaker was mounted at the base of a cryostat. The various parts of the apparatus will be separately described.

The Cryostat Frame (Figure VI.1)

The frame had been designed to be, as far as possible, vibration-free. It had been bolted on to a concrete pit, itself isolated from the building by resting on springs. The frame was cross-braced to minimize torsional vibration and supported a heavy steel plate on damped springs. Two brass collars to hold glass liquid helium dewars were bolted on to opposite ends of this steel plate, and flexible hoses, two inches in diameter, looped away from the collars to the valves and the main pumping line. The hose was spring-supported from the ceiling. While an experiment was in progress, a counter-weight to compensate for the weight of a helium dewar and cryostat, was placed on the end opposite the experimental dewar to ensure a highly damped system with a period of about two seconds.

The glass liquid nitrogen dewar, which enveloped the helium dewar was supported from the collar of a copper

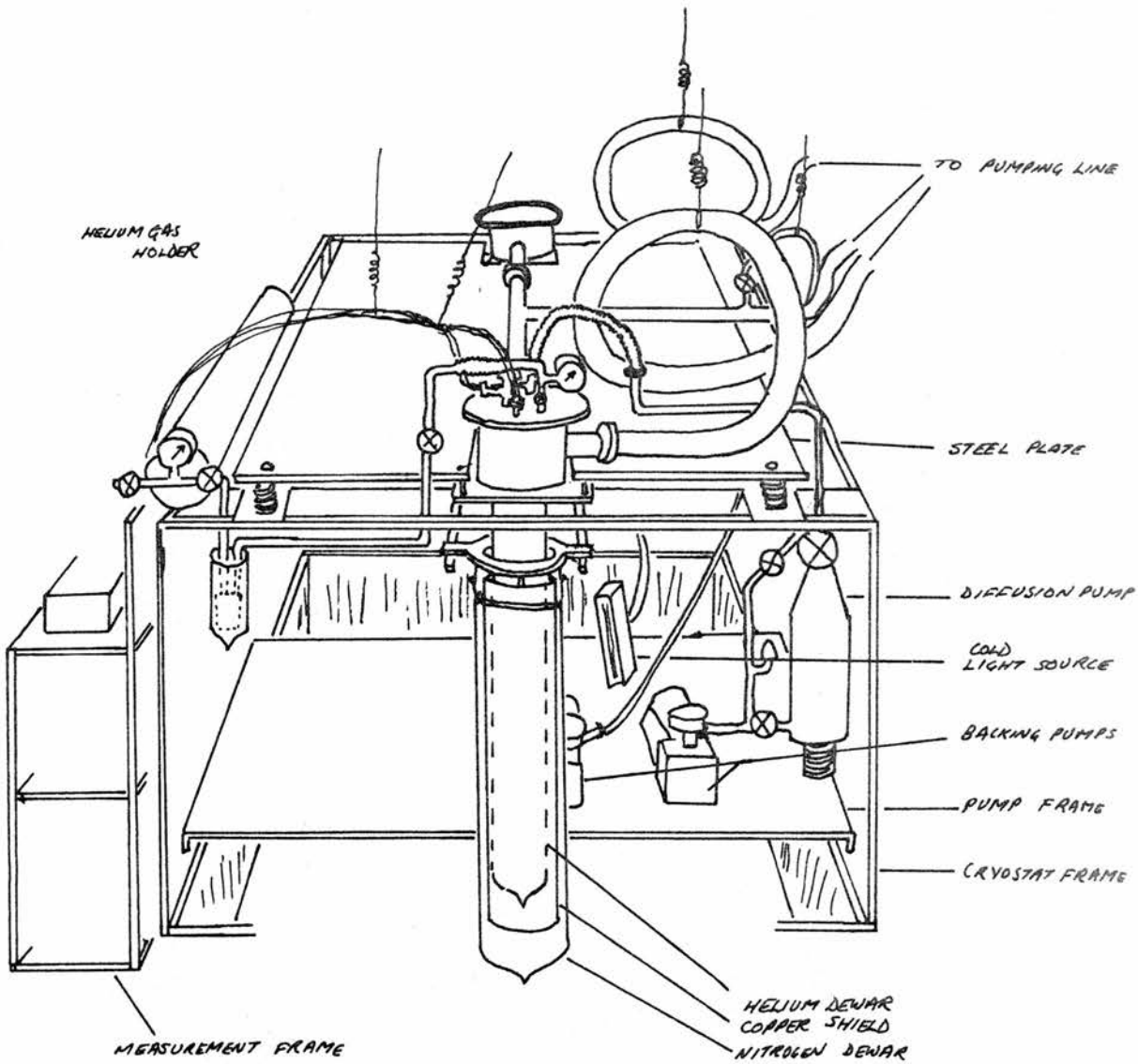

FIGURE VI.1 THE CRYOSTAT FRAME

cylinder which rested on protrusions from the cryostat frame, in such a way that it was not in contact with either the steel plate or the helium dewar. This copper cylinder acted as an efficient liquid nitrogen temperature shield when its lower end was immersed in liquid nitrogen. Because the level of liquid nitrogen could then be kept below the tit of the helium dewar, the vibration from liquid nitrogen boiling against the side of the helium dewar was eliminated.

Both dewars were silvered, and both had narrow slits about two centimetres wide running axially along the length of the dewars to allow visual observation of the helium level. During the course of an experiment, the nitrogen dewar was rotated so that the observation slits in the helium dewar were obscured, ensuring that no room temperature radiation shone into the helium dewar.

All the subsidiary apparatus, such as the measuring equipment and the vacuum pumps was housed on a separate frame.

The Cryostat

The cryostat itself was used to support rigidly the experimental glass beaker and to provide a means of leading the electrical leads to the capacitors. It was initially designed with two needle valves, one to seal a glass chamber in which the beaker was mounted, and the other to seal the experimental beaker.

The cryostat consisted of two brass flanges connected by a pair of thin walled stainless-steel tubes one metre long. One tube was joined to the lower flange via a copper tube bent

into a semi-circle to act as a radiation trap. Through this tube, all the electrical leads connected to the experimental beaker and leads for a carbon resistance thermometer and a wire-wound heater which rested in the glass chamber, were taken. The other tube, through which the remaining electrical leads to the thermometer and heater in the helium dewar were taken, was in two sections, the one offset from the other to reduce the heat leak into the lower chamber due to room temperature radiation. To restrict further this radiation, several circular stainless steel baffle plates were situated along the length of the cryostat above the lower flange. Rigidity was enhanced by the thin walled stainless steel tubing originally used to guide the push-rods of the needle valves.

To minimize the radiation entering the lower chamber a copper can, with heat absorbent Chance galss covering the two narrow observation slits, enclosed the glass chamber.

Two meters of 0.5 mm cupro-nickel tubing were coiled down the cryostat, passing through the lower flange and into the glass chamber. Through this, helium gas was condensed into the experimental beaker. About 75 cm of the tubing was coiled just above and below the lower flange. Narrow gauge copper wire was closely wound round the lowest few turns of the tubing above the lower flange and anchored several times to the copper radiation trap. The next two highest turns of the tubing were wrapped about with narrow strips of thin copper sheet and similarly anchored (Figure VI.2).

The leads to the capacitors were Lakeshore Cryogenic

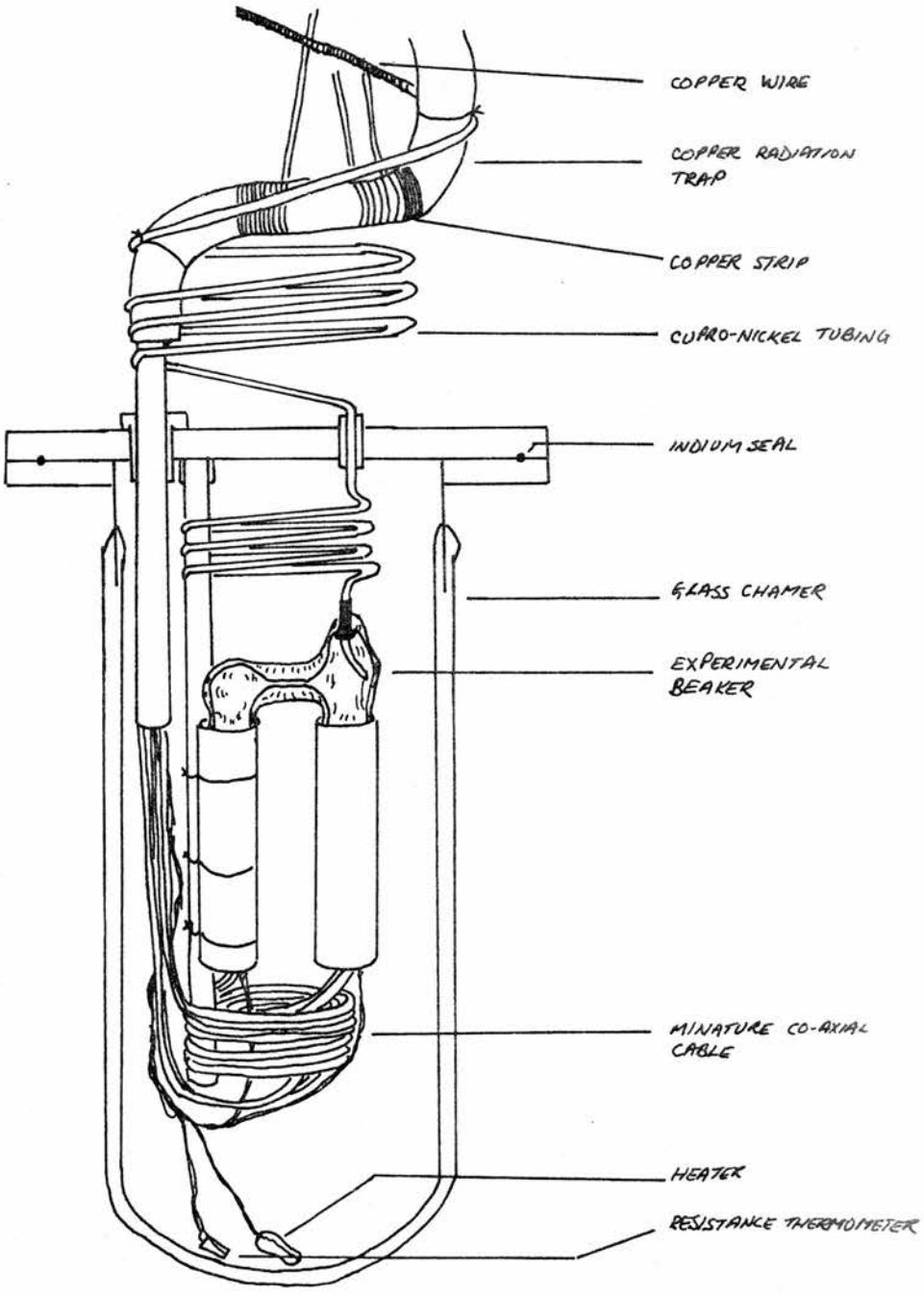

FIGURE VI.2 THE GLASS CHAMBER

minature co-axial cables, coiled at the base of the glass chamber before being attached to the capacitors. The upper ends of the leads terminated in co-axial mountings on an insulating perspex plate, so that the screens of the cables could be separately earthed. The leads to all the carbon resistance thermometers and the wire-wound heaters were of narrow gauge silk-coated manganim wire.

The Experimental Beaker

The beaker consisted of a horizontal glass capillary linking two side arms whose bases were the two reservoirs (capacitors) discussed below. A capillary was used so as to be able to have a well-defined area in the flow path from one reservoir to the other across which the dissipation would be dominant over dissipation occurring across any other area of the flow path. Being horizontal, it was independent of the direction of liquid helium film flow.

The experimental beaker was constructed from Kovar glass. The side arms incorporated Kodial metal seals onto which the reservoirs were soldered using Woods' metal. One of the side arms had a second Kodial metal seal at the top end to receive the cupro-nickel tubing down which the condensed helium gas flowed. The end of the tubing was directed at the glass wall so that the liquid helium would flow down the side-arm walls and not fall as droplets onto the reservoir. The capillary too was made from Kovar glass. It was drawn down from a larger tube and when measured, found to have a uniform elliptical cross-section over its length. The major

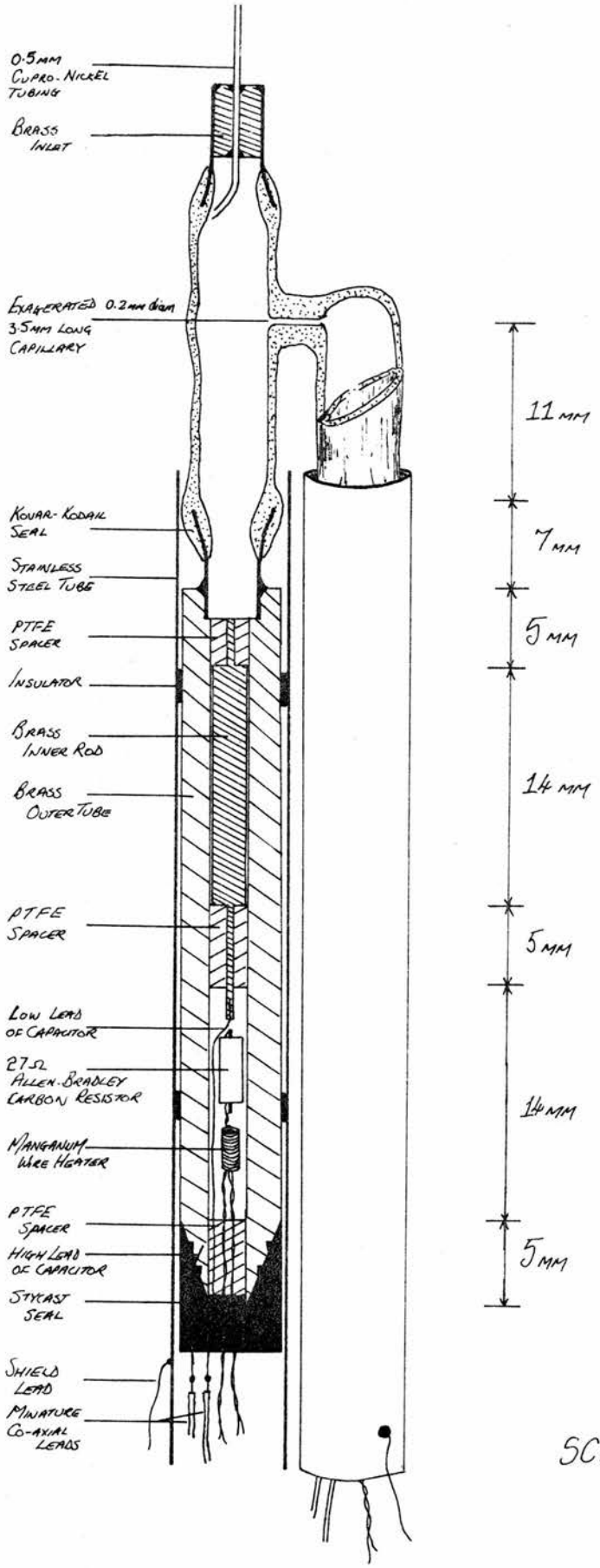

SCALE: Approximately
2 1/2 life size

FIGURE VI.3 THE EXPERIMENTAL BEAKER

and minor diameters were 0.266 and 0.193 (±0.005) mm respectively. In the calculations and description of the equations of motion for the beaker (ChapterVII), a diameter of 0.232 mm is used which gives the same perimeter as the elliptic section. After the beaker was constructed, the whole assembly was left in a furnace to ensure that the glass was fully annealed. A sketch of the beaker together with its dimensions is given in Figure VI.3.

The Capacitors

Two nearly identical capacitors were built to form the reservoirs of the experimental beaker. Because the narrow annular areas of the two capacitors were the same, capillarity effects in one arm of the beaker were balanced by those in the other.

The capacitors were machined from brass rod. The completed capacitor consisted of a short rod positioned by spacers inside the top of a longer tube. In the cavity below the rod there was space for a carbon resistance thermometer and a wire-wound heater.

(i) Inner Rod The inner rod was turned from a 5 mm diameter brass rod, to several microns oversize. A 2 mm long protrusion and a 5 mm long protrusion were turned down at the top and bottom of the rod respectively, around which the spacers were to be fixed. A hole was drilled in the centre of the lower protrusion into which a length of manganin wire was soldered as the electrical connection. To obtain a smooth and uniform surface the rod was ground down using a paste made from jewellers' rouge. This procedure resulted

in an inner rod with a central section 14 mm long which was uniform to within 2 μm (as measured on a micrometer) and free of visible blemishes.

(ii) Outer Tube The outer tube was made from the same brass rod as the inner rod. The tube was first cut to a length of 43 mm, and a 2 mm deep, 1/8" diameter hole was milled into the top. The lower end was tapered over the last 5 mm down to 1/8" diameter, and a groove incised in the middle of this taper. (This taper and groove was to ensure a good seal between the brass and the Stycast which was used to cover the base).

A hole was drilled down the centre of the rod with an unused 1.5 mm drill bit. The hole was then reamed using an unused 1/16" diameter reamer. Finally, the hole was slightly widened and very effectively polished by forcing 3/32" diameter hardened-steel ball-bearings down the barrel using a drill press and lubricating the ball-bearings with light machine oil. The result was an extremely smooth surface (even under a microscope neither scratches nor ridges could be discerned) and a circular hole. A manganin wire was soldered to the tapered region, just below the groove, providing the other electrical connection to the capacitor.

(iii) Assembly Circular spacers were fashioned from teflon rod and were machined to be a very tight fit both onto the protrusions on the inner rod and into the outer tube. The spacers were trimmed to an almost rectangular shape in cross-section to allow the flow path along the spacer to be large relative to the flow path in the annular

gap of the capacitor. The inner rod was forced up the tube until the surface of the top spacer was flush with the surface milled out to receive the Kodial of the glass-metal seal.

Into the cavity below the rod, a 27Ω Allen-Bradley carbon thermometer was inserted. Also, in one of the capacitors, a small manganin wire-wound heater was inserted. A teflon plug with holes drilled through for the electrical leads was fitted into the base of the tube. In the second capacitor a 0.5 mm diameter cupro-nickel tube protruded just through this plug. (This was originally connected to a needle valve but after the needle valve proved unreliable, this tube was sealed with solder). The capacitors were then placed in a mould, and the ends sealed over using Stycast.

The capacitors were leak-checked at room and liquid nitrogen temperatures using a helium mass spectrometer, and re-checked after then had been soldered using Woods' metal, onto the experimental beaker. The brass tube was then insulated with PTFE tape and stainless-steel cylinders were placed about the capacitors, extending about one centimetre above the end of the glass- metal seal and about an equal distance below the Stycast. These cylinders, which provided the screens about the capacitors, were earthed to the cryostat.

The Gas Handling System

Pure helium gas was stored under pressure in a gas cylinder (about 7.4 litres in volume) strapped to the framework supporting the electrical measuring system. The

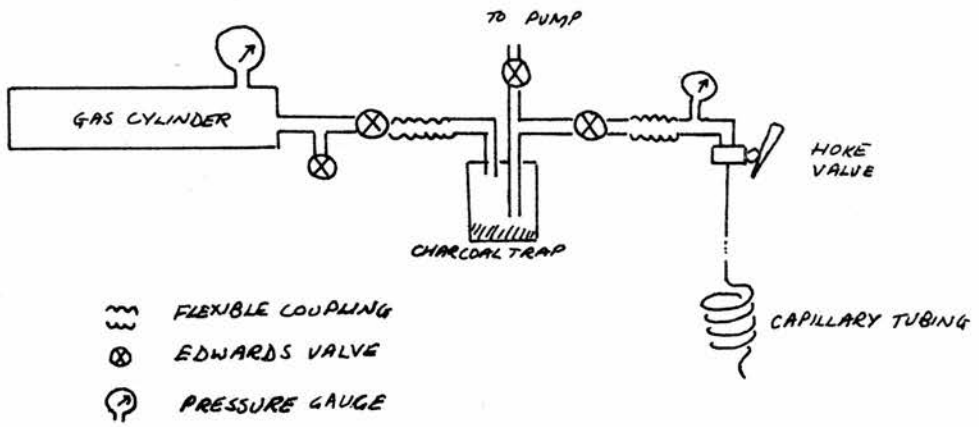

FIGURE VI.4 SCHEMATIC GAS HANDLING SYSTEM

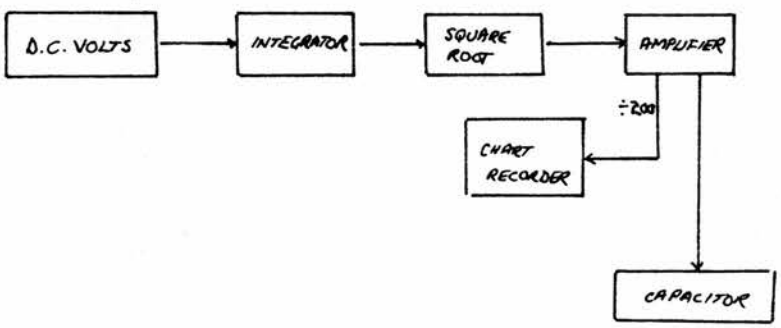

FIGURE VI.5 BLOCK DIAGRAM OF ELECTRICAL SYSTEM

gas was taken from the cylinder to the top flange of the cryostat via $\frac{1}{4}$" copper tubing, and to maintain vibration isolation flexible bellows connections were used to link the tubing whenever it passed from one framework to another. Immediately after the gas cylinder, a liquid nitrogen charcoal trap was placed in the line. An outlet to the vacuum pump was also fixed to the charcoal trap to enable the tubing and the experimental beaker to be evacuated. A pressure meter was fitted to the line just before the Hoke valve into which the cupro-nickel tubing leading down to the experimental beaker was soldered. This is schematically illustrated in Figure VI.4.

Once assembled, the gas handling system and experimental beaker were flushed through with helium gas and evacuated using an oil diffusion pump several times. Additionally, before each experiment, the system was again purged at liquid nitrogen temperatures. Between experiments the system was left under vacuum.

When an experiment had been prepared, the charcoal trap was pressurised using the gas cylinder which was then sealed off from the rest of the gas handling system. The Hoke valve to the capillary tubing was opened and helium gas was slowly allowed into the tubing until the gauge at the head of the tubing read atmospheric pressure. All valves were then sealed, and liquid helium was transferred into the helium dewar. Once a bath temperature of about 1.2K had been reached, the tubing between the charcoal trap and the Hoke valve was brought up to atmospheric pressure. The trap was

then sealed and the Hoke valve opened until the gauge read ten inches mercury. The valve to the capillary was closed and the gas allowed to condense down the capillary tubing These last two stages were repeated. This allowed the experimental beaker to be filled in a controllable manner without flooding both reservoirs with liquid helium.

Measuring Equipment

The capacitance of the two capacitors was measured using two ASL 1055 Manual Displacement Bridges. The standard capacitors used for both bridges were General Radio 10 pF standard capacitors. These were placed in a polystyrene lined box to minimize drift due to temperature variation in the laboratory. The capacitance bridge had an accuracy greater than 1% full-scale deflection. With a capacitance of 1 pF and a cable capacitance of 100 pF, using a band-width of 0.3 Hz, a change of 10^{-6}pF could have been detected. The temperature drift was zero in the balance position and 0.1% per degree celcius in the off-balance position.

The off-balance signals from the bridges were recorded on a two-pen Servoscribe chart recorder.

When driven flow was being examined, the following electrical system was used (a block diagram is shown in Figure VI.5):

A labpak supplied a d.c. voltage from 0.2 volts to 10 volts as the input of an integrating circuit which had two possible time constants (given by RC = 33 and RC = 4.7 seconds). The output from this integrator was thus a

voltage increasing from zero volts to a maximum of 10 volts. The linearity of the output was checked over the time range using the chart recorder. The voltage could be linearly decreased by reversing the polarity of the labpak. There was an upward drift on the integrator at zero volts input. This rate was less than when any of the ranges were used, and did not affect the output if a definite voltage was applied to the input of the integrator.

The output from the integrating circuit served as the input to a square-root circuit constructed using a Texas Instrument Decoder chip. The output was equal to the square root to ten times the input voltage, provided the input was negative with respect to earth. The accuracy was checked by feeding in voltages and measuring the output using a digital voltmeter. The graph of $\ln(V_{output})$ against $\ln(V_{input})$ yielded the equation

$$\ln(V_{output}) = 1.1424 + 0.5030 \ln(V_{input}) ,$$

as compared with the theoretical

$$\ln(V_{output}) = 1.1513 + 0.500 \ln(V_{input}) .$$

The correlation coefficient of the experimental straight line plot was 0.999996, suggesting a small bias voltage but an accurate square root function.

The output from the square root function was fed into a Lansing High Voltage D C Amplifier (Model 80.310) and from this, the voltage was applied across the capacitor. The maximum voltage applied was 140 volts; the voltage

necessary for dielectric breakdown was about 150 volts. The Lansing amplifier also had a terminal whose output was a two-hundredth of the output to the capacitors. This was used to monitor the voltage on the Servoscribe recorder.

Precautions were taken to ensure the absence of ground loops in the electronics, and the leads to the capacitors were very carefully shielded to prevent any cross-talk, particularly between the two capacitance bridges.

CHAPTER VII

ANALYSIS AND DISCUSSION OF THE EXPERIMENTAL RESULTS

(i) Equation Of Motion

The basic equation governing the flow of the superfluid is given by

$$\frac{\partial v}{\partial t} + \nabla \mu = - D(v)$$

where v is the superfluid velocity, μ is the chemical potential and D is some dissipative function dependent on the superfluid velocity. The chemical potential is found from

$$\mu = \mu_0(P,T) + \frac{1}{2}\frac{\rho_s}{\rho} v^2 + gh - \frac{\alpha}{\delta^n}$$

where μ_0 is the chemical potential for bulk liquid and α/δ^n is the van der Waals energy for a film of thickness δ.

Consider the experimental beaker (Figure VI.1) and integrate the equation of motion along a streamline from one arm (reservoir) to the second. Then

$$\frac{\partial}{\partial t}\int_1^2 v\,dl - s\Delta T + \frac{1}{\rho}\Delta P + gz = -\int_1^2 D(v)\,dl$$

where ΔT and ΔP are the difference in temperature and pressure between the two reservoirs and z is the level difference between them. If at any time the flow rate along the flow path is constant i.e. $a_f v$ = constant, then the flow rate is defined at any point along the flow path by

$$a_f v = a_f(l) v(l) \quad ,$$

where $a_f(\ell)$ is the cross-sectional area of the film. Experimentally, it is the change in the levels of the reservoirs which is measured; writing

$$a_f(\ell)v(\ell) = \frac{\rho}{\rho_s} A_1 \frac{\partial}{\partial t}(h_1) = -\frac{\rho}{\rho_s} A_2 \frac{\partial}{\partial t}(h_2)$$

allows v in the equations above to be replaced by the rate of change of level difference z:

$$\frac{\rho A}{\rho_s} \frac{d^2 z}{dt^2} \int_1^2 \frac{d\ell}{a_f(\ell)} - s\Delta T + \frac{1}{\rho}\Delta P + gz = -\int_1^2 D(v)\,d\ell$$

where A is the reduced area of the two reservoirs ($A^{-1} = A_1^{-1} + A_2^{-1}$). If the dissipation is dominated by its occurrence over a length l where v is at its largest value (for example, along a constriction where a_f is smaller than elsewhere along the flow path) the above equation can be written as

$$\frac{\rho A}{\rho_s} I \frac{d^2 z}{dt^2} - \left(s - \frac{1}{\rho}\frac{dP}{dT}\right)\Delta T + gz = -D(v)\ell \qquad (1)$$

where $\int_1^2 \frac{d\ell}{a_f(\ell)}$ has been replaced by I and the assumption that $\Delta P = \frac{dP}{dT}\Delta T$ has been made.

A further relationship between the temperature difference and the level difference can be found by considering conservation of entropy. Since the superfluid carries no entropy, the change in the total entropy of each reservoir must equal the heat flow $\dot{Q}/T$ where $T \simeq T_1 \simeq T_2$, that is,

$$\frac{d}{dt}(\rho s V_1) = -\kappa \Delta T/T$$

and

$$\frac{d}{dt}(\rho s V_2) = \kappa \Delta T/T \quad .$$

As s is a function of T, the derivative $\frac{ds}{dt} = \frac{ds}{dT} \cdot \frac{dT}{dt} = \frac{c}{T} \frac{dT}{dt}$, where c is the specific heat. This yields the equation

$$\frac{d}{dt} \Delta T + \frac{\kappa}{\rho c V} \Delta T + \frac{sAT}{cV} \frac{dz}{dt} = 0 \qquad \text{—— (2)}$$

where V is the reduced volume ($V^{-1} = V_1^{-1} + V_2^{-1}$) and κ is the effective thermal conductivity such that $\dot{Q} = \pm \kappa \Delta T$. This equation allows the removal of the ΔT term in equation (1), resulting in a third order equation in z.

The integral I contains the cross-sectional area of the film a_f, which is the product of the film thickness and the perimeter at all points along the flow path. The perimeter is fixed by the geometry of the experimental apparatus; the film thickness is a function both of the height of any point above the bulk liquid level and of the superfluid velocity (Kontorovich, 1956):

$$\delta = k \left(\frac{1}{2} \frac{\rho_s}{\rho} \frac{v^2}{g} + h \right)^{-1/n} .$$

The change in film thickness due to a change in velocity Δv is given by

$$\frac{\Delta \delta}{\delta} = - \frac{\rho_s v}{\rho g n \left(\frac{1}{2} \frac{\rho_s v^2}{\rho g} + h \right)} \Delta v .$$

During most of these experiments, h was of the order of 3 cm and v $\sim$ 25 cm s^{-1}, so that with a van der Waals' exponent of n = 3, $\Delta\delta/\delta \simeq 2.5 \times 10^{-3} \times \Delta v$ at low temperatures. Thus, when calculating the film thickness during dynamic equilibrium conditions, the mean value of v only was used, as even relatively large changes in v will not significantly alter the value of the film thickness.

(ii) Data Collection

In order to introduce bulk liquid into the experimental beaker, helium gas was condensed into one of the arms of the beaker and the liquid was transferred to the other arm via flow through the helium film. The levels in the two arms were monitored using two capacitance bridges and the output from the bridges recorded on a two-channel chart recorder. As the "empty" reservoir filled up, there was a slow and fairly irregular response on the chart recorder, until the dead volume had filled up and the bulk liquid had reached the narrow annular region where the area of the reservoir was uniform and well defined. Measurements were not taken until then. By that time, however, the bath temperature was stable and well regulated. As the levels decayed towards equilibrium, it was necessary to continually adjust the null of the capacitance bridges. These adjustments were used to calibrate the sensitivity of the traces (in terms of chart deflection per capacitance change) and additionally, once equilibrium had been reached, the balance point on the bridge was adjusted on either side of the null position to confirm the sensitivity measurement. Because thermal cycling produced small changes in the valves of the capacitors in the two arms, and because it was not possible to meter accurately the volume of gas condensed into the experimental beaker, the equilibrium position of the bulk liquid in the reservoirs was different from day to day and can only be deduced from the observed period of the potential oscillations and from the position on the chart recorder traces when the "empty"

capacitor first showed a large response to changes in the bulk liquid level.

The initial flow to equilibrium was initiated by the level difference between the "full" and "empty" reservoirs. Flow was also initiated by applying a d.c. voltage across one of the capacitors while monitoring the response on the other capacitor. Applying an electric field across the helium forming the dielectric of the capacitor, changes its chemical potential. This change is most conveniently expressed as an equivalent change in level in the reservoir, h_v, given by

$$h_v = \frac{\pi \epsilon_0 (\epsilon_r - 1) V^2}{\rho g A_2 \ln(b/a)} \quad ,$$

where V is the applied voltage, A_2 is the cross-sectional area of the capacitor, and b and a are the outer and inner radii of the concentric capacitor. If a voltage V is applied across the one capacitor, then the change in chemical potential (characterized by h_v) will draw helium from the other reservoir until the chemical potentials again balance; if the change in that reservoir is h_f, then $h_f = \frac{1}{2} h_v$. This was used to confirm that the two capacitors were nearly identical: the change in capacitance (level of liquid) was monitored for a given voltage across the other capacitor; the results showed that the areas are the same to 1% (of the order of the error in the measured values).

Experimental data was taken from the chart recorder traces. The slopes of the lines were measured to yield the flow rate σ , and the times at which changes in the slope first occurred. Thus most of the data consisted of a series

of times between which flow rates (measured as pF sec^{-1}) were constant. As it was not possible to monitor the level in the reservoir across which a d.c. voltage was applied, data has been calculated from the measured changes in the other reservoir. The flow rate was defined by

$$\sigma = A_1 \dot{h}_1 / (2\pi R) \quad cm^2\, sec^{-1} \quad ,$$

where $A_1 \dot{h}_1$ is the rate of volume change in the measured reservoir, and R is the radius of the smallest constriction in the flow path (the capillary tube of Figure VI.1). The superfluid velocity can then be obtained from

$$v = \frac{\rho}{\rho_s} \frac{\sigma}{\delta} \qquad cm\ sec^{-1} \quad .$$

The rate of change of level in one arm is related to the rate of change of level in the other by

$$\dot{h}_2 = -\frac{A_1}{A_2} \dot{h}_1$$

$$\therefore \quad \dot{z} = \dot{h}_1 - \dot{h}_2 = \frac{2\pi R \sigma}{A} = \dot{h}_1 A_1 \left(1 + \frac{A_1}{A_2}\right) \quad .$$

At equilibrium, z = 0 (since $\dot{h}_2$ includes any effect of h_v), so integrating $\dot{z}$ from the time the level first moved from or crossed over the equilibrium position to any time t, gave the level difference z(t) as a function of time.

(iii) Accuracy

Temperature Stability. Once the required temperature had been reached by reducing the vapour pressure, it was controlled using an Oxford Instruments resistance bridge. As described in Chapter VI, the temperature detector for the bridge was a 27 Ω Allen-Bradley miniature carbon resistor,

and the offset was used to drive a current through a 250 wire-wound resistor. It was found that the best position for the detector was inside the sealed glass vessel in which the experimental beaker hung. The heater resistor used was outside this vessel in the main liquid helium bath. The carbon resistor was cycled many times and then calibrated against the temperature, calculated from the vapour pressure (measured using a mercury manometer) as given in the 1958 He^4 Scale of Temperatures. When checking stability, a second resistance bridge was used to measure the temperature inside one of the arms of the experimental beaker. (Because of the power dissipated during measurement, temperature inside the arm of the beaker was not measured during experiments). Stability was measured at $\pm 7\mu K$ at $T \simeq 1.2K$. Calibration of the detector resistor between 1.2K and 4K gave a straight line fit, $T^{-1} = 3.0947 \ln R + 4.9753$, with a correlation coefficient of 0.998, but because measuring temperature from the resistance bridge meant interrupting either the experiments or the control of temperature, temperatures were measured during runs using the vapour pressure of the helium bath.

Instrument Sensitivity. The liquid levels were monitored using the ASL Model 1055 Manual Dispalcement meter. This is a ratio arm transformer bridge where the tapping position on a winding is altered until the signal passing through the variable capacitor balances that passing through a standard capacitor. A sensitivity of one part in 10^6 is possible. The nominal capacitance of the capacitors was ~12.2 pF when flooded by liquid helium at 1.2K. As has already been said, the

capacitance was not constant from day to day, and therefore no absolute measures of liquid level could be made. Discrimination of levels less than 0.5 micron are theoretically possible using the bridge; however, the physical linearity and construction of the capacitors limits the resolution. The parallel-ness and smoothness of the capacitors was of the order of 0.1%. That would limit the resolution to ± 3 micron.

Measurement Errors. The measurements taken off the chart recorder traces were those of time and of slopes. The sensitivity of the chart recorder was adjusted so that either the chart span equaled full scale deflection of the ASL capacitance bridge or, when flow was initiated by a voltage across one capacitor, the chart span was able to measure the extremes of the oscillations when the voltage was turned on or off. The sensitivity was of the order of 10^{-2} pF per chart span: this suggests a resolution of 10^{-5} pF. This error is smaller than the $\pm 3\mu$ imposed by the physical manufacture.

The error in measuring time was much greater and depended on the chart speed used. The chart speeds varied from 60 cm min^{-1} to 3 cm min^{-1}, and the best resolution possible (because of the width of the traces) was $\pm$ 0.02 cm, an error of approximately $\frac{1}{2}$ second at the slow chart speeds. At slow speeds, changes in slope (and hence changes in the flow rate, σ) were harder to distinguish, and in particular, where the slope change was less well defined. The discrimination in the slopes ranged from 0.1% to 2% and the error

in the duration of each rate of flow could be as high as 2%. When integrating the slopes to obtain the level difference, a cumulative error could be introduced from the errors in time and in the slopes. Except for the initial run-in, the flows that were initiated went from one equilibrium position to another. At each equilibrium position, the difference in chemical potential between the reservoirs must be zero. This means that the effective level difference (including the effect due to voltage, h_v) must be zero. In calculating the level difference, a percentage correction was applied such that this condition was true. The percentage correction varied in sign and was between 4 and 10%. This correction reflects the condition

$$(\sum^{n} \sigma_i \Delta t_i)\, e = \sum^{n} (\sigma_i + \varepsilon_{\sigma_i})(\Delta t_i + \varepsilon_{t_i}) - \sum^{n} \sigma_i \Delta t_i \,.$$

Assuming that products of the errors can be neglected,

$$(\sum^{n} \sigma_i \Delta t_i)\, e = \sum^{n} (\sigma_i \varepsilon_{t_i} + \Delta t_i \varepsilon_{\sigma_i}) \,.$$

If the ε are a constant fraction for each pair $(\sigma_i, \Delta t_i)$, then

$$(\sum^{n} \sigma_i \Delta t_i)\, e \simeq n\,(\bar{\sigma}\,\varepsilon_t + \overline{\Delta t}\,\varepsilon_\sigma) \,.$$

Taking a value for the errors ε of 5% for both σ and Δt (as the slope measurement involves time, it seems reasonable to suppose that the errors in the rates of flow and in time should be of the same order), and using n = 6 with typical value of the means $\bar{\sigma}$ and $\overline{\Delta t}$,

$$7\times10^{-4}\,.\,e = 6\,(8\times10^{-5}\times 0.25 + 5\times 4\times10^{-6}) \,.$$

e is found to be 6%, of the same order as the error in time. Except where otherwise stated, the error in the flow rate or the superfluid velocity will be taken as 7% (the mean of the percentage correction values).

(iv) The Run-In

The run-in was defined as that period of measurement from the time when the bulk liquid level in both reservoirs had reached the narrow annular region where the cross-sectional areas are well defined, to the point in time when the levels first reached their equilibrium position. The last part of such a run-in as measured by the change in capacitance of one **reservoir** is shown in Figure VII.1. Also shown are the inertial oscillations that follow the run-in as the levels oscillate about the equilibrium position. From the slope of the trace (chart roll divisions sec^{-1}) and the sensitivity of the chart recorder (pF per chart roll division), the rate of capacitance change in a reservoir could be calculated (pF sec^{-1}). Dividing by the change in capacitance per unit length (pF cm^{-1}) and multiplying by the cross-sectional area of the reservoir (cm^2) yielded the volume flow into (or out of) the reservoir ($cm^3 sec^{-1}$). This can be expressed either as the flow rate σ = volume flow /(circumference of smallest constriction) (cm^2 sec^{-1}) or as the superfluid velocity, $v = \rho_s$ x volume flow / (ρ x film area) (cm sec^{-1}) where the film area is the cross-section area of the helium film in the smallest constriction.

To obtain the level difference which is responsible for driving the liquid helium from one reservoir to the other, the trace was considered in reverse, namely, from the position of equilibrium backwards, until one of the liquid levels left the well-defined narrow annular region. The measured flow rates σ_i were constant for a time period

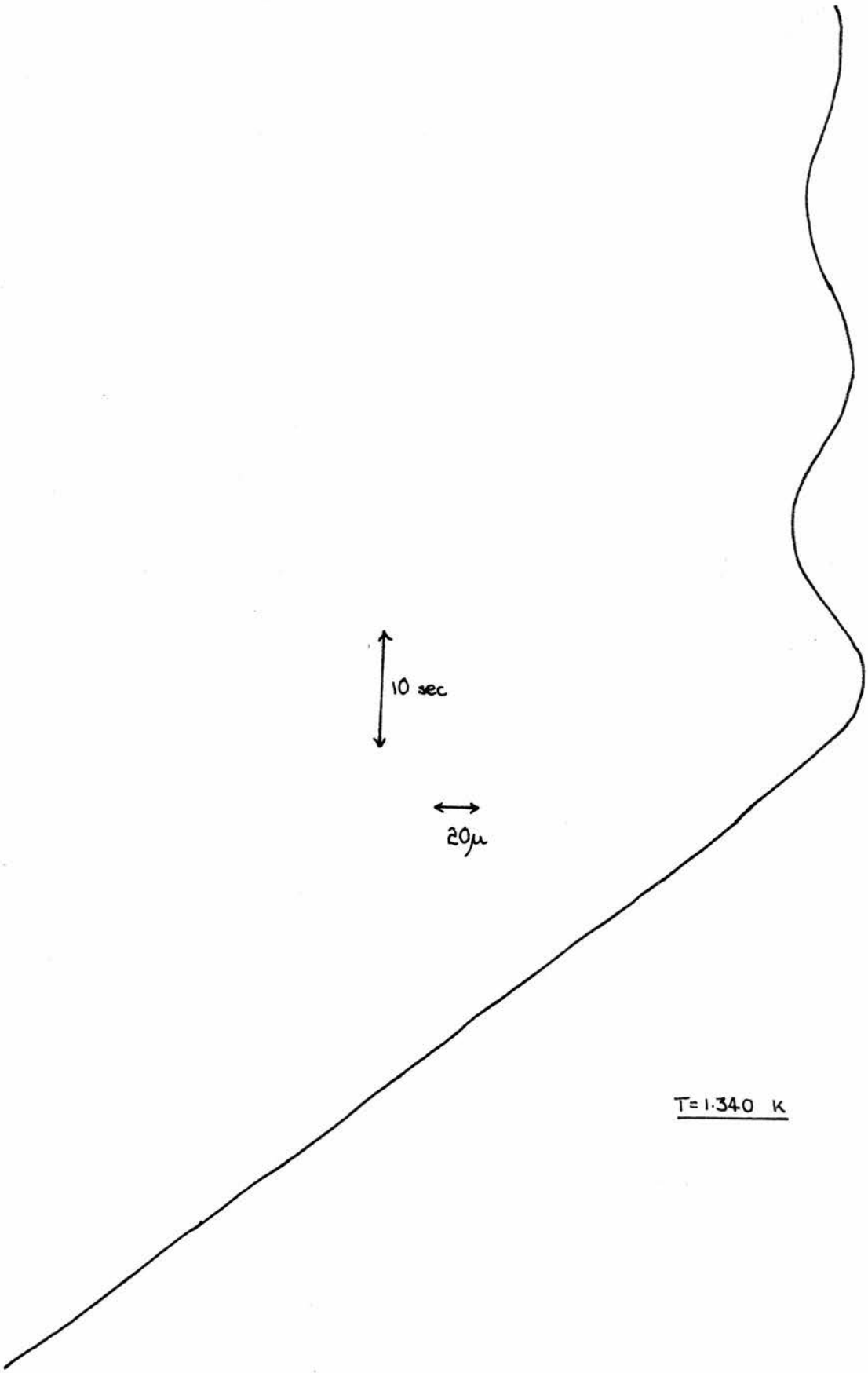

FIGURE VII.1 END OF RUN-IN AND START OF OSCILLATIONS

The volume of liquid flowing out of one reservoir during Δt_i was thus $2\pi R \sigma_i \Delta t_i$ (where $2\pi R$ is the circumference of the restriction) and the change in liquid level in that capacitor was given by

$$\Delta h_i(1) = 2\pi R \sigma_i \Delta t_i / A_1 \quad .$$

A similar expression exists simultaneously for the second reservoir, where the flow is in the opposite sense:

$$\Delta h_i(2) = -2\pi R \sigma_i \Delta t_i / A_2 \quad .$$

Hence the change in the level difference was

$$\begin{aligned} \Delta z_i &= \Delta h_i(1) - \Delta h_i(2) \\ &= 2\pi R \sigma_i \Delta t_i \left(1/A_1 + 1/A_2 \right) \\ &= 2\pi R \sigma_i \Delta t_i / A \quad . \end{aligned}$$

If this is integrated (summed), then the level difference as a function of time is

$$z(t_n) = 2\pi R / A \sum_{i=1}^{n} \sigma_{i-1} (t_i - t_{i-1})$$

where a flow rate σ_i is constant from time t_i to time t_{i+1} .

Figures VII.2 - VII.4 show the level difference a plotted as a function of time, at three different temperatures. The straight lines are a least squares fit to the data. The method of calculating z involves summing the $\sigma_i \Delta t_i$, so that every data point shown has resulted from a change in the measured flow rate σ_i. This can be accentuated by plotting

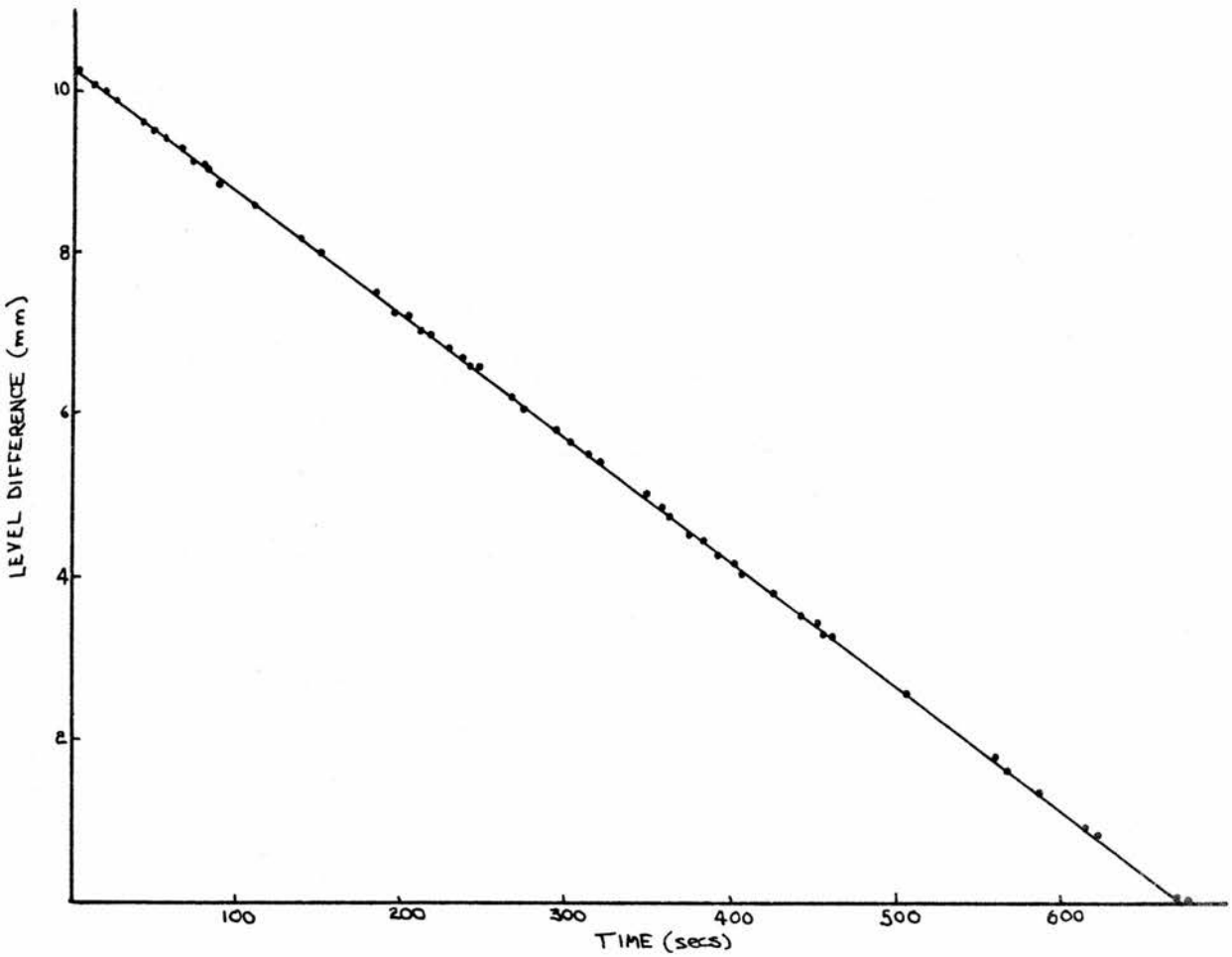

FIGURE VII.2 RUN-IN T = 1·340

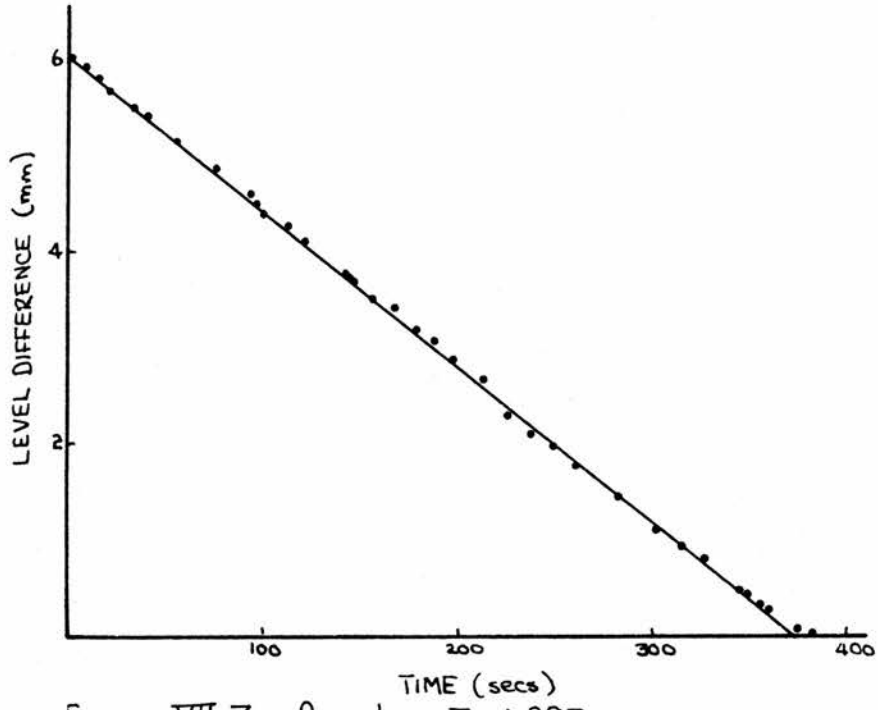

FIGURE VII.3 RUN-IN T= 1.293

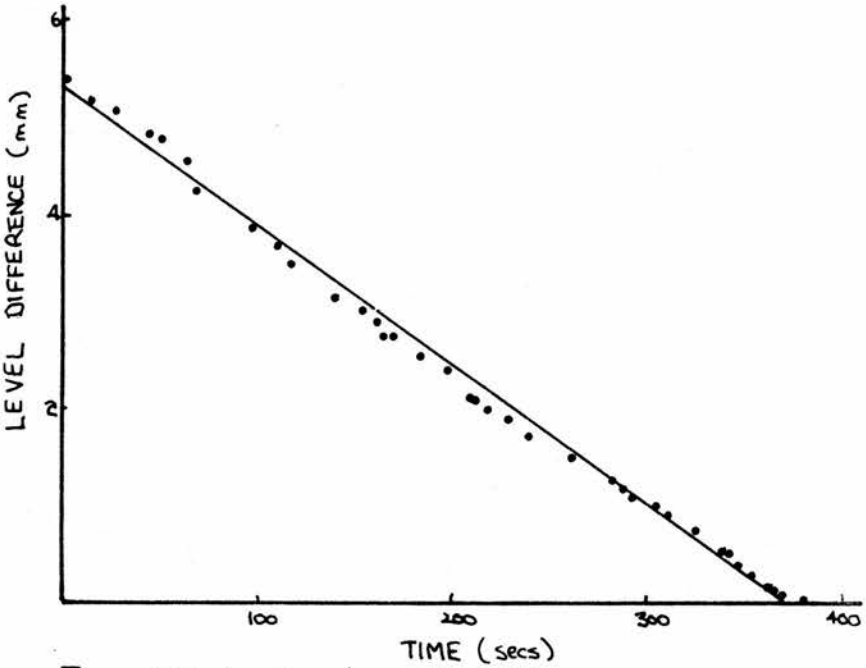

FIGURE VII.4 RUN-IN T= 1·212

the measured flow rate as a function of the calculated level difference, as in Figures VII.5 - VII.7. These show that the rate of level change is only very approximately linear, that changes in rate can both increase and decrease and that there is not a pattern that emerges which is common to all three figures, either in respect of the changes in flow rate, or in respect of the relationship between the flow rate and the driving force (this will be further discussed together with the results of driven flow).

The nearly linear decay of the level difference with time has been used to indicate the existence of a limiting or critical superfluid velocity whose value is obtained from the slope of Figures VII.5 - VII.7. The straight lines represent the following flow rates:

$$\text{At } T = 1.340 \;,\; \sigma = 8.34 \times 10^{-5} \text{ cm}^2 \text{ sec}^{-1} \;,$$
$$T = 1.293 \;,\; \sigma = 8.73 \times 10^{-5} \text{ cm}^2 \text{ sec}^{-1} \;,$$
$$T = 1.212 \;,\; \sigma = 7.83 \times 10^{-5} \text{ cm}^2 \text{ sec}^{-1} \;.$$

The superfluid velocity v was found from

$$v = \frac{\rho}{\rho_s} \frac{\sigma}{\delta}$$

where the film thickness δ is

$$\delta = k \left(\tfrac{1}{2} \frac{\rho_s}{\rho} \frac{v^2}{g} + h \right)^{-1/n} .$$

Taking a van der Waals exponent of n = 3, and using the value of $k = 4.0 \times 10^{-6}$ cm$^{4/3}$, the corresponding velocity v could be calculated. The value of h, the height of film in the dissipative area, was found from the geometry of the experimental beaker and from the liquid level in the narrow

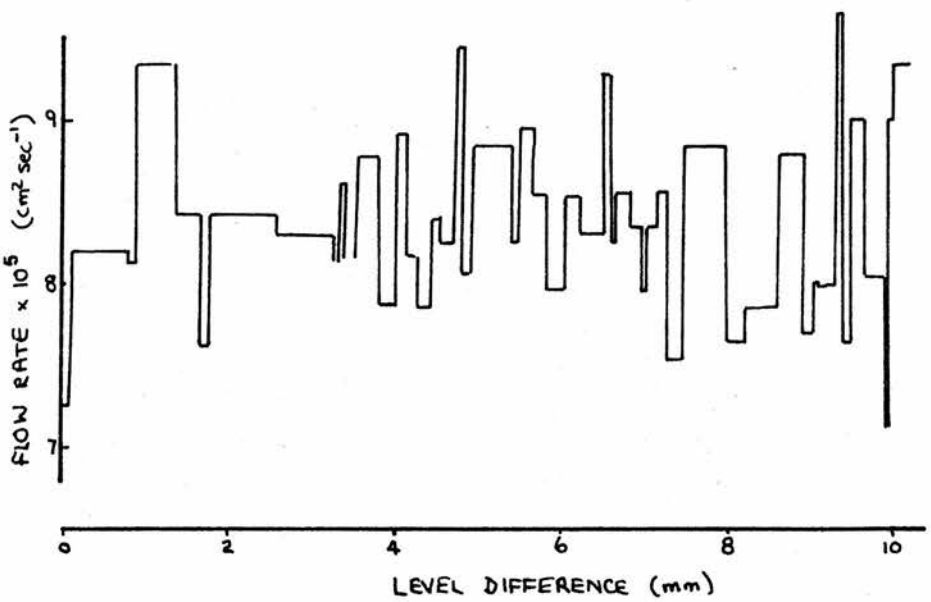

FIGURE VII.5 FLOW RATE AS A FUNCTION OF LEVEL DIFFERENCE
T = 1·340

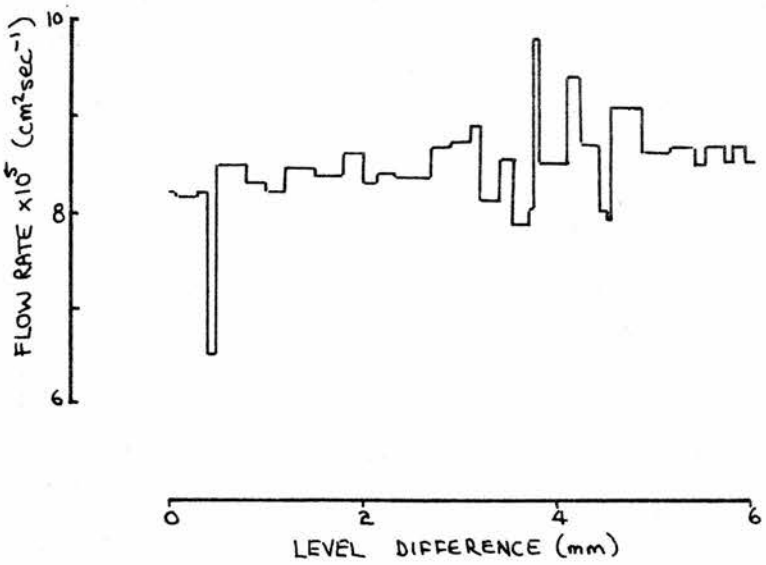

FIGURE VII.6 FLOW RATE AS A FUNCTION OF LEVEL DIFFERENCE
T= 1.293

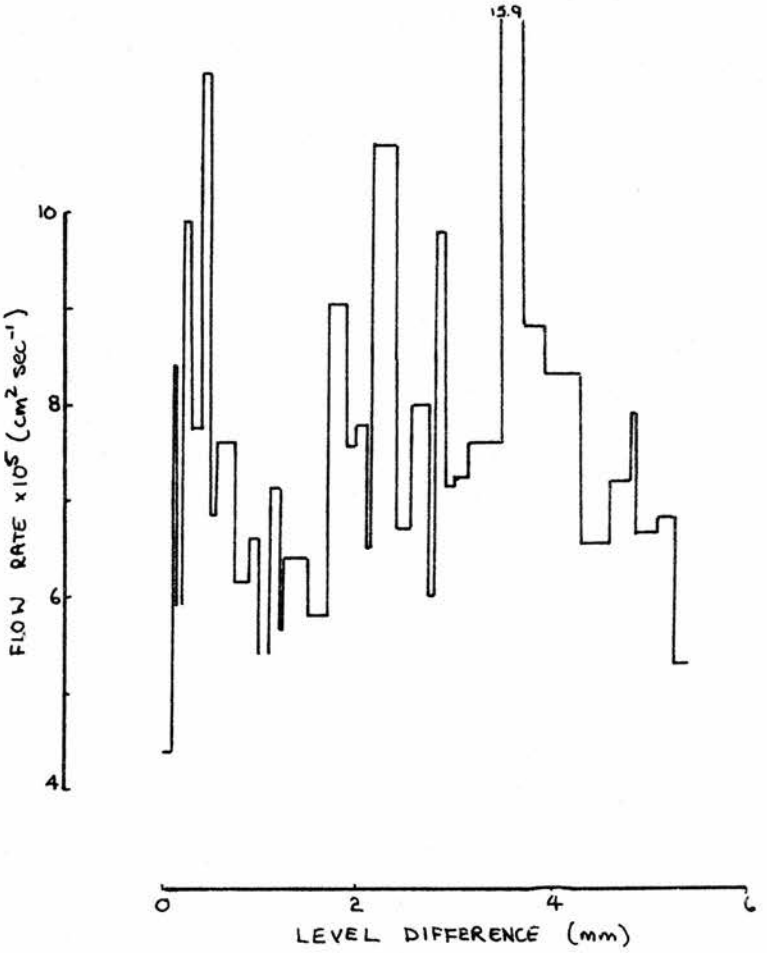

FIGURE VII.7 FLOW RATE AS A FUNCTION OF LEVEL DIFFERENCE
T = 1.212

annular region as inferred from the maximum level difference shown on the run-ins (Figures VI.2 - VI.4). The values obtained are:

$$T = 1.340 \quad , \quad v = 25.5 \quad \text{cm sec}^{-1} \quad ,$$

$$T = 1.293 \quad , \quad v = 25.8 \quad \text{cm sec}^{-1} \quad ,$$

$$T = 1.212 \quad , \quad v = 23.3 \quad \text{cm sec}^{-1} \quad .$$

The equations of motion suggest that if there was zero acceleration then

$$gz = -D(v_c)\, l \quad .$$

The form of the dissipation function that has recently most often been applied to the flow of superfluid helium is that suggested by Langer and Fisher (1967):

$$D = a_f \kappa f \, e^{-v_b/v}$$

where a_f is the cross-sectional area over which dissipation occurs, $\kappa = \hbar/m$ is the quantum of circulation and f, the attempt frequency, and v_b, the barrier velocity, are the two parameters of the equation. If the flow was 'critical', then

$$v_c = v_b \left(\ln \frac{l a_f \kappa f}{gz} \right)^{-1} \quad .$$

Typical values for f and v_b, obtained from an experimental beaker similar to the one used in this work (Campbell et al [1976]) are

$$f \simeq 10^{29} \quad \text{sec}^{-1} \quad ,$$

$$v_b \simeq 1500 \quad \text{cm sec}^{-1} \quad .$$

Thus, if the Langer-Fisher dissipation function were to fit the experimental results, the theory would suggest a 'critical' velocity of the order of 40 cm sec^{-1} for a level difference of 1 cm.

To see whether Langer-Fisher or any other theory fitted the experimental data, it was necessary to solve the complete equations of motion (Equations [1] and [2] of section [i]). Expressed in terms of the level difference z, this becomes

$$\frac{d^3z}{dt^3} + e\frac{d^2z}{dt^2} + \left(1 + \frac{sbAT}{gcV}\right)\omega_o^2\frac{dz}{dt} + e\omega_o^2 z = -\frac{\omega_o^2 l}{g}\left(\frac{dD(v)}{dt} + eD(v)\right)$$

where $e = \kappa/(\rho cV)$, $b = (s - \frac{1}{\rho}\frac{d\rho}{dt})$ and $\omega_o^2 = g\rho_s/(\rho AI)$. This equation would require prior knowledge of the parameters of the dissipative function and is not in a suitable form to allow a graphical test of the function to the experimental data.

Two assumptions can be made:

(i) Since the data consisted of a series of constant flow rates, the second derivative of the flow rate must be very small and $d^3z/dt^3 = 0$. To get the form of the equation into a suitable form, an assumption must also be made about the rate of change of the dissipative factor, namely, either $dD(v)/dt = 0$ or $eD(v) >> \frac{dD(v)}{dt}$. This would yield the equation

$$\frac{d^2z}{dt^2} + \left(\frac{\rho cV}{\kappa} + \frac{sbAT\rho}{g\kappa}\right)\omega_o^2\frac{dz}{dt} + \omega_o^2 z = -\frac{\omega_o^2 l}{g}D(v) \quad \text{—— (3a)}$$

(ii) If, in equation (2), $\frac{d\Delta T}{dt} = 0$, then an equation similar to (3a) can be obtained

$$\frac{d^2z}{dt^2} + \frac{sbAT\rho}{g\kappa}\omega_o^2\frac{dz}{dt} + \omega_o^2 z = -\frac{\omega_o^2 l}{g}D(v) \quad \text{—— (3b)}$$

This assumption can be justified by considering the magnitudes of the terms in equation (2). Taking a value of $dz/dt = 15 \times 10^{-6}$ m sec^{-1} (the slopes of Figures VII.2 - VII.4) and assuming $\frac{d\Delta T}{dt} = 0$, $\Delta T \simeq 8 \times 10^{-7}$K. The magnitudes of the terms $s\Delta T \frac{dz}{dt} / (cV)$ and $\kappa \Delta T / (\rho c V)$ are both $\simeq 2 \times 10^{-5}$K sec^{-1}; thus even a change in ΔT of one hundred per cent over one second will only affect the result by 2%. Furthermore, Campbell et al (1976) have shown that in the oscillatory region of the flow, the better accuracy of the two approximations can be found by considering the geometrical and thermodynamic properties of the experimental system. For the experimental apparatus used in this work, $\frac{d\Delta T}{dt} = 0$ is the better approximation (see Appendix).

If the Langer-Fisher dissipation function can be applied, then

$$D(v) = \kappa f 2\pi R\delta \exp(-v_b/v)$$

where $2\pi R\delta$ is the cross-sectional area of film over which dissipation occurs. Thus equation (3b) can be expressed as

$$F = Gf \exp(-v_b/v)$$

and a plot of $\ln(F/G)$ against $(1/v)$ would yield a straight line of slope $-v_b$ and intercept equal to $\ln(f)$. Such a plot is shown in Figure VII.8 and illustrates the inadequacy of the Langer-Fisher model in explaining the experimental results. That it would not be satisfactory was apparent from Figure VII.5. The function F is dominated by the term in z; for the Langer-Fisher model to hold, the flow

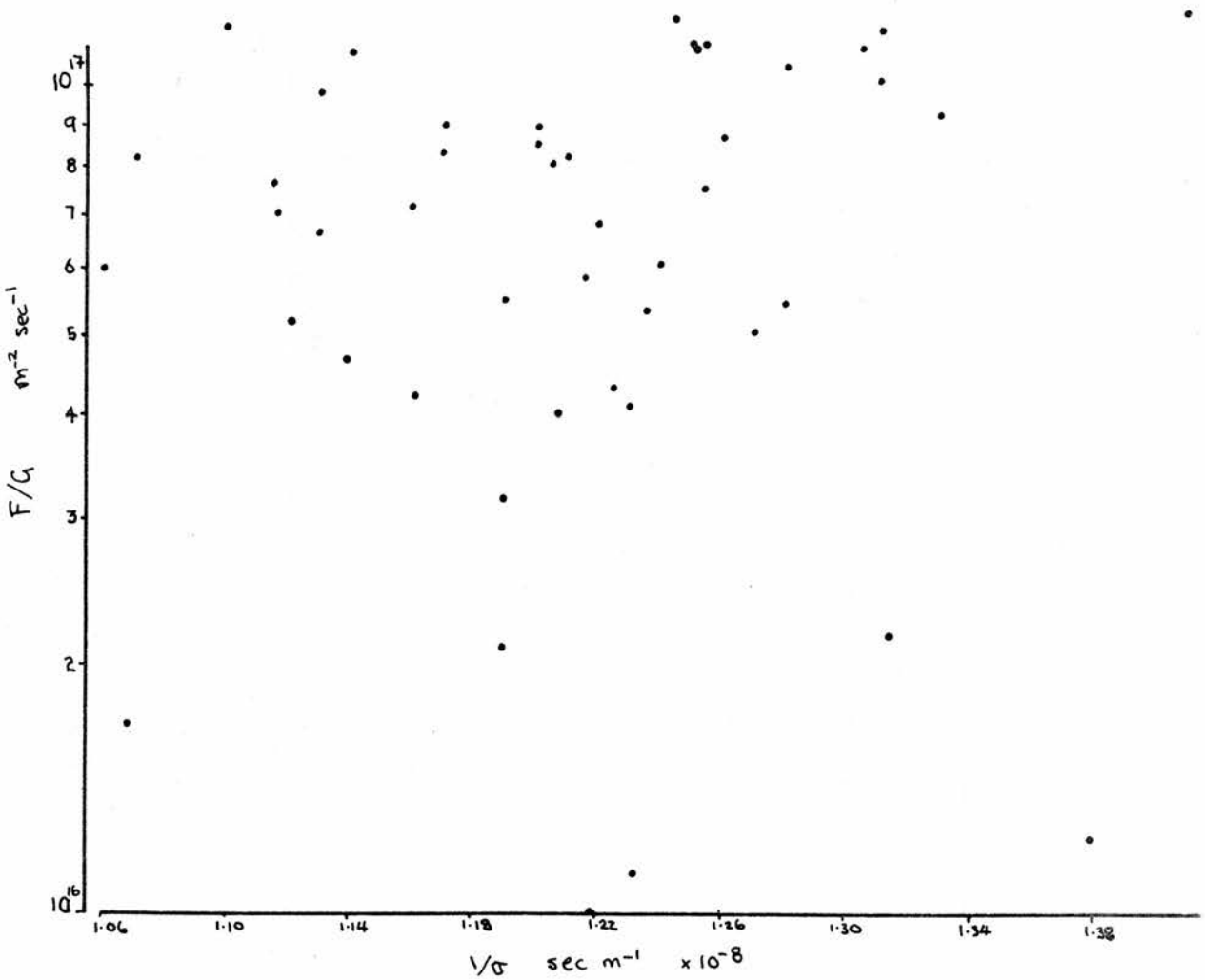

FIGURE VII.8 TEST OF LANGER-FISHER THEORY

rate should fall off exponentially at least at lower level differences. Flow rates at low level differences will be looke at in section (vi).

(v) Oscillations

Figure VII.1 shows the onset of oscillations following a run-in. These inertial oscillations arise as the mass of liquid helium transported in the film transforms the kinetic energy of flow into potential energy; this change in the chemical potential drives the liquid helium in a damped oscillatory fashion. The theoretical basis for these oscillations was first described by Robinson (1951). The equations were derived for flow through narrow channels and are of the same form as equations (1) and (2), except that there was no dissipative function in Robinson's treatment. The damping of the oscillations is due to thermal effects, because the term proportional to the rate of change of level difference is dependent on the temperature difference. The equation which governs the flow of liquid helium when the intrinsic dissipation can be neglected is

$$\frac{d^3z}{dt^3} + \frac{\kappa}{\rho c V}\frac{d^2z}{dt^2} + \omega_0^2\left(1 + \frac{\left(1-\frac{1}{\rho^3}\frac{d\rho}{dT}\right)s^2 AT}{gcV}\right)\frac{dz}{dt} + \frac{\omega_0^2\kappa}{\rho c V} z = 0 .$$

The general solution to this equation is of the form

$$z(t) = A_1 e^{a_1 t} + A_2 e^{a_2 t}\sin(a_3 t + \phi) .$$

The a_i are found by solving the characteristic equation of the differential equation:

$$a^3 + \frac{\kappa}{\rho c V} a^2 + \omega_0^2\left(1 + \frac{\left(1-\frac{1}{\rho^3}\frac{d\rho}{dT}\right)s^2 AT}{gcV}\right)a + \frac{\omega_0^2\kappa}{\rho c V} = 0 .$$

The appendix shows the detailed calculation both for ω_o^2 (from $\omega_o^2 = {}^{g\beta}/_{\rho AI}$) and for the roots of the above equation; at a temperature of T = 1.2K the solution is

$$z(t) = A_1 e^{-(22.74)t} + A_2 e^{-(9.42\times10^{-3})t} \sin[(0.261)t + \phi] ,$$

the decay of the first term is very much more rapid than the second (after one second $e^{-22.74t} = 1.3 \times 10^{-10}$, whereas $e^{-9.42 \times 10\ t} = 0.99$), so that it can be neglected and the solution

$$z(t) = A e^{a_2 t} \sin(a_3 t + \phi)$$

is that of a second order differential equation. Campbell et al (1976) in discussing the two approximations that will give rise to a second order differential equation, have shown that whenever (H - 1)/ G < 1, then the approximation ${}^{d\Delta T}/_{dt} = 0$ gives a smaller error than the approximation ${}^{d^3z}/_{dt^3} = 0$. The expression (H - 1)/ G can be written as

$$sT\left(s - \frac{1}{\rho}\frac{d\rho}{dT}\right)A\ /(gcV) .$$

For the apparatus used, (H - 1)/ G $\simeq$ 0.7, hence the use of the approximation ${}^{d\Delta T}/_{dt} = 0$ (for definitions see Appendix).

Because of the small error in approximating the equation of motion through ${}^{d\Delta T}/_{dt} = 0$, the value of the thermal conductivity was deduced from the observed period and damping, using the equation

$$2q\alpha|K| \simeq \omega_o^2 \left(1 - \frac{1}{\rho s}\frac{d\rho}{dT}\right)\rho s^2 AT .$$

For the experimental results at 1.212 K, the period of the oscillations was measured and the logarithmic decay constant was calculated from a plot such as Figure VII.9. These give a value for ω_o^2 of 6.847×10^{-2} sec^{-2}, about 2% higher than the predicted value given in the appendix. As has been stated by other researchers, for example, Hallock and Flint (1974), the Robinson description of the behaviour of a system linked via the superfluid helium, is in good quantitative agreement with these experimental results.

Oscillations were also observed after changes to the chemical potential of one reservoir by applying a voltage across the reservoir. Figure VII.10 shows the response to a step change of voltage as monitored on the second reservoir. The traces show alternatively, the application of a voltage, followed by the removal of the voltage (the second and fourth traces are upside down). These too, show the same characteristics as the oscillations after the run-in. Figure VII.11 shows the average decay constant.

(vi) Driven Flow

It has already been stated that applying a voltage V across one of the reservoir capacitors would result in a change in the chemical potential equal to a change in level of

$$h_v = \frac{\pi \epsilon_o (\epsilon_r - 1) V^2}{A_2 \rho g \ln(b/a)} .$$

Suddenly applying a voltage of 140V was equivalent to applying a step change in the level of the reservoir of about 310×10^{-6}m. This method of producing a change in the chemical potential has three major advantages over the more

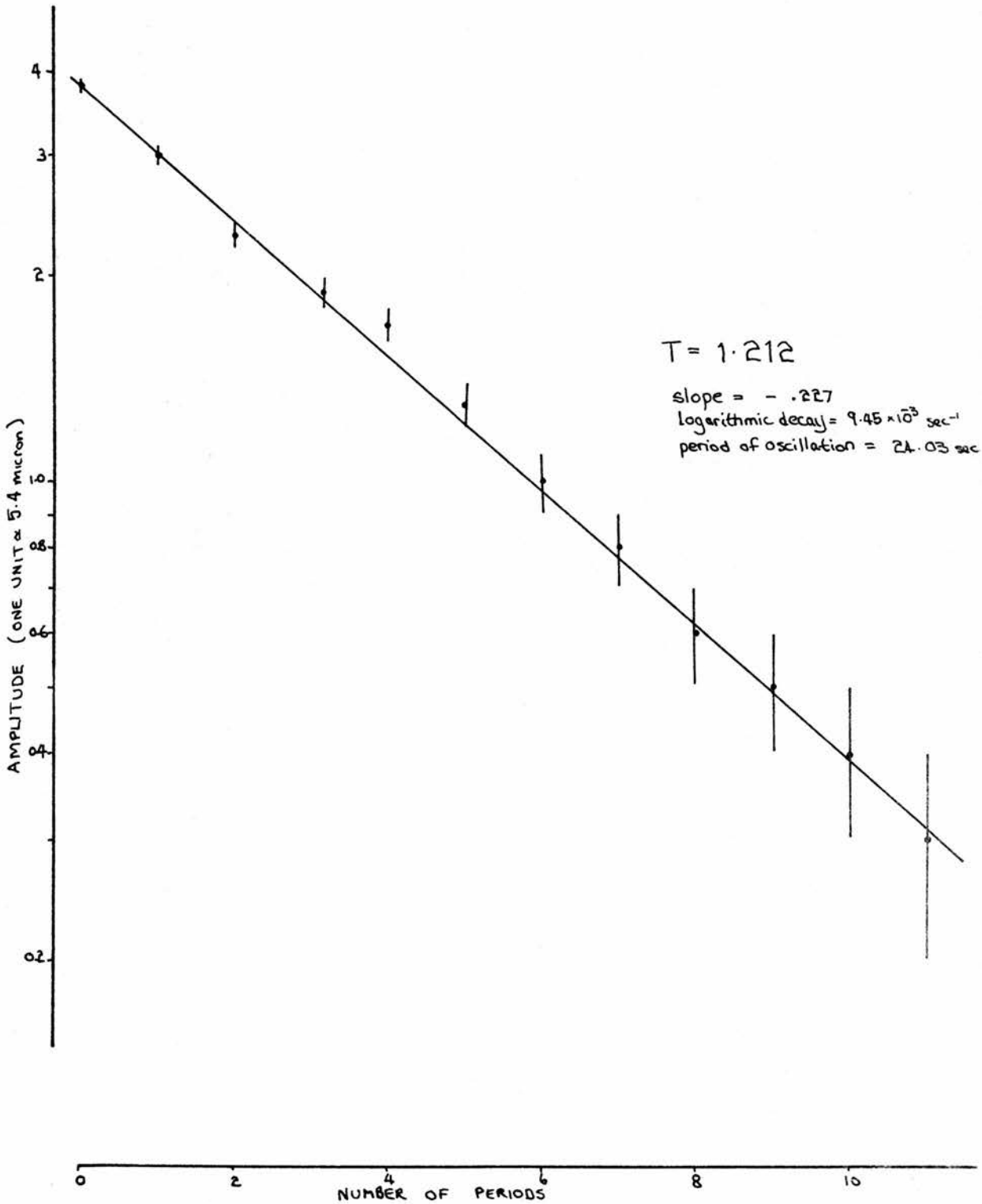

FIGURE VII.9 DECAY OF OSCILLATIONS AFTER RUN-IN

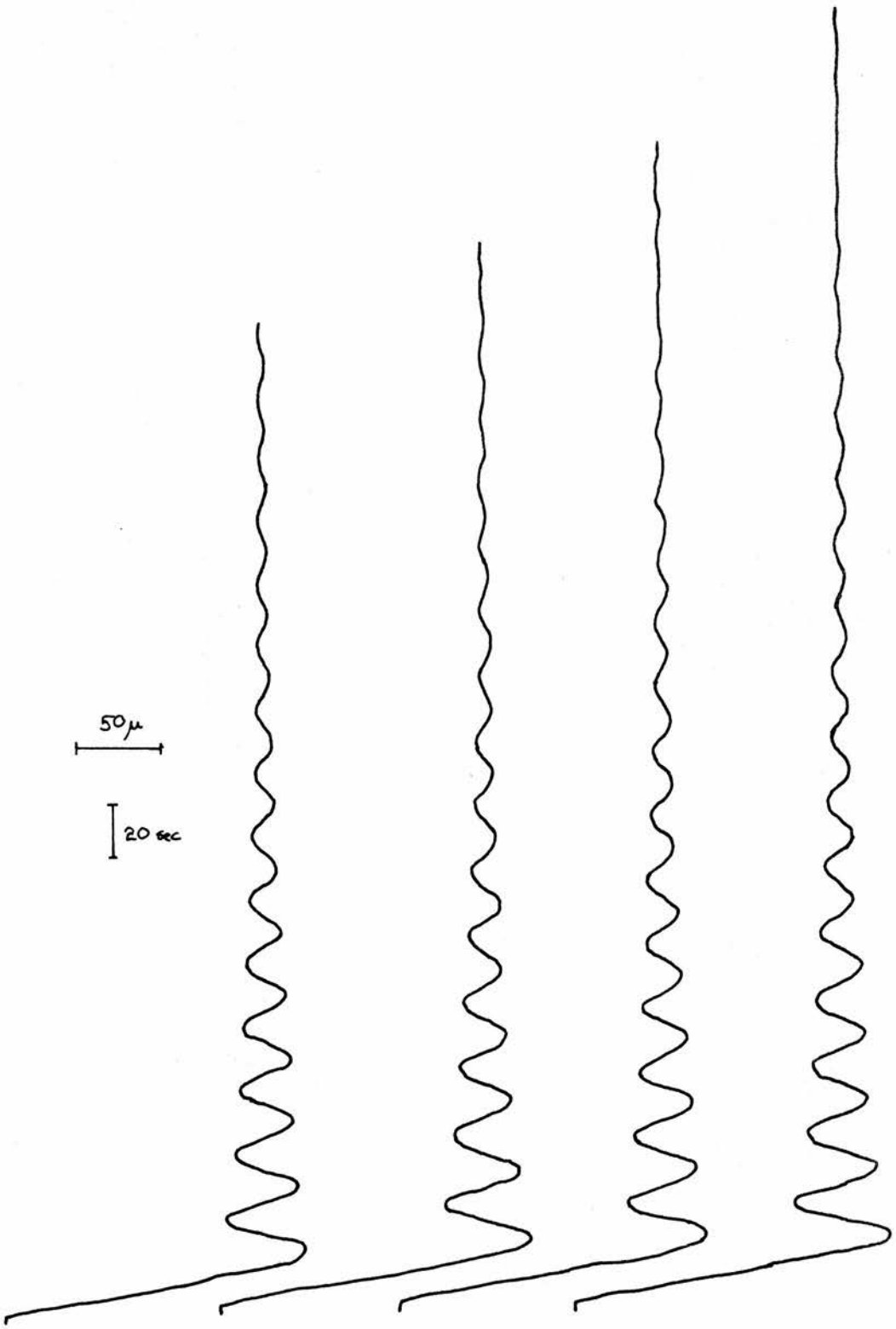

FIGURE VII.10 OSCILLATIONS AFTER STEP INPUT T= 1.212

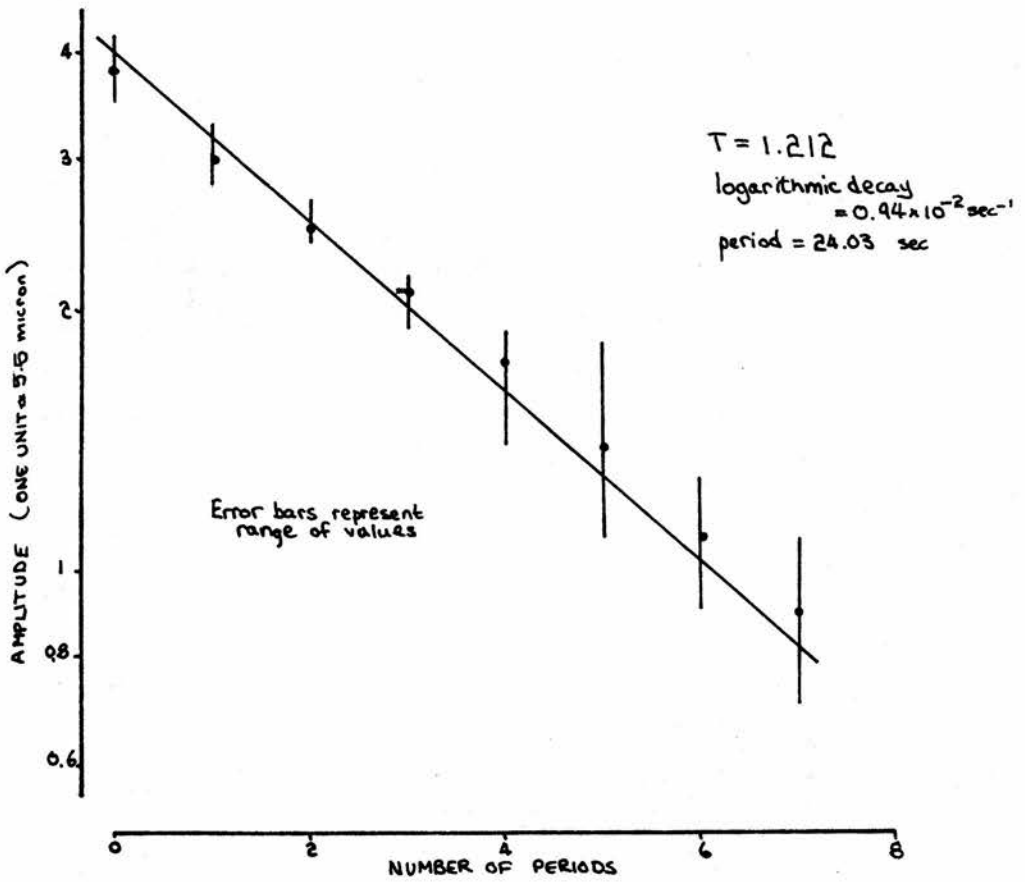

FIGURE VII.11 DECAY OF OSCILLATIONTIONS AFTER STEP INPUT

conventional means of driving flow:

1) The means of applying the drive is free of any mechanical linkage system (bellows or plunger) whose movement can induce vibrational oscillations.

2) There is no thermal change is applying a voltage across the capacitor and the leads to the capacitor can readily be thermally anchored to prevent conduction of heat into the experimental system.

3) The control over the drive system is very precise as voltage can easily be regulated.

If the voltage applied across the capacitor is such that the chemical potential increases or decreases linearly with time, then there will be an out-or inflow of liquid helium into that reservoir trying to maintain a zero chemical potential difference between the two reservoirs. At any instant of time, the "level" in the reservoir across which a voltage was being applied is

$$h_2(t) = h_v(t) - \frac{2\pi R}{A_2}\int \sigma\, dt$$

and the level in the second reservoir would be

$$h_1(t) = \frac{2\pi R}{A_1}\int \sigma\, dt$$

Thus the equivalent level difference at time t was

$$z(t) = h_v(t) - \frac{2\pi R}{A}\int \sigma dt \quad .$$

If $h_v(t)$ is linear with time, then if $h_v(t)$ goes from a value of zero at t = 0 to a maximum value of h_v at t = τ , then

$$h_v(t) = \frac{h_v \cdot t}{\tau} \quad \text{for} \quad t \leq \tau$$

$$h_v(t) = h_v \quad \text{for} \quad t > \tau \ .$$

As for the run-in, $\int \sigma dt$ is replaced by the sum of the discrete flow rates over the time:

$$\int \sigma dt = \sum_{i}^{n} \sigma_{i-1}(t_i - t_{i-1}) \ .$$

The chart recorder traces for the driven flow were of the level in the one capacitor and of the voltage applied across the other capacitor. Thus, the same information as used during the run-in on rates of flow and the times over which the flow was constant could be obtained. As explained in Chapter VI, the voltage across the capacitor was varied with time so that

$$V^2(t) = t V_{max} / \tau$$

where τ is the (variable) time taken to reach V_{max}. The chart recorder trace allowed a more accurate measure of τ and provided a means of synchronizing the flow to the beginning of the drive. Since the range of equivalent level differences is small where using an applied voltage to drive the liquid helium from one reservoir to the other, it was hoped that the results would be able to throw some light on the results of the run-ins.

Examples of driven flow at T = 1.203 K are shown in Figures VII.12 and VII.13. Plotted on the graphs are the liquid level in the measured reservoir, the chemical potential change due to the applied voltage (expressed as an equivalent liquid level h_v), the flow rate and the equivalent pressure

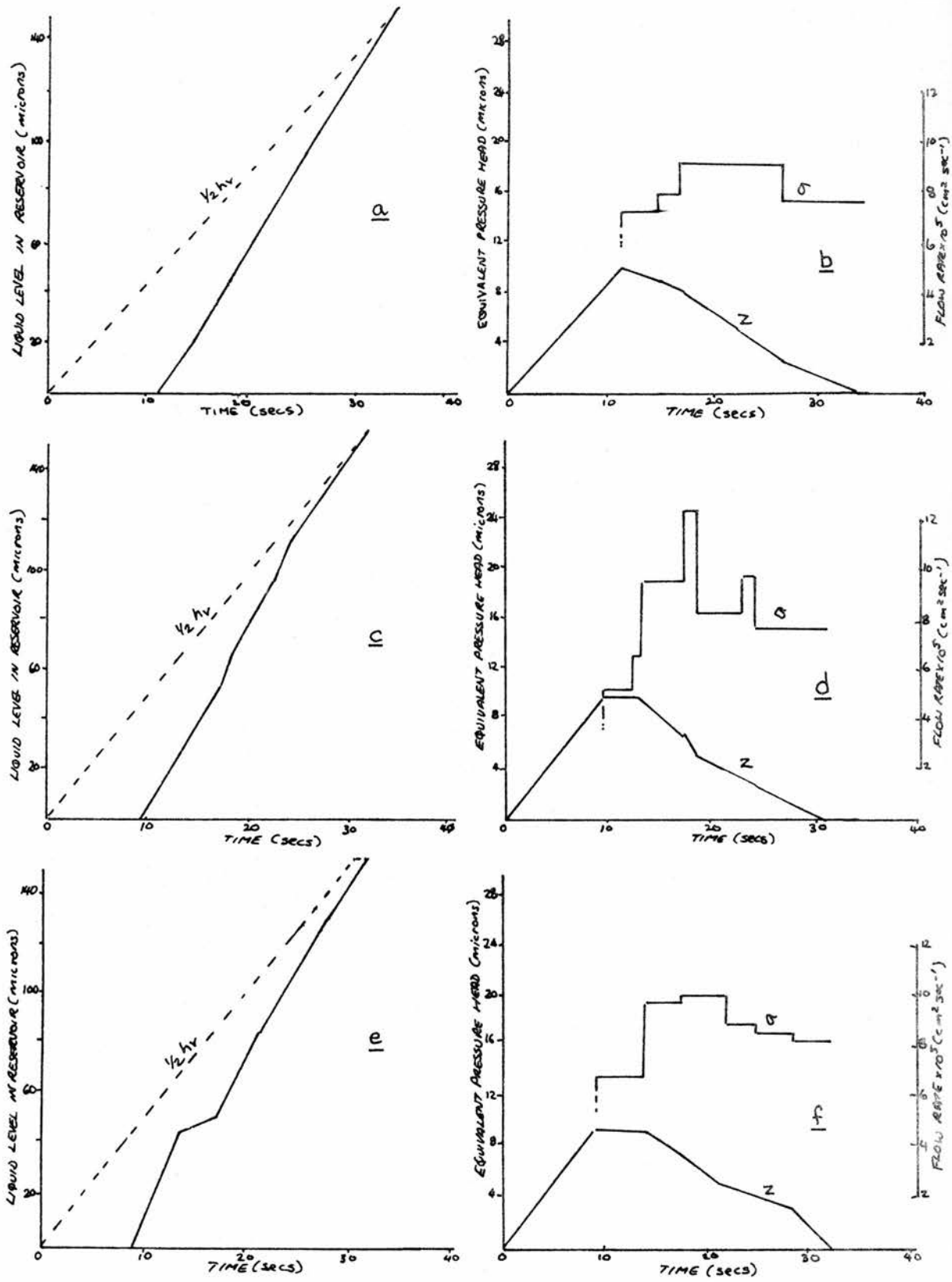

FIGURE VII.12 VARIATION OF FLOWRATE, LEVEL DIFFERENCE & LIQUID LEVEL WITH TIME AND CHEMICAL POTENTIAL CHANGE
T = 1.203

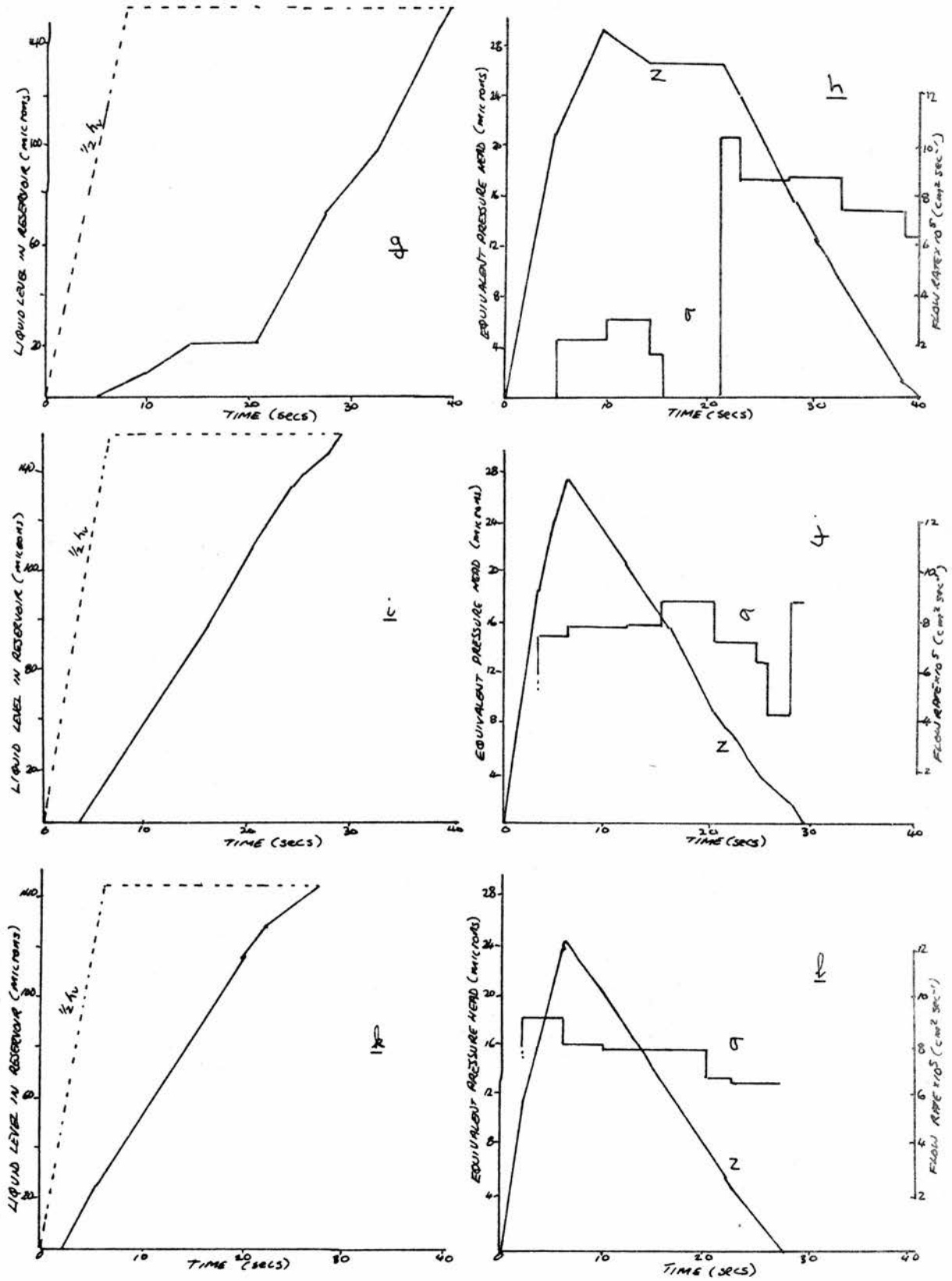

FIGURE VII .12 (CONTINUED)

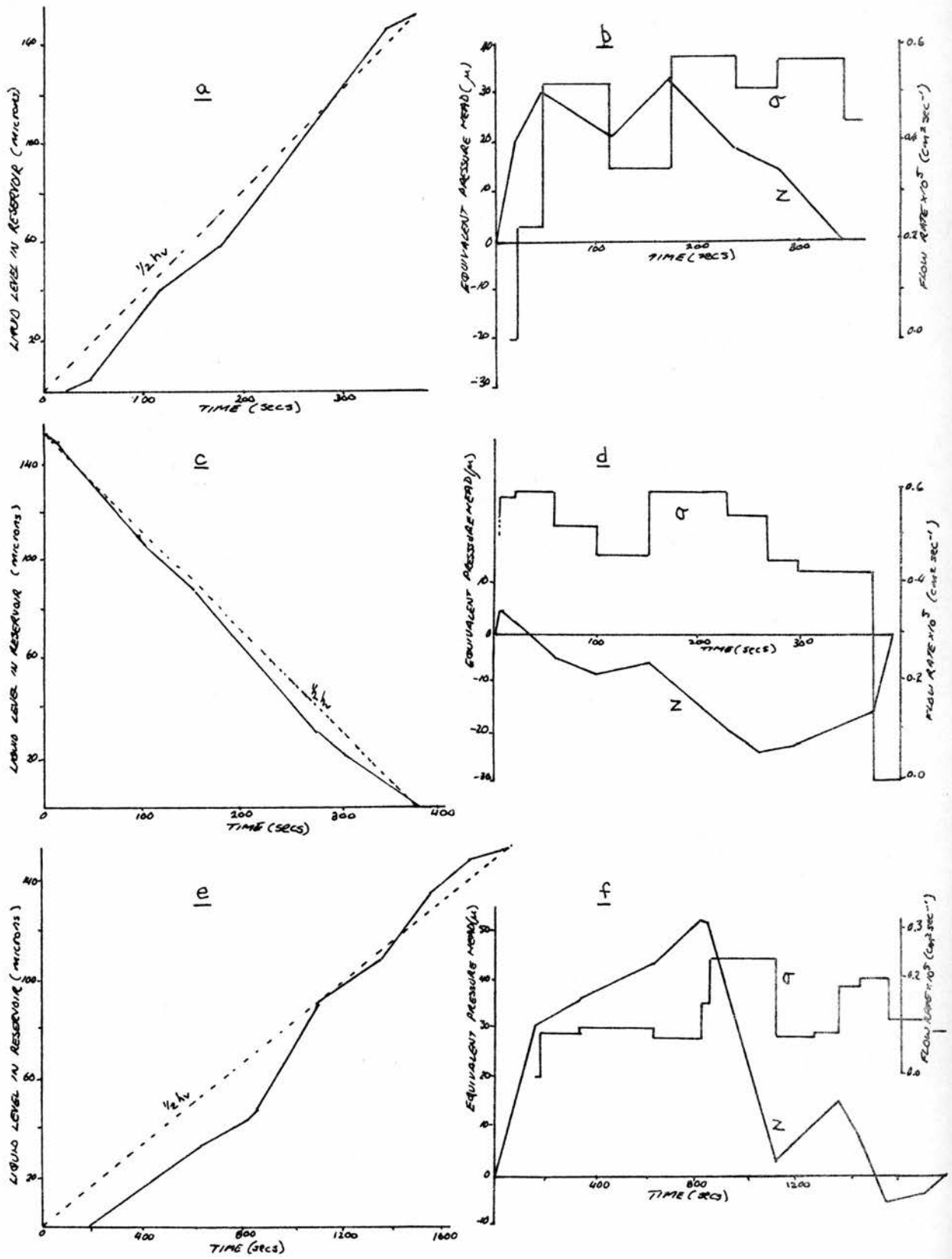

FIGURE VII.13 VARIATION OF FLOW RATE, LEVEL DIFFERENCE & LIQUID LEVEL DURING SLOWLY DRIVEN FLOW
T = 1.203

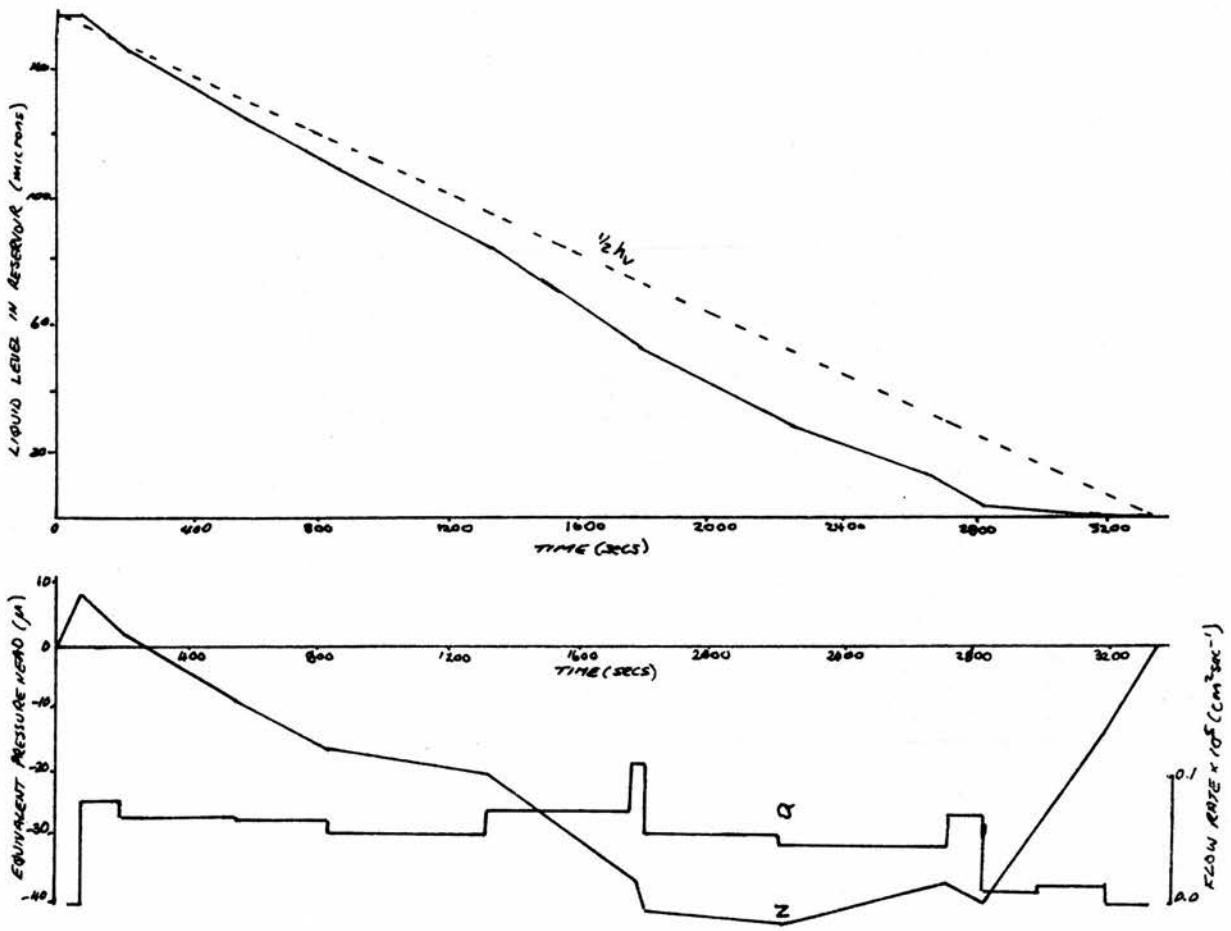

FIGURE VII.13 (CONTINUED)

TABLE VII.1

head driving the flow, $z(t)$, as defined in the earlier equations. Considering Figure VII.12, a dotted line, $\frac{1}{2}h_v$, indicates the way the liquid level in the measured reservoir would change if there could be an instantaneous and ideal superfluid response to the change in the chemical potential due to the applied voltage across the second reservoir. The solid line shows the actual change in the level of the reservoir. There were several obvious features to the observed results:

(i) There was a delay before the level in the measured reservoir changed.

(ii) Looking at the level changes alone, they appear to change approximately linearly with time.

(iii) When driven over longer periods (generally greater than thirty seconds), the change in level often crossed over the line of $\frac{1}{2}h_v$ (see Figure VII.13).

(iv) The flow rate both increased and decreased during driven flow, seemingly independently of the direction in which the driving force for the flow was changing.

Some of these results are explicable; collectively, they do not fit comfortably into any of the theories discussed in Chapter V. The delay before flow commenced seems partly due to the need to overcome the inertia of the mass of helium film before the driving force will accelerate it into movement. A reasonable time to use would be approximately one-quarter of the period of the inertial oscillations. Table VII.1 gives the average observed time delays and also the average chemical potential (expressed as an equivalent level difference between the reservoirs) before flow actually

commenced. The delay times were all within the quarter-period time of the inertial oscillations; the equivalent pressure head that had been reached by the time flow commenced was not constant, even at the same temperature and there was a distinct difference between flow driven upwards (i.e. while the voltage was increasing) and flow driven downwards, despite the geometrical symmetry of the experimental beaker.

One set of experiments was carried out at T = 1.203 K using a very slowly changing voltage as the driving force. The change in chemical potential due to the applied voltage was equivalent to a change in liquid level of 310×10^{-6}m. The voltage was over four times: increasing over six minutes, decreasing over six-and-a-half minutes, increasing over thirty minutes and decreasing over fifty-six minutes. These results are shown in Figure VII.13. Two results might have been expected: that the helium film flow would remain in a state of dynamic equilibrium whereby the increase in chemical potential due to the applied voltage would be balanced by the decrease as fluid left the reservoir via film flow, and that the behaviour of the film flow would be simpler and thus provide some means of explaining the results of Figure VII.12. However, Figure VII.13 shows many of features of the former figure. Of interest, is the observation of stable flow rates whose magnitude is one hundred times smaller than that reported in the literature (Figure VII.13h). The values of the flow rate correspond to superfluid velocity of 0.3 to 0.03 cm sec^{-1}. It is unlikely that so small a driving force could have been applied by any other method than that of applying a slowly

changing voltage across the capacitor-reservoir.

The nearly linear rate of change in level that was noticed during the run-in (Figure VII.2), is also seen during driven flow. As before, the plot of liquid level against time, disguises the changing flow rate as the graphs of flow rate against time show.

The way in which the flow rate changed during the driven flow is contradictory to the present theories on dissipation in the helium film. The Iordanskii-Langer-Fisher theory suggests that the rate of change of flow rate would be proportional to the exponentional of the "barrier" flow rate divided by the flow rate (Langer & Fisher, 1967); the Harris-Lowe theory proposes a rate of change of flow rate proportional to the three halves power of the difference between the flow rate and some "critical" flow rate (Harris-Lowe, 1977). Both these theories require that the flow rate should be a monotonic function of the parameter used as the measure of the driving chemical potential force. As suggested by Figures VII.12 and VII.13, the experimental results obtained are multi-valued functions of the effective level difference, z.

The results of driven flow can be divided into two parts. The first part concerns the results obtained while the applied voltage was changing; the second, the results obtained when the applied voltage was constant but there still existed a difference in the chemical potential of the two reservoirs. The dependence of the flow rate on the effective pressure head is shown in Figures VII.14 - VII.16, for both types of results. In all cases, although a curve rising exponentionally towards

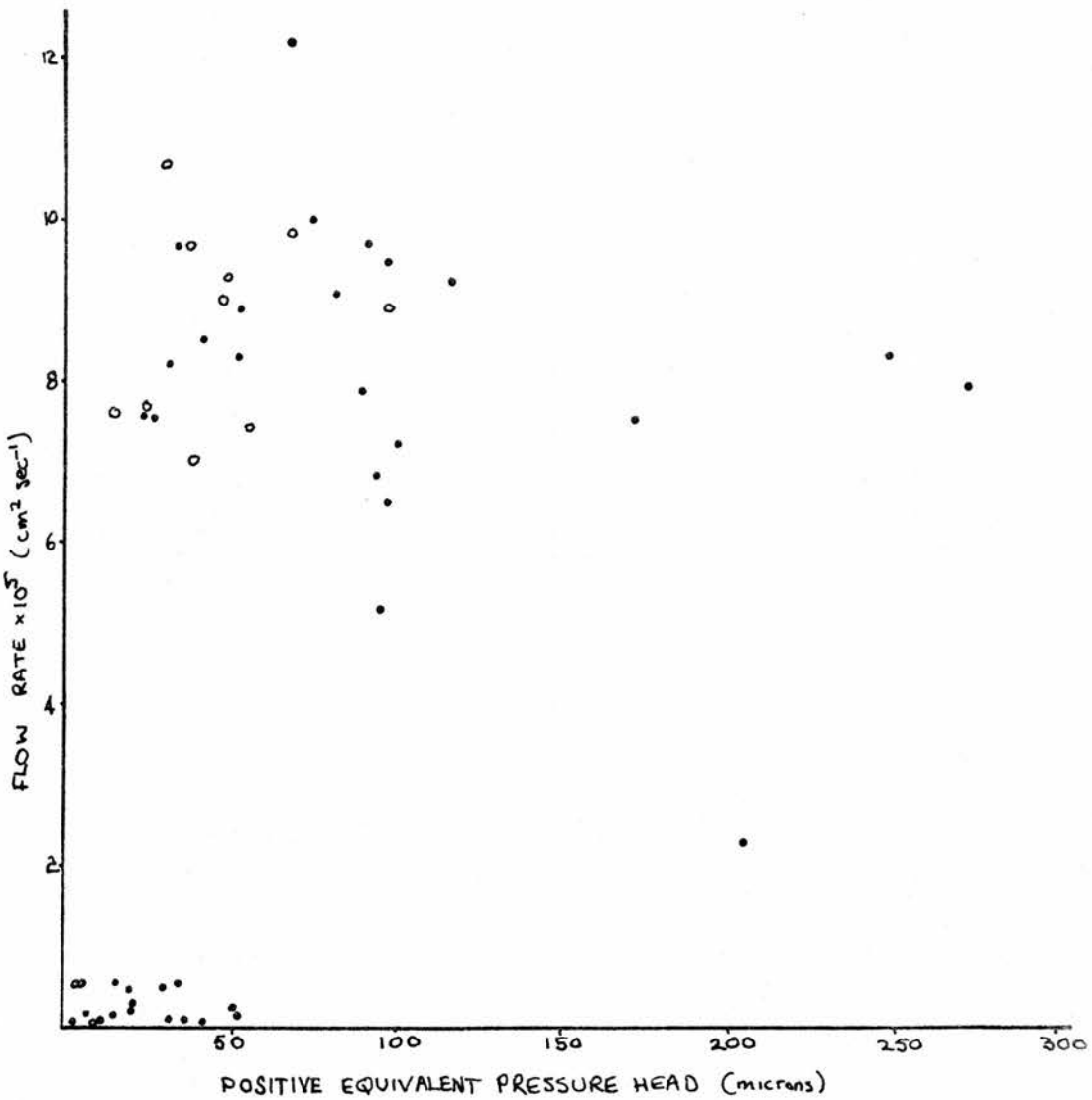

a. DURING TIME OF CHANGING APPLIED VOLTAGE
o - driven down • - driven up

FIGURE VII.14 FLOW RATE VS. PRESSURE HEAD
T = 1·203

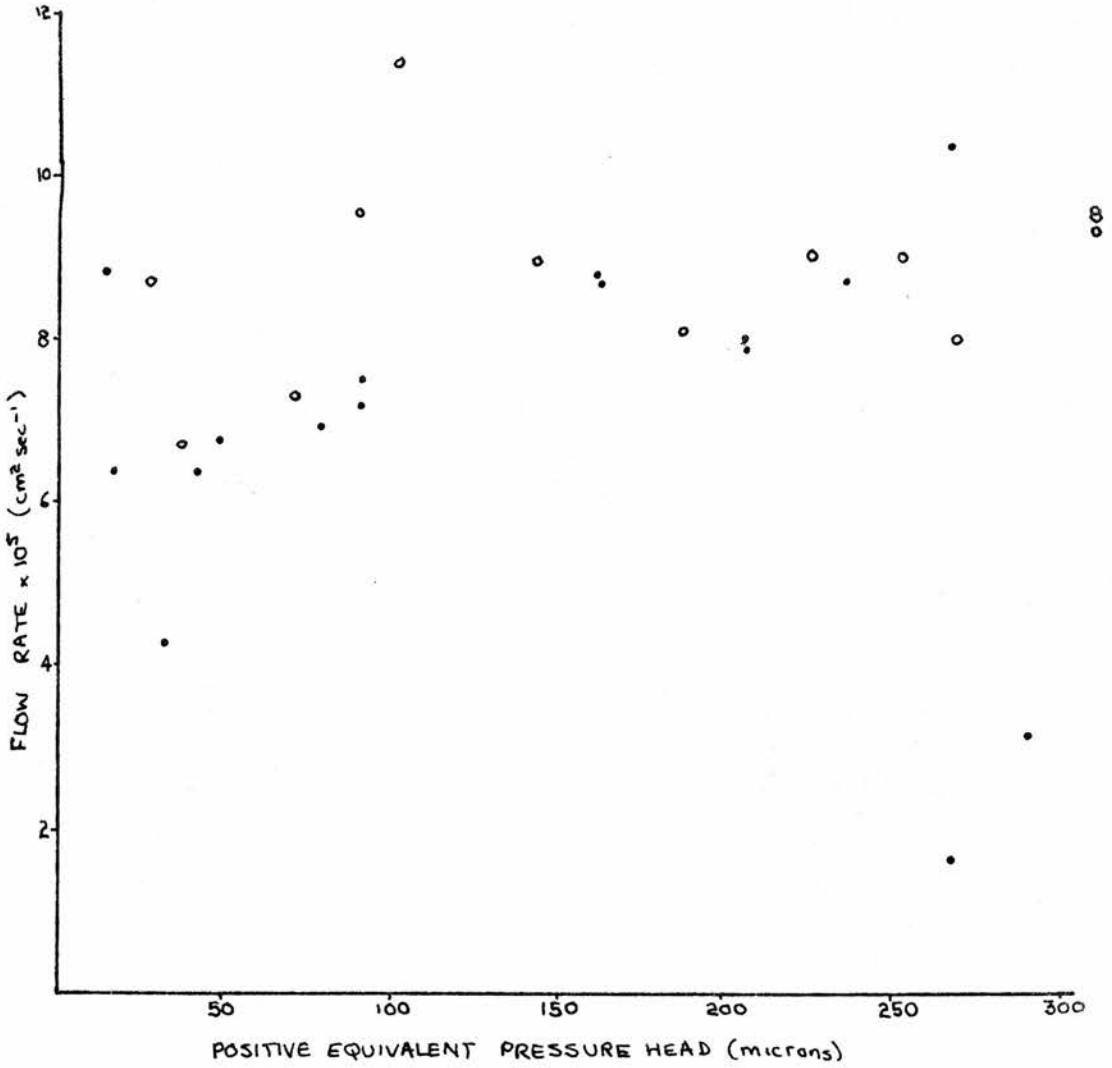

b. APPLIED VOLTAGE CONSTANT

o - driven down • - driven up

FIGURE VII.14 (CONTINUED)

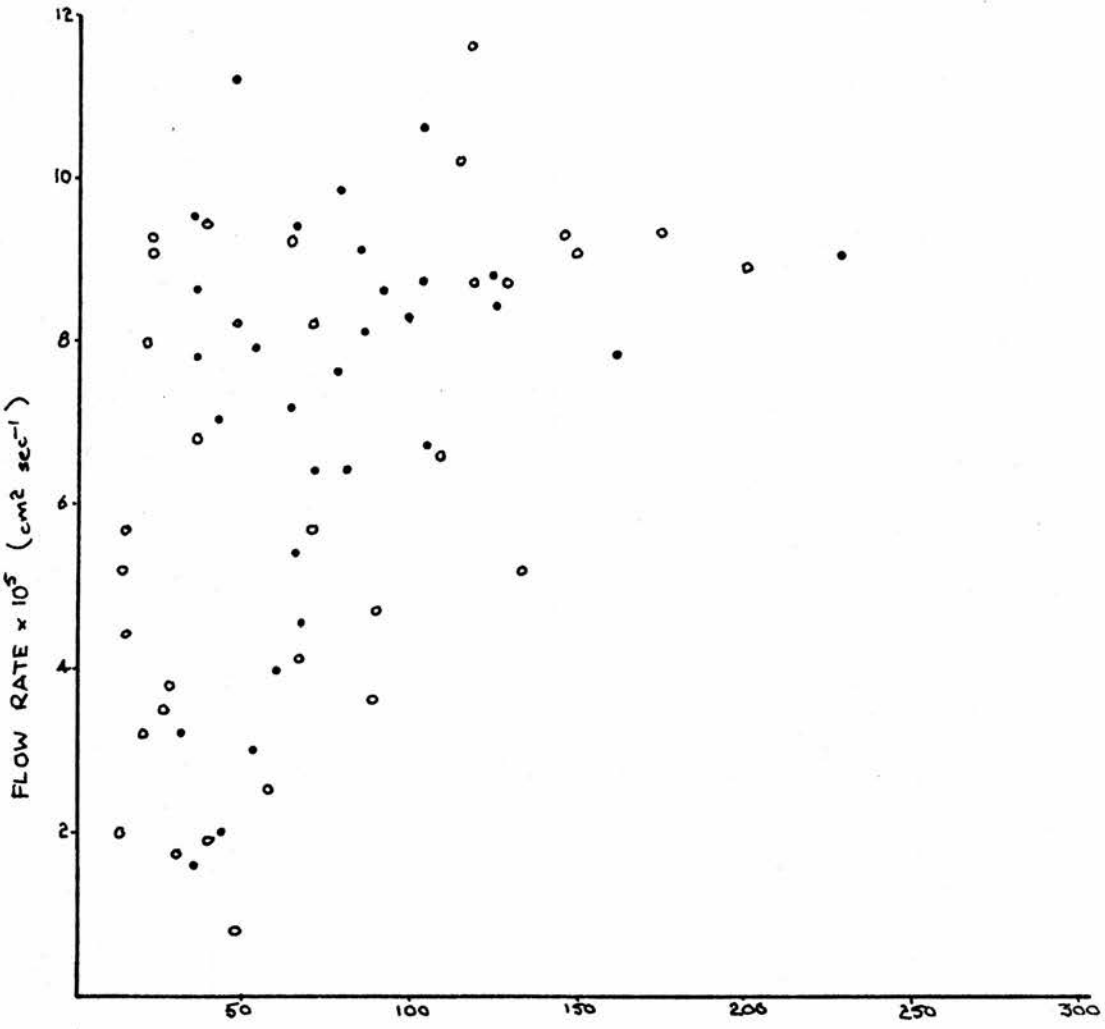

a. DURING TIME OF CHANGING APPLIED VOLTAGE
o - driven down • - driven up

FIGURE VII. 15 FLOW RATE VS. PRESSURE HEAD
T = 1.212

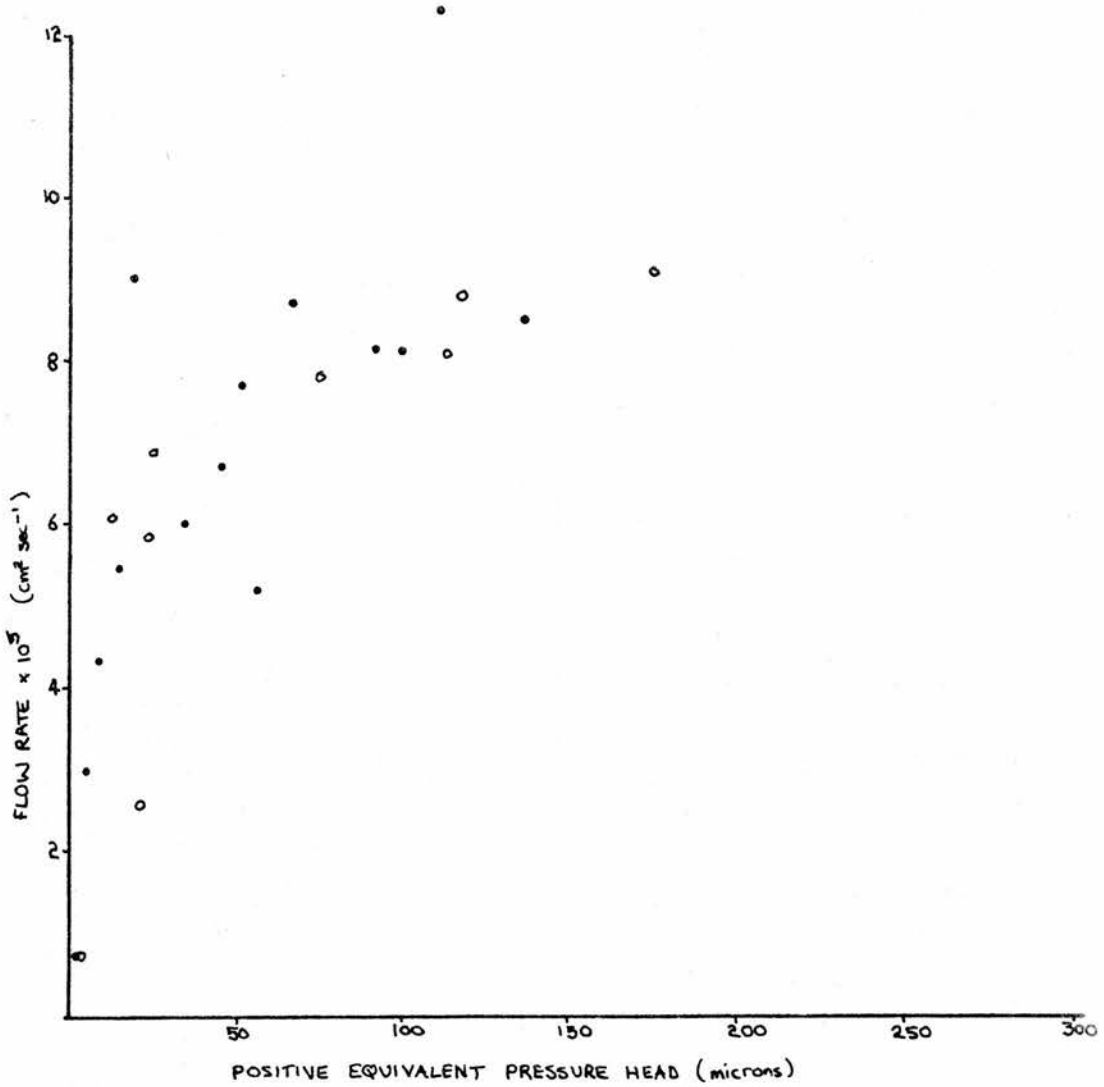

b. APPLIED VOLTAGE CONSTANT

o – driven down • – driven up

FIGURE VII.15 (CONTINUED)

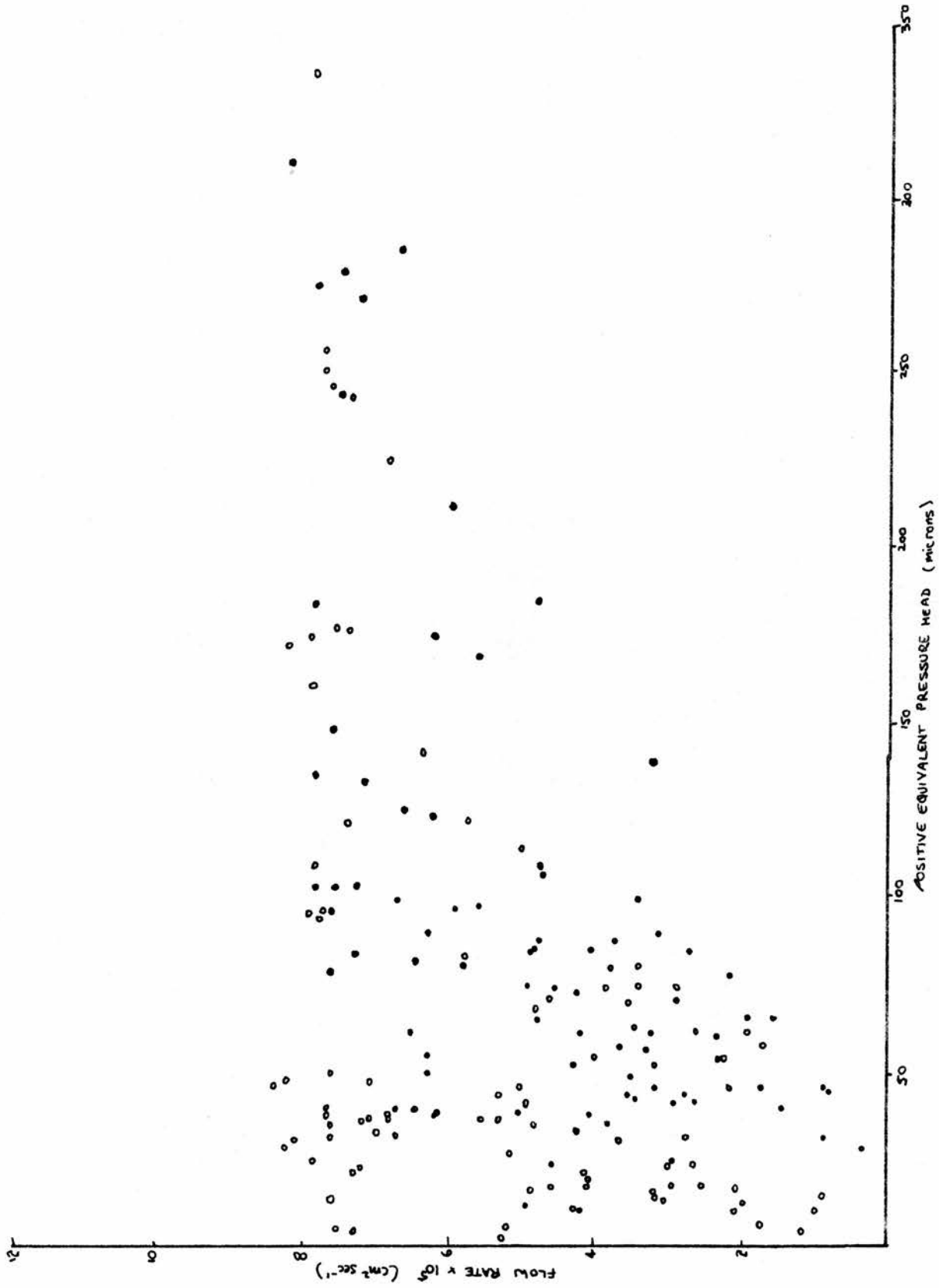

a. DURING TIME OF CHANGING APPLIED VOLTAGE
o - driven down • - driven up

FIGURE VII.16 FLOW RATE VS. PRESSURE HEAD
T = 1.634

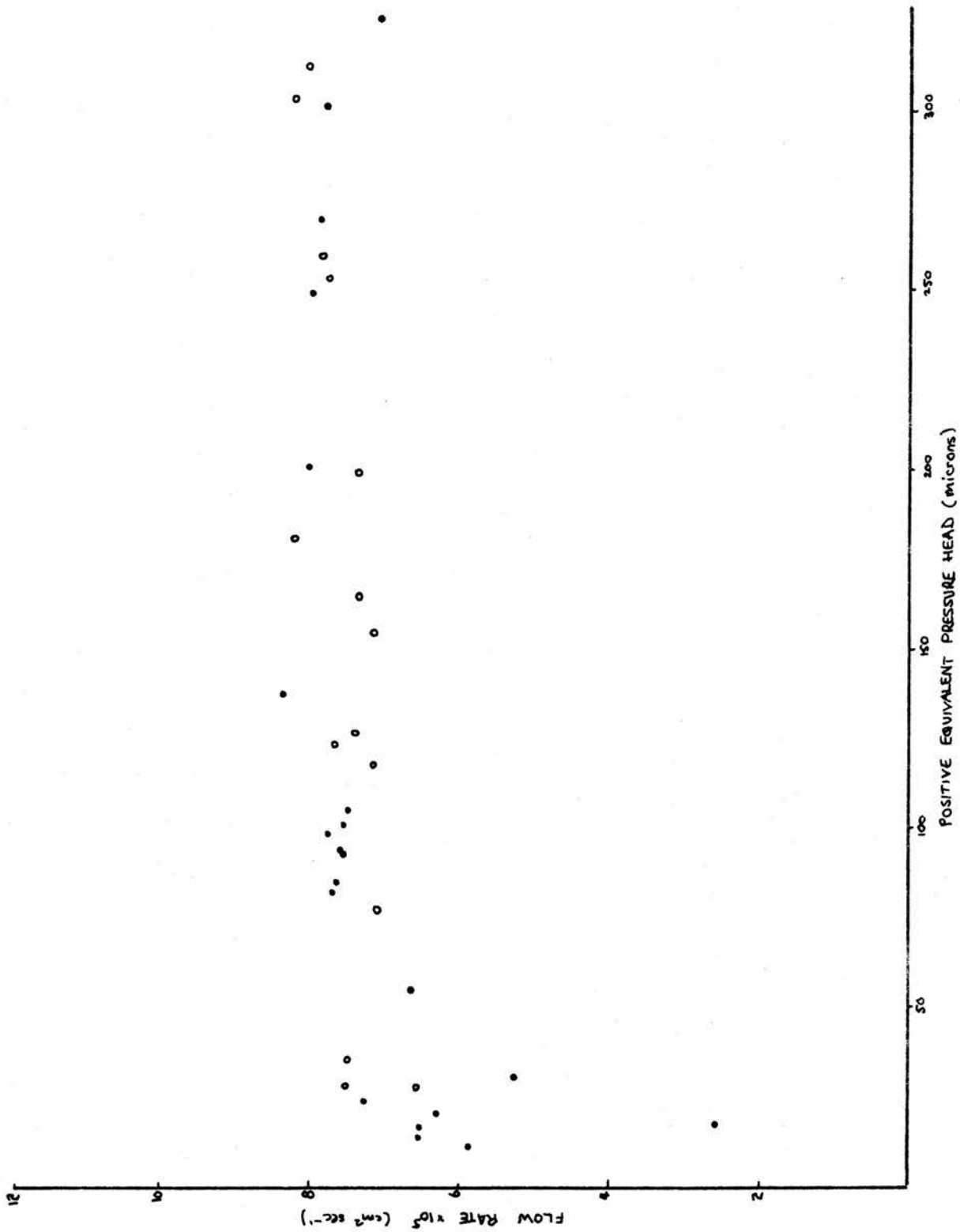

b. APPLIED VOLTAGE CONSTANT

FIGURE VII.16 (CONTINUED)

TABLE VII.2

TABLE VII. 3

some constant value (as would be expected from the thermal nucleation theories) could have been drawn through the data, the scatter would have been too large to draw any conclusions about the dissipation function in the helium film. Instead, it was decided to look at that part of the data which showed a monotonic increase in flow rate with increasing effective pressure head.

Two functional forms were tried:

(i) A straight line fit of the data in the form of logarithm of the effective pressure head against the inverse of the flow rate (it has already been shown in the section on the run-in, that the term in z dominates the other terms that should be included in a functional fit to the Langer and Fisher prediction), and

(ii) A straight line fit of the data expressed as the logarithm of the flow rate as a function of the logarithm of the effective pressure head (this form, mentioned in Chapter V, was suggested as being appropriate to dissipation in the helium film).

The criterion used to decide between the two forms was the correlation coefficient of the straight line to the data. Table VII.2 lists the results. In almost every case the correlation coefficient for the second form is closer to unity when compared to those for the first form. Graphs of the fit of the data to $\ln v$ against $\ln z$ are given in Figures VII.17 - VII.24, and the details of the straight lines in Table VII.3. Three-quarters of the lines obtained are nearly coincident.

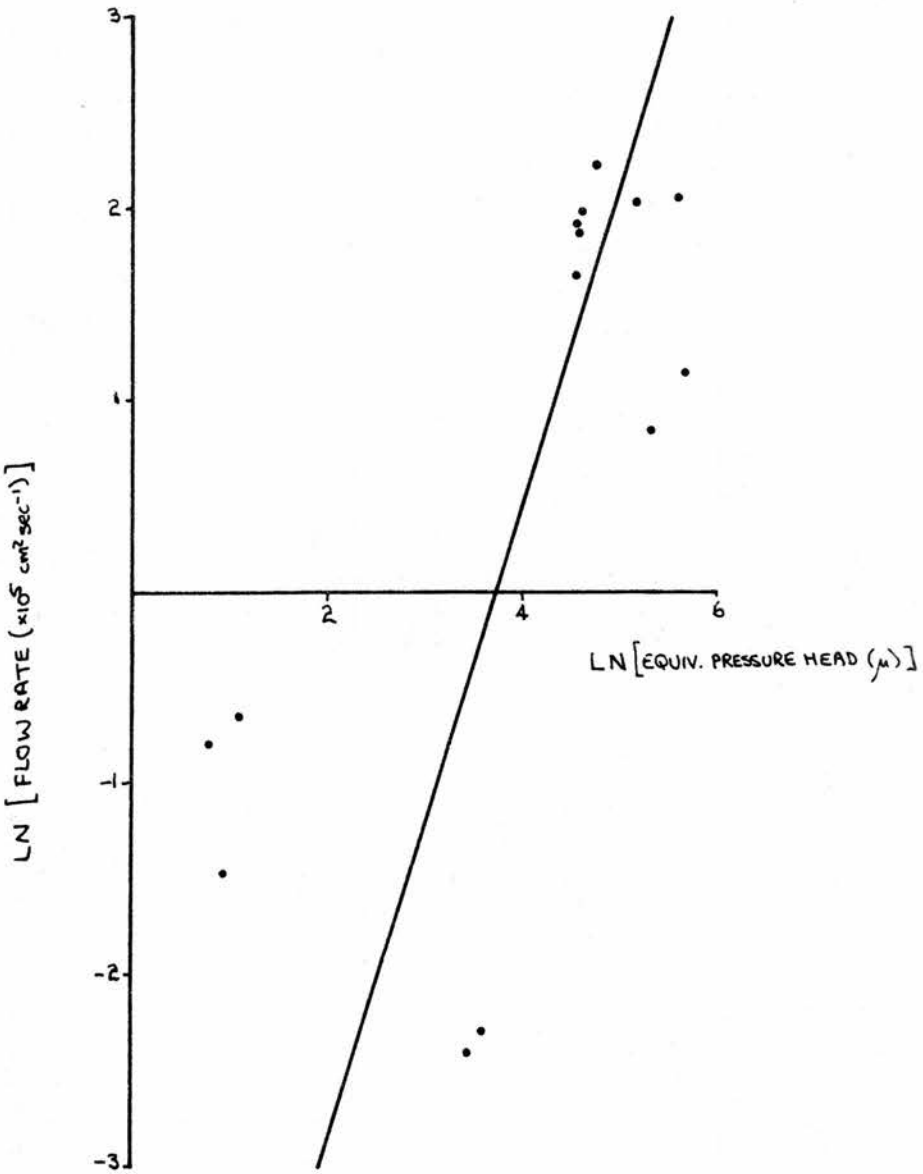

FIGURE VII.17 MONOTONIC INCREASE OF FLOW RATE WITH PRESSURE HEAD
T = 1.203 (DRIVEN UP)

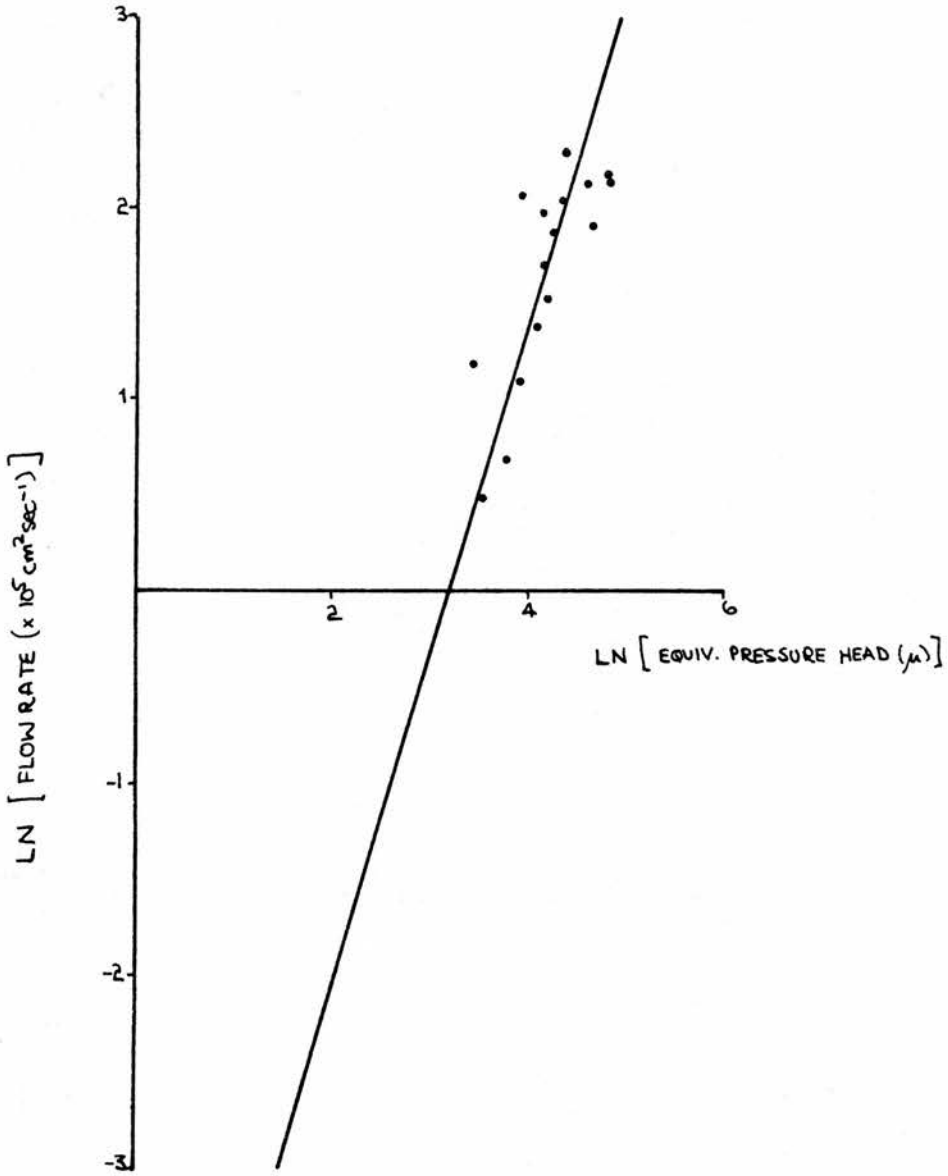

FIGURE VII.18 MONOTONIC INCREASE OF FLOW RATE WITH PRESSURE HEAD
T = 1·212 (DRIVEN UP)

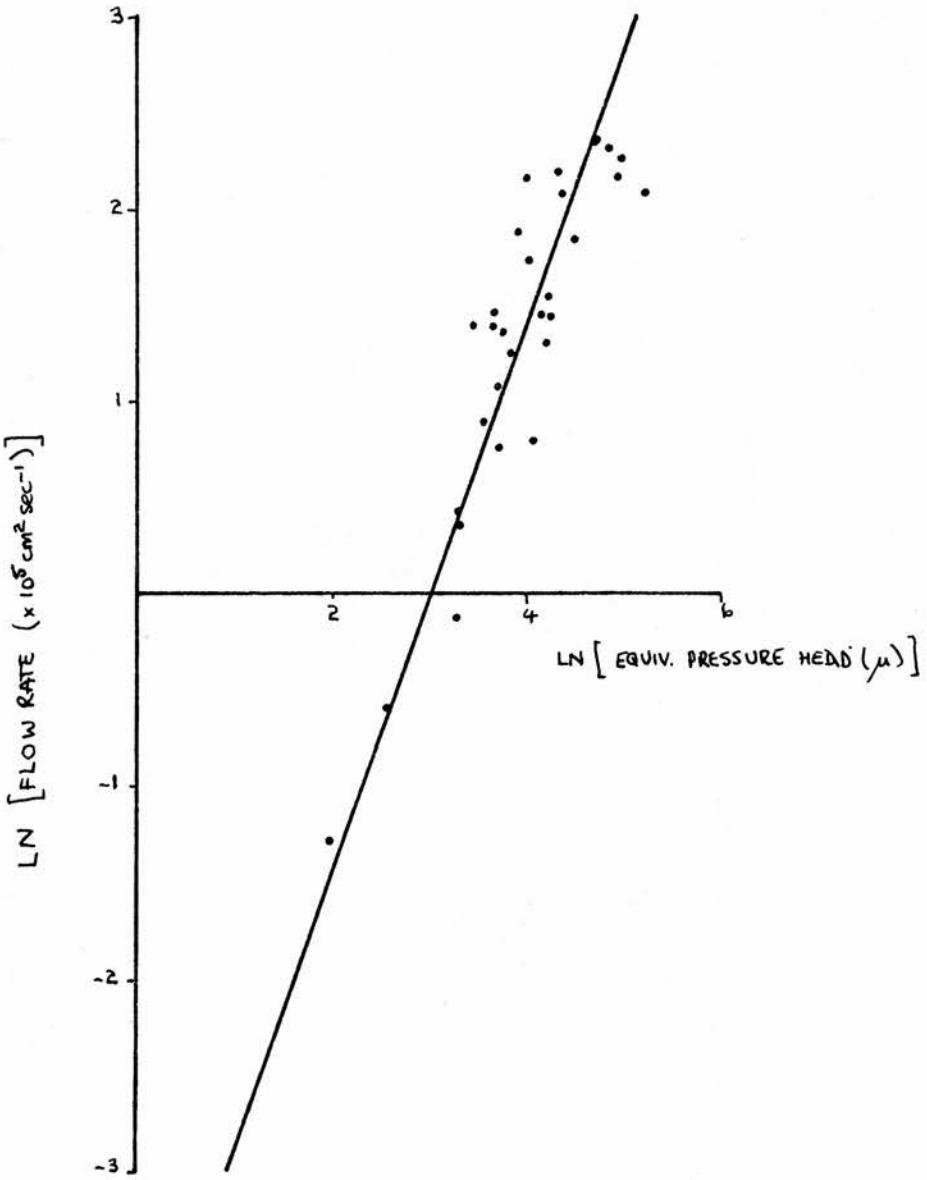

FIGURE VII.19 MONOTONIC INCREASE OF FLOW RATE WITH PRESSURE HEAD
T= 1.340 (DRIVEN UP)

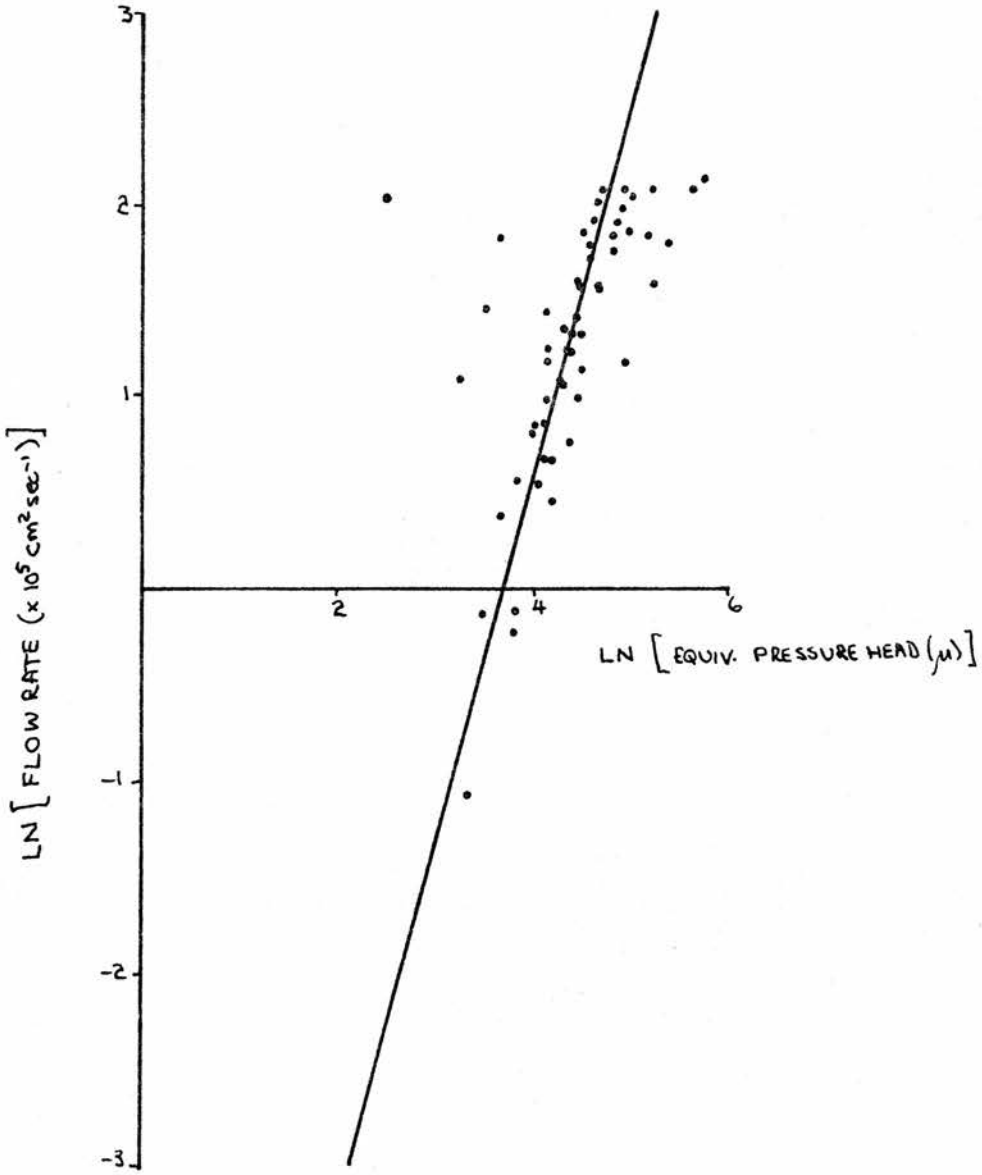

FIGURE VII.20 MONOTONIC INCREASE OF FLOW RATE WITH PRESSURE HEAD
T = 1.634 (DRIVEN UP)

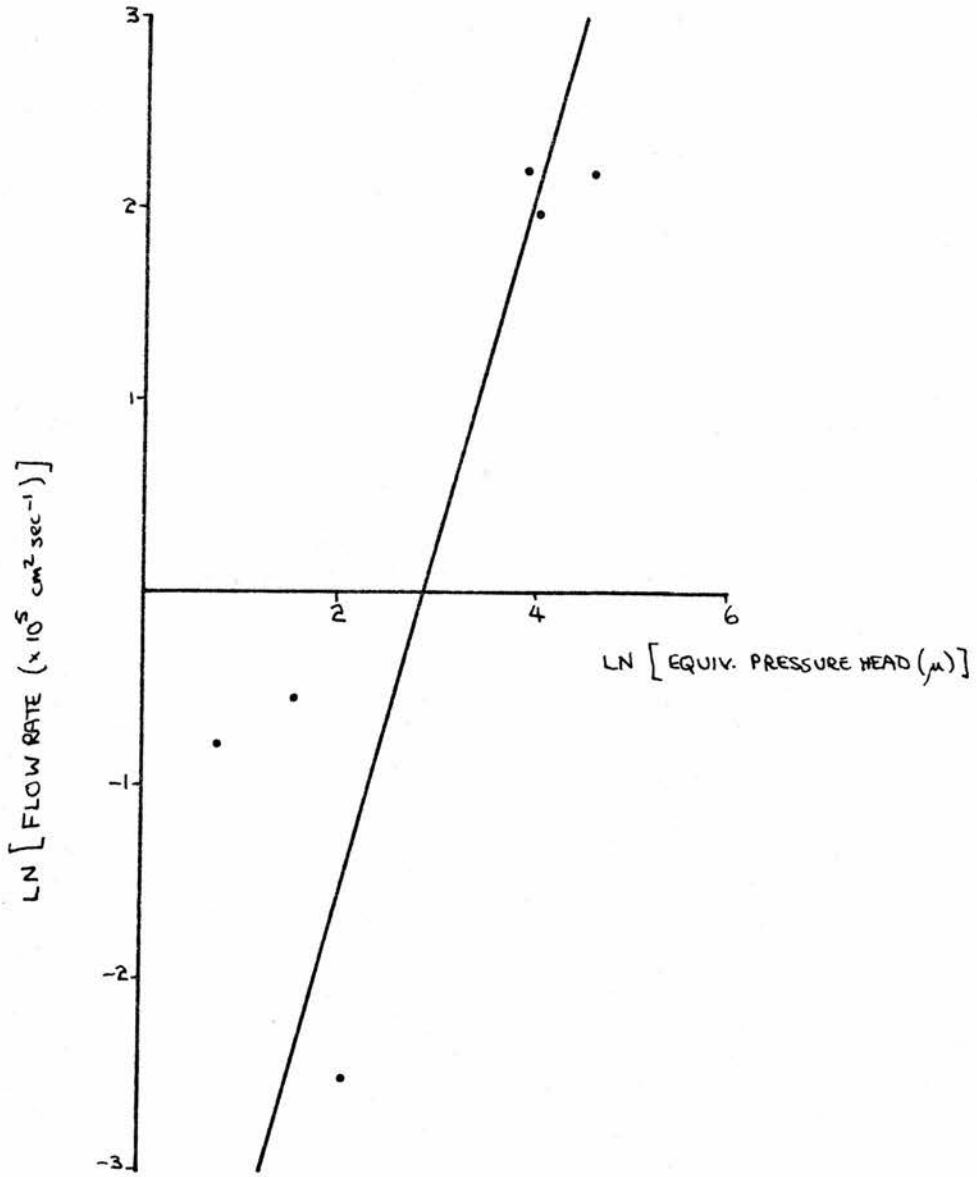

FIGURE VII. 21 MONOTONIC INCREASE OF FLOW RATE WITH PRESSURE HEAD
T = 1·203 (DRIVEN DOWN)

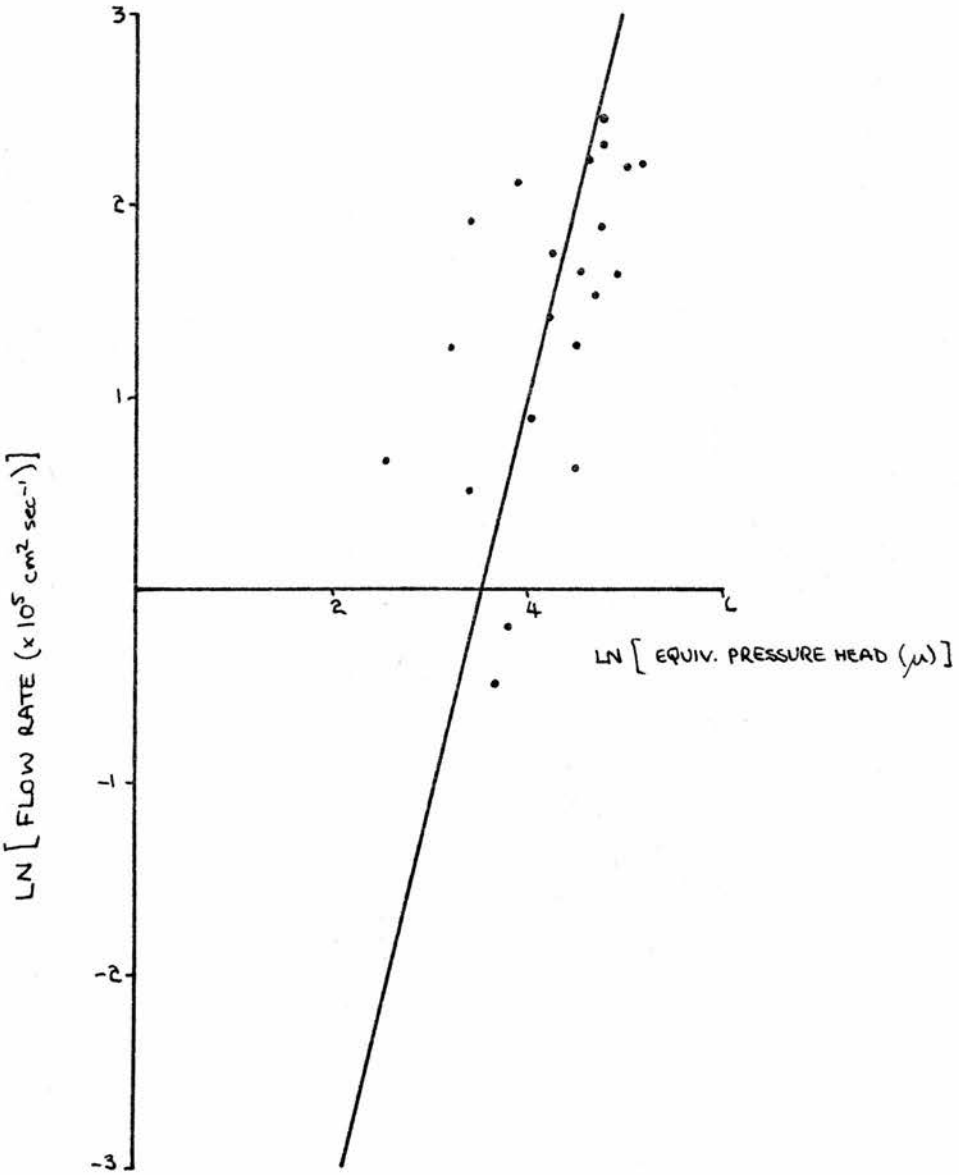

FIGURE VII.22 MONOTONIC INCREASE OF FLOW RATE WITH PRESSURE HEAD
T=1·212 (DRIVEN DOWN)

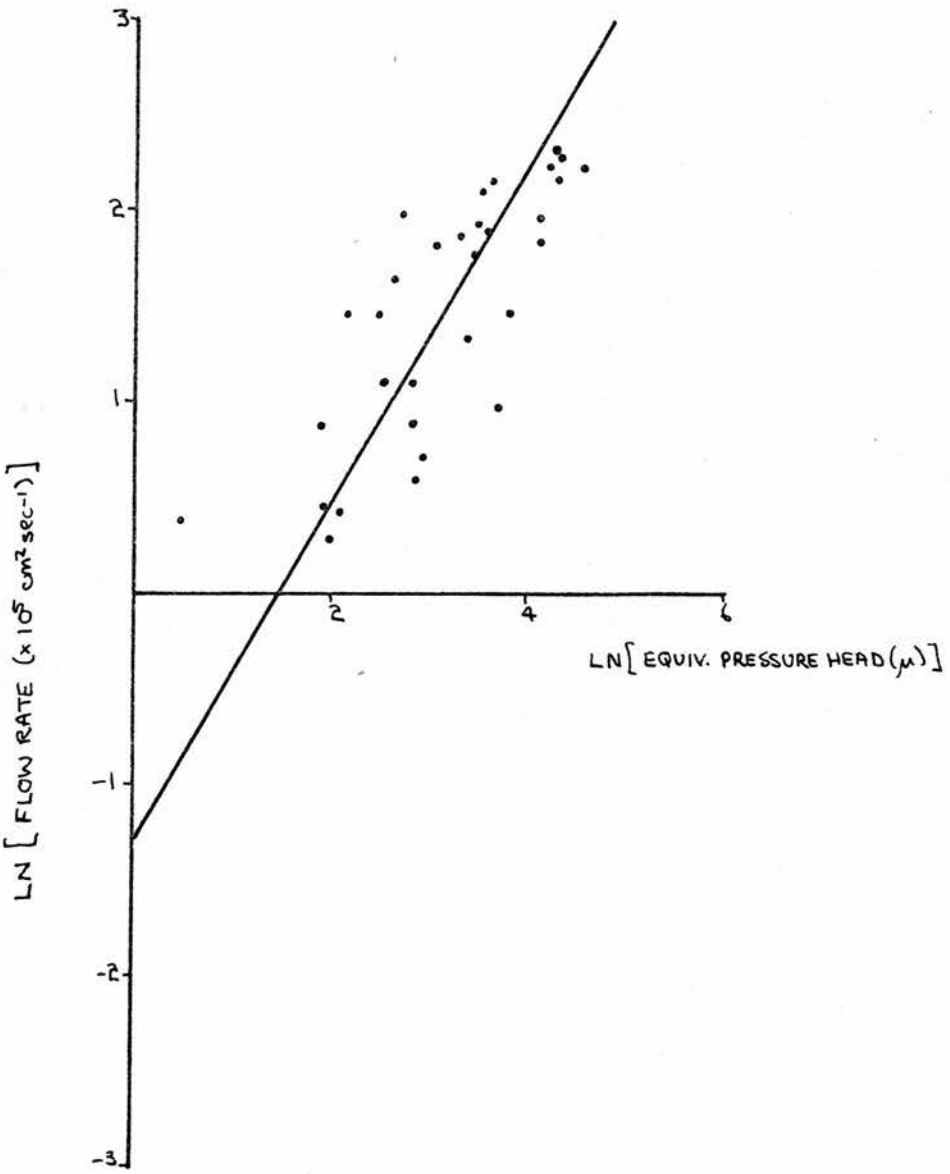

FIGURE VII.23 MONOTONIC INCREASE OF FLOW RATE WITH PRESSURE HEAD
T=1.340 (DRIVEN DOWN)

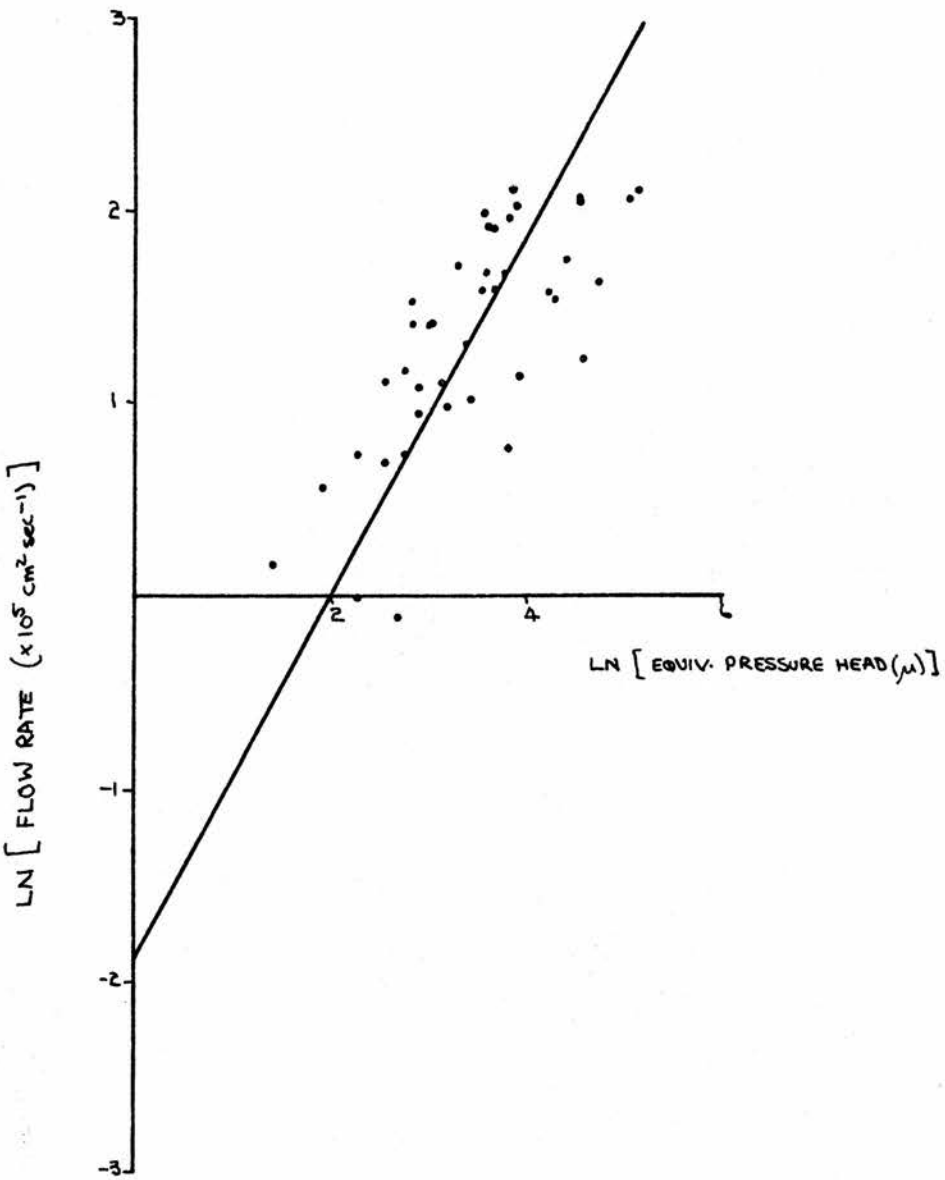

FIGURE VII. 24 MONOTONIC INCREASE OF FLOW RATE WITH PRESSURE HEAD
T = 1·634 (DRIVEN DOWN)

It has already been shown in section (iv) that in equation (3b) describing the equation of motion of the superfluid, the term in z is dominant among the terms on the left hand side of the equation. Using this to simplify the equation and incorporating the form of the dissipation function suggested by the experimental results,

$$|z| \simeq \frac{\omega_0 l a_f H f}{g} \left(\frac{\rho \sigma}{\rho_s \delta}\right)^c$$

$$\text{or} \quad \ln z - \ln(\omega_0 l a_f H f/g) = c \ln(\rho/\rho_s \delta) + c \ln \sigma \ .$$

The straight line intercept would yeild the value of f, the gradient, the value of c. From Table VII.3,

slope = 0.570

and intercept = 3.35

where z is in microns and σ in units of 10^5 cm^2 sec^{-1}. The value of f will change according to the value of ω_0 ; as ω_0 is a temperature dependent parameter, the value of f will have the inverse temperature dependence.

The changes in flow rate shown in Figures VII.12 and VII.13 are shown in more detail in Figures VII.25 and VII.26. The only theory which allows for macroscopic changes in the flow rate is that of Vinen (1958; 1961a). Flow steps have been studied (although not in terms of the Vinen theory) by Turkington et al (1972). The steps observed do not fall into distinct patterns: there was a peak in the distribution of values of flow rate at about $\sigma = 8 \times 10^{-5}$ cm^2 sec^{-1} (corresponding to a superfluid velocity of about 25 cm sec^{-1}); there was no indication of any forbidden rate of flow.

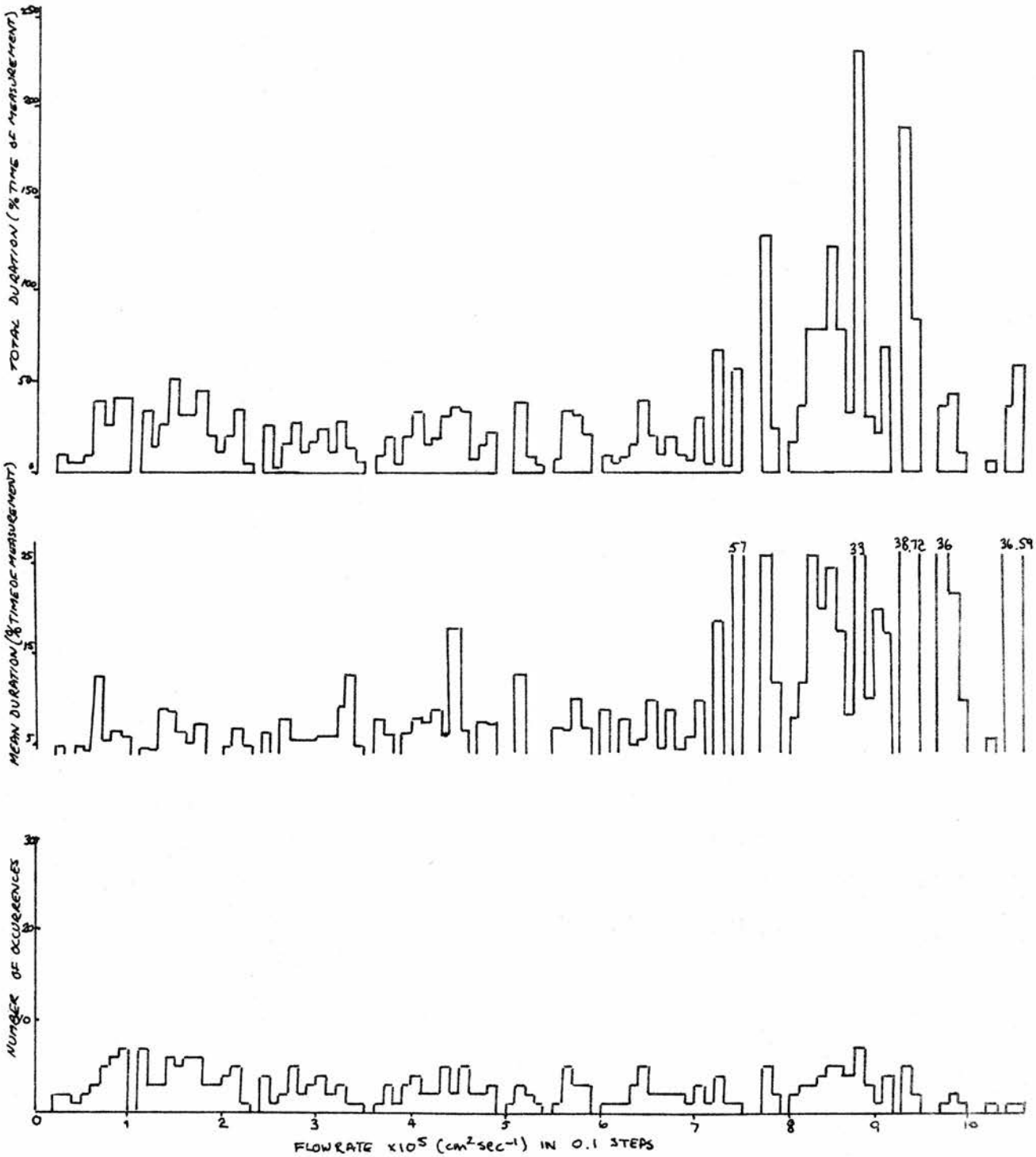

FIGURE VII.25 CHANGES IN FLOW RATE $T = 1.340$

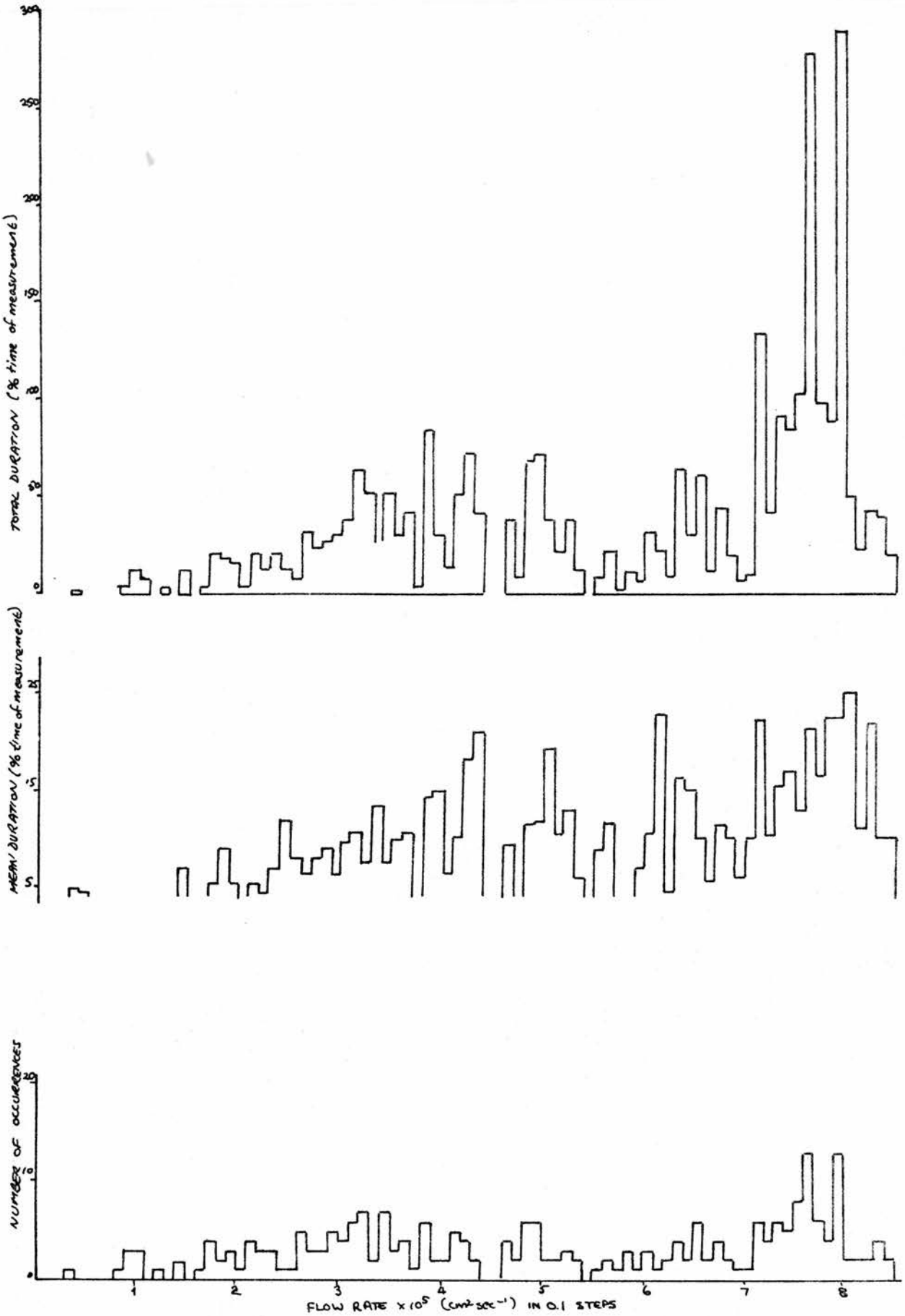

FIGURE VII.26 CHANGES IN FLOW RATE T = 1.634

(vii) Conclusions

Helium film flow has been studied for some thirty years. During that time there have been many advances in the understanding of the properties of liquid helium and many theories have been put forward to explain the experimental data that has been collected. The original concept of a "critical" velocity has been superceded by one in which the time rate of change of velocity is too small to be experimentally observed. There have, however, been only two theories on the dissipation in helium flow that seem to have been able to explain the observed experimental results. The Vinen theory has been successfully applied to thermal counterflow in narrow channels (Childers & Tough, 1975). The basis of this theory, discussed in Chapter IV, was the dynamic equilibrium of a tangled mass of vortex lines. The Iordanskii-Langer-Fisher theory, modified to allow for temperature dependent parameters, has been used to explain experimental results near T_λ, and its use has been extended to lower temperatures.

The experimental data presented in this thesis does not show the agreement previously reported with the thermal fluctuation theories, at least not in the form usually used. The flow rate would appear to have been dominated throughout by flow steps, whose existence has been reported, but whose significance has not found its way into any theory of dissipation. Superfluid velocities have been observed having values as low as 0.03 cm sec^{-1} and restricting the data to those when the flow rate is a monotonic function of the driving force supports the original suggestion of Langer and

Reppy's, that if thermal fluctuation theory is to be applied to film flow, the mechanism to consider is vortex lines parallel to the free surface, and not the vortex ring. No support is found for the Harris-Lowe theory, the existence of a critical velocity, v_o, cannot be deduced from the experimental data, and the power dependence of the superfluid velocity would be roughly $\frac{2}{3}$, and not the $\frac{3}{2}$ predicted. The use, however, of an empirical formulation of the equilibrium of a length of vortex line is the only one that allows the multi-valued dependence of velocity on driving force observed.

The experimental apparatus used is not dissimilar to that used by Campbell et al (1976) in their experiments. One reason for the great difference between their results and those presented here, may be the value of $a_f l$, the annular cylinder formed by helium film in the narrow capillary where the dissipation should dominate the flow. In Campbell's apparatus $a_f l$ has a value of approximately 3×10^{-6} cm^3 while in the apparatus used for this work, $a_f l \simeq 8 \times 10^{-8}$ cm^3.

APPENDIX

CALCULATION OF ω_o^2 AND SOLUTION TO EQUATION OF MOTION

(i) Calculation of ω_o^2

In Chapter VII, ω_o^2 was defined as

$$\omega_o^2 = g\beta/\rho AI$$

where

$$I = \int_1^2 \frac{dl}{a_f(l)} .$$

The area of the film $a_f(l)$ is the product of the perimeter and the film thickness δ where

$$\delta = a\left(\frac{1}{2}\frac{\beta}{\rho}v^2 + h\right)^{-1/n}$$

h being the height of the film above the bulk level and $a = 4.0 \times 10^{-8}$m for a glass surface.

The apparatus is sketched below:

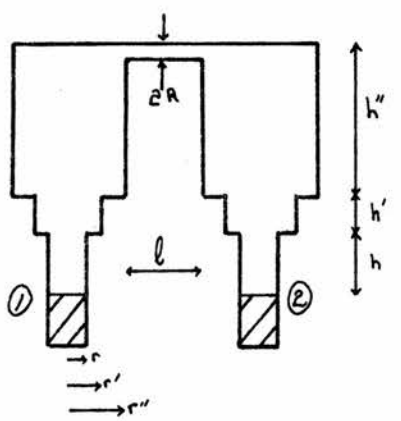

$l = 3.5 \times 10^{-3}$ m $R = 1.16 \times 10^{-4}$ m
$h'' = 1.3 \times 10^{-2}$ m $r'' = 2.0 \times 10^{-3}$ m
$h' = 1.0 \times 10^{-2}$ m $r' = 1.25 \times 10^{-3}$ m
$h = 3.0 \times 10^{-3}$ + liquid m $r = 1.185 \times 10^{-3}$ m

As each section is cylindrical,

$$I = \int_1^2 \frac{dl}{a_f(l)}$$
$$= \int_1^2 \frac{1}{2\pi} \frac{dl}{r(l)\,\delta(l)}$$
$$= \frac{1}{2\pi a} \int_1^2 \frac{(\tfrac{1}{2}\beta_s/\rho\, v^2 + h(l))^{1/n}}{r(l)}\, dl \,.$$

Letting $\tfrac{1}{2}\beta_s/\rho\, v^2 = b$, letting liq be the helium level below the top of the capacitors, and using a van der Waals coefficient of n = 3,

$$2\pi a I = \frac{2(b+h)^{4/3}}{4/3} + 2\times\frac{3}{4r'}\left[(b+h+h')^{4/3} - (b+h)^{4/3}\right]$$
$$+ 2\times\frac{3}{4r''}\left[(b+h+h'+h'')^{4/3} - (b+h+h')^{4/3}\right]$$
$$+ \frac{l}{R}(b+h+h'+h'')^{1/3} \,.$$

Using the values for the run-in at 1.212K, where $V = 0.232$ m sec^{-1} and hence $b = 2.7\times10^{-3}$ m,

$$2\pi a I \times 10^{4/3} = 9.87 + 17.50 + 17.55 + 44.14$$
$$= 89.06 \ \text{m}^{1/3} \,.$$

This shows that the largest contribution to the integral was the capillary section, and the value of I was then

$$I = 3.54\times10^{8} \ \text{m}^{-1} \,.$$

Hence

$$\omega_0^2 = 6.693\times10^{-2} \ \text{sec}^{-2} \,.$$

(ii) Equation of Motion

The equation to be solved is

$$\frac{d^3z}{dt^3} + \frac{K}{\rho CV}\frac{d^2z}{dt^2} + \omega_0^2\left(1 + \frac{(1-\frac{1}{\rho}\frac{\partial\rho}{\partial T})sAT}{gCV}\right)\frac{dz}{dt} + \frac{\omega_0^2 K}{\rho CV} = 0 \,.$$

Expressed in non-dimensional form

$$\frac{1}{\omega_0^3}\frac{d^3z}{dt^3} + \frac{K}{\rho cV\omega_0^3}\frac{d^2z}{dt^2} + \frac{1}{\omega_0}\left(1+\frac{(1-\frac{1}{\rho}\frac{d\rho}{dT})sAT}{gcV}\right)\frac{dz}{dt} + \frac{K}{\rho cV\omega_0}z = 0.$$

The characteristic equation for the differential equation is

$$\frac{1}{\omega_0^3}a^3 + \frac{K}{\rho cV\omega_0^3}a^2 + \frac{1}{\omega_0}\left(1+\frac{(1-\frac{1}{\rho}\frac{d\rho}{dT})sAT}{gcV}\right)a + \frac{K}{\rho cV\omega_0} = 0.$$

Letting $\lambda = \frac{a}{\omega_0}$, $G = \frac{K}{\rho cV\omega_0}$ and $H = 1+\frac{(1-\frac{1}{\rho}\frac{d\rho}{dT})sAT}{gcV}$,

$$\lambda^3 + G\lambda^2 + H\lambda + G = 0 \quad .$$

Let $\lambda = y - \frac{1}{3}G$.

Then, $$y^3 + 3py + 2q = 0$$

where

$$3p = \frac{3H - G^2}{3} \quad ,$$

$$2q = \frac{2G^3}{27} - \frac{GH}{3} + G \quad .$$

Defining $$u^3 = -q + (q^2+p^3)^{1/2}$$

and $$v^3 = -q - (q^2+p^3)^{1/2} \quad ,$$

the solution to the equation in y is

$$y_1 = u+v$$

$$y_2 = -\tfrac{1}{2}(u+v) - i\frac{\sqrt{3}}{2}(v-u)$$

$$y_3 = -\tfrac{1}{2}(u+v) - i\frac{\sqrt{3}}{2}(u-v)$$

For the experimental system at 1.2K,

$$G = 86.982$$

$$H = 7.281$$

$$p = -838.2$$

$$q = 24311.$$

$$u = -28.38$$

$$v = -29.54 \quad ;$$

thus $y_1 = -57.92$

$$y_{2,3} = 28.96 \pm i\, 0.999 \quad ,$$

giving

$$\lambda_1 = -86.91$$

$$\lambda_{2,3} = -0.036 \pm i\, 0.999 \quad ,$$

and finally

$$a_1 = -22.74$$

$$a_{2,3} = -9.42 \times 10^{-3} \pm i\, 0.261 \quad .$$

Therefore

$$z(t) = A e^{-(22.74)t} + B e^{-(9.42\times 10^{-3})t} \sin(10.261t + \phi) .$$

REFERENCES

Allen, J.F. Nature 185 831 (1960)

Allen, J.F. "Liquid Helium" (Enrico Fermi School XXI) 305 (Academic Press 1963)

Allen, J.F. & Armitage, J.G.M. Phys. Lett. 22 121 (1966)

Allen, J.F., Armitage, J.G.M. & Saunders, B.L. Proc. Int. Conf. LT13 258 (1972a)

Allen, J.F., Armitage, J.G.M. & Saunders, B.L. E.P.S. Low Temp. Conf. (1972b)

Allen, J.F. & Jones, H. Nature 141 243 (1938)

Allen, J.F. & Matheson, C.C. Proc. Phys. Soc. A290 1 (1965)

Allen, J.F., Matheson, C.C. & Walker, C.M. Phys. Lett. 19 199 (1965)

Allen, J.F. & Misener, A.D. Nature 141 75 (1938)

Allen, J.F. & Misener, A.D. Proc. Roy. Soc. A172 467 (1939)

Allum, D.R., McClintock, A.V.E., Phillips, A. & Bowley, R.M. Phil. Trans. Roy. Soc. 284 199 (1977)

van Alphen, W.M., de Bruyn Ouboter, R., Taconis, K.W. & de Haas, W. Physica 40 469 (1969a)

van Alphen, W.M., de Bruyn Ouboter, R., Taconis, K.W. & de Haas, W. Phsyica 40 470 (1969b)

Ambler, E. & Kurti, N. Phil. Mag. 43 260 (1952)

Amit, D. & Gross, E.P. Phys. Rev. 145 130 (1966)

Anderson, P.W. "Quantum Fluids" (ed. Brewer, D.F.) 146 (North Holland 1966a)

Anderson, P.W. Rev. Mod. Phys. 38 298 (1966b)

Andronikashvili, E.L. J. Phys. (USSR) 10 201 (1946)

Andronikashvili, E.L. & Marmaladze, Yu.G. Rev. Mod. Phys. 38 567 (1966)

Armitage, J.G.M., Allen, J.F. & Toft, M. Proc. Int. Conf. LT15 preprint (1978)

Ashton, R.A. & Northby, J.A. Phys. Rev. Lett. 30 1119 (1973)

Atkins, K.R. Proc. Roy. Soc. A203 119 (1950a)

Atkins, K.R. Proc. Roy. Soc. A203 239 (1950b)

Atkins, K.R. Phys. Rev. 92 1571 (1953)

Atkins, K.R. Canad. J. Phys. 32 347 (1954)

Atkins, K.R., Rosenbaum, B. & Seki, H. Phys. Rev. 113 751 (1959)

Atkins, K.R. & Rudnick, I. Prog. L.T. Phys. (ed. Gorter, C.J.) 6 37 (1970)

Banton, M.E. Jnl. L.T. Phys. 16 211 (1974)

Beliaev, S.T. J.E.T.P. 7 289 (1958a)

Beliaev, S.T. J.E.T.P. 7 299 (1958b)

van den Berg, G.J. Physica 17 797 (1951)

Bergman, D.J. Proc. Roy. Soc. A333 261 (1973)

Bogoliubov, N. J. Phys. (USSR) 11 23 (1947)

Boorse, H.A. & Dash, J.G. Phys. Rev. 79 1008 (1950)

Bowers, R. & Mendelssohn, K. Proc. Phys. Soc. A63 1318 (1950)

Brewer, D.F. & Edwards, D.O. Phil. Mag. 6 775 (1961)

Brooks, J.S. & Hallock, R.B. Phys. Lett. 63A 319 (1977)

de Bruyn Ouboter, R. Jnl. L.T. Phys. 12 3 (1973)

de Bruyn Ouboter, R., Taconis, K.W. & van Alphen, W.M. Proc. L.T. Phys. (ed. Gorter, C.J.) 5 (1967)

Calvani, P., Grenlich, K. & Maraviglia, B. Nuov. Gm. Lett. 6 536 (1973)

Campbell, L.J. Jnl. L.T. Phys. 3 175 (1970)

Campbell, L.J. Jnl. L.T. Phys. 8 105 (1972a)

Campbell, L.J. Proc. Int. Conf. LT13 268 (1972b)

Campbell, L.J. Physica 78 245 (1974)

Campbell, L.J. "The Helium Liquids" (ed. Armitage, J.G.M. & Farquhar, I.E.) Chapter 4, 127 (Academic Press, 1975a)

Campbell, L.J. Phys. Rev. B11 4721 (1975b)

Campbell, L.J., Hammel, E.F., Hoffer, J.K. & Keller, W.E. Jnl. L.T. Phys. 24 527 (1976)

Campbell, L.J. & Liebenberg, D.H. Phys. Rev. Lett. 29 1065 (1972)

Chandrasekhar, B.S. Phys. Rev. 86 414 (1952)

Chandrasekhar, B.S. & Mendelssohn, K. Proc. Phys. Soc. A65 226 (1952)

Chester, G.V. "The Helium Liquids" (ed. Armitage, J.G.M. & Farquhar, I.E.) Chapter I (Academic Press) (1975)

Childers, R.K. & Tough, J.T. Phys. Rev. Lett. 31 911 (1973)

Childers, R.K. & Tough, J.T. Jnl. L.T. Phys. 15 53 (1974a)

Childers, R.K. & Tough, J.T. Jnl. L.T. Phys. 15 63 (1974b)

Childers, R.K. & Tough, J.T. Phys. Rev. B13 1040 (1976)

Clow, J.R. & Reppy, J.D. Phys. Rev. Lett. 19 289 (1967)

Craig, P.P. Phys. Lett. 21 385 (1966)

Crum, D.B., Edwards, D.O. & Sarawinski, R.E. Phys. Rev. A9 1312 (1974)

Dash, J.G. & Boorse, H.A. Phys Rev. 82 851 (1951)

Daunt, G. & Mendelssohn, K. Nature 141 911 (1938a)

Daunt, G. & Mendelssohn, K. Nature 142 475 (1938b)

Daunt, G. & Mendelssohn, K. Nature 143 719 (1939a)

Daunt, G. & Mendelssohn, K. Proc. Roy. Soc. A170 423 (1939b)

Daunt, G. & Mendelssohn, K. Proc. Roy. Soc. A170 439 (1939c)

Daunt, G. & Mendelssohn, K. Nature 160 385 (1947)

Daunt, G. & Mendelssohn, K. Proc. Roy. Soc. A63 1305 (1950)

Donnelly, R.J. & Roberts, P.H. Phil. Trans. Roy. Soc. 271A 41 (1971)

Duthler, C.J. & Pollack, G.L. Phys. Lett. 31A 390 (1970)

Duthler, C.J. & Pollack, G.L. Phys. Rev. A3 191 (1971)

Dzyaloshinskii, I.E., Lifshitz, E.M. & Pitaevskii, L.P. Adv. In Phys. 10 165 (1961)

Ekholm, D.T. & Hallock, R.B. Phys. Rev. B19 2485 (1979a)

Ekholm, D.T. & Hallock, R.B. Phys. Rev. Lett. 42 449 (1979b)

Esel'son, B.N., Ivanov, V.G. & Scherbachenko JETP Lett. 15 435 (1972)

Esel'son, B.N., Ivanov, V.G. & Scherbachenko Phys. Lett. 47A 29 (1974)

Fairbank, H.A. & Lane, C.T. Phys. Rev. 76 1209 (1949)

Fehl, D.L. & Dillinger, J.R. Phys. Lett. 49A 243 (1974)

Fetter, A.L. Phys. Rev. 138A 429 (1965a)

Fetter, A.L. Phys. Rev. 138A 709 (1965b)

Fetter, A.L. Phys. Rev. 162 143 (1967)

Feynman, R.P. Rev. Mod. Phys. 20 367 (1948)

Feynman, R.P. Phys. Rev. 91 1291 (1953)

Feynman, R.P. Phys. Rev. 91 1301 (1953)

Feynman, R.P. Phys. Rev. 94 262 (1954)

Feynman, R.P. Prog. in L.T. Phys. (ed Gorter, C.J.) 1 17 (1955)

Feynman, R.P., & Cohen, M. Phys. Rev. 102 1189 (1956)

Fineman, J.C. & Chase, C.E. Phys. Rev. 129 1 (1963)

Flint, E.B. & Hallock, R.B. Phys. Rev. B11 2062 (1975)

Frenkel, J. J. Phys. (USSR) 2 345 (1940)

Galkiewicz, R.K. & Hallock, R.B. Phys. Rev. Lett. 33 1073 (1974)

Ginzberg, V.L. & Pitaevskii, L.P. JETP 1 858 (1958)

Glaberson, W.I. & Donnelly, R.J. Phys. Rep. 141 208 (1966)

Glick, F.I. & Werntz, I.H., Jnr. Proc. Int. Conf. LT9A 214 (1964)

Gopal, see Raja Gopal

Goodstein, D.L. & Saffman, P.G. Proc. Roy. Soc. A325 447 (1971)

Goodstein, D.L. & Saffman, P.G. Jnl. L.T. Phys. 18 435 (1975)

Gorter, C.J. & Mellink, J.H. Physica 15 285 (1949)

Graham, G.M. & Vittoratos, E. Phys, Rev. Lett. 33 1136 (1974)

Gribbon, P.W.F. & Jackson, L.C. Canad. J. Phys. 41 1047 (1963)

Hall, H.E. Adv. in Phys. 9 89 (1960)

Hall, H.E. & Vinen W.F. Proc. Roy. Soc. A238 204, (1956a)

Hall, H.E. & Vinen W.F. Proc. Roy. Soc. A238 215 (1956b)

Hallock, R.B. Phys. Lett. 51A 457 (1975)

Hallock, R.B. & Flint, E.B. Phys. Lett. 45A 245 (1973a)

Hallock, R.B. & Flint, E.B. Phys. Rev. Lett. 31 1381 (1973b)

Hallock, R.B. & Flint, E.B. Phys. Lett 42A 417 (1974a)

Hallock, R.B. & Flint, E.B. Phys. Rev. A10 1285 (1974b)

Harris-Lowe, R.F. Jnl. L.T. Phys. 28 489 (1977)

van der Heijden, van der Boog, A.G.M., Giezen, J.J. & Kramers, H.C. Physica 59 493 (1972a)

van der Heijden, van der Boog, A.G.M., Giezen, J.J., & Kramers, H.C. Physica 61 556 (1972b)

van der Heijden, van der Boog, A.G.M., Giezen, J.J. & Kramers, H.C. Physica 77 487 (1974)

Herbet, G.R., Chopra, K.L. & Brown, J.B. Phys. Rev. 106 391 (1957)

Hess, G.B. Phys. Rev. Lett. 27 977 (1971)

Hess, G.B. Phys. Rev. Lett. 29 96 (1972a)

Hess, G.B. Low Temp. Conf. LT 13 1 302 (1972b)

Hess, G.B. Phys. Rev. A8 899 (1973)

Hoffer, J.K., Fraser, J.C., Hammell, E.F., Campbell, L.J. Keller, W.E. & Sherman,R.H. Proc. Int. Conf. LT13 253 (1972)

Helenberg, P.C. & Martin, P.C. Ann. Phys. 34 291 (1965)

Huang, K., Yang, C.N. Phys. Rev. 105 767 (1957)

Huang, K., Yang, C.N. & Luttinger, J.M. Phys. Rev. 105 776 (1957)

Hugenholtz, N.M. & Pines, D. Phys. Rev. 116 489 (1959)

Huggins, E.R. Phys. Rev. A1 332 (1970a)

Huggins, E.R. Phys. Rev. Lett. 24 573 (1970b)

Huggins, E.R. Phys. Rev. Lett. 24 699 (1970c)

Hulin, J.P., D'Humieres, D., Perrin, B. & Libchaber, A. Phys. Rev. A9 885 (1974)

Hulin, J.P., Laroche, C., Libchaber, A. & Perrin, B. Phys. Rev. A5 1830 (1972)

Iordanskii, S.V. J.E.T.P. 21 467 (1965)

Jackson, L.C. & Burge, E.G. Nature 164 660 (1949)

Jackson, L.C. & Grimes, W.G. Adv. in Phys. 7 435 (1958)

Josephson, B.D. Ann. Phys. 70 229 (1972)

Kadonoff Rev. Mod. Phys. 39 395 (1967)

Kalos, M.H., Levesque, D. & Verlet, L. Phys. Rev. A9 (1974)

Kammerlingh Onnes, H. Leiden Comm. 159 (1922)

Kapitza, P.L. Nature 141 74 (1938)

Keesom, W.H. & Macwood, G.E. Physica 5 737 (1938)

Keller, W.E. "Helium ^{3} and Helium ^{4}" Chapter 7 (Plenum Press 1969a)

Keller, W.E. "Helium ^{3} and Helium ^{4}" 289 (Plenum Press 1969b)

Keller, W.E. Phys. Rev. Lett. 24 569 (1970)

Keller, W.E. & Hammel Ann. Phys. 10 202 (1960)

Keller, W.E. & Hammel Physics (NY) 2 221 (1961a)

Keller, W.E. & Hammel Phys. Rev. 124 (1641b)

Khalatnikov "An Introduction to the Theory of Superfluidity" (Benjamin Press, 1965)

Kidder, J.N. & Blackstead, H.A. Low Temp. Conf. LT9 331 (1965)

Kidder, J.N. & Fairbank, W.M. Phys. Rev. 127 987 (1962)

Kikoin, A.K. & Laserew, B.G. Nature 141 912 (1938)

Kikoin, A.K. & Laserew, B.G. Nature 142 289 (1939)

Kontorovich, V.M. J.E.T.P. 3 770 (1956)

Kukich, G., Henkel, R.P. Reppy, J.D. Low Temp Conf. LT11 140 (1968a)

Kukich, G., Henkel, R.P. Reppy, J.D. Phys. Rev. Lett. 21 197 (1968b)

Ladner, Childers, R.K. & Tough, J.T. Phys. Rev. B13 2918 (1976)

Lamb, H. "Hydrodynamics" (Cambridge Univ. Press 1932)

Landau, L. J. Phys. (USSR) 5 71 (1941)

Landau, L. J. Phys. (USSR) 10 389 (1946)

Landau, L. J. Phys. (USSR) 11 91 (1947)

Landau, L. Phys. Rev. 75 884 (1949)

Landau, L. & Lifshitz, E. "Fluid Mechanics" Chapter 16 (Pergamon Press 1959)

Langer, J.S. Ann. Phys. 41 108 (1967)

Langer, J.S. & Fisher, M.E. Phys. Rev. Lett. 19 560 (1967)

Langer, J.S. & Reppy, J.D. Prog. L.T. Phys (ed Gorter, C.J.) 6 1 (1970)

Larochen, C., Perrin, B. & Libchaber, A. Phys. Lett. 55A 29 (1975)

Lee, T.D., Huang, K. & Yang, C.N. Phys. Rev. 106 1135 (1957)

Lee, T.D. & Yang,C.N. Phys. Rev. 106 1119 (1957)

Lee, T.D. & Yang, C.N. Phys. Rev. 112 1419 (1958)

Lee, T.D. & Yang, C.N. Phys. Rev. 113 1165 (1959a)

Lee, T.D. & Yang, C.N. Phys. Rev. 116 25 (1959b)

Lee, T.D. & Yang, C.N. Phys. Rev. 117 12 (1960a)

Lee, T.D. & Yang, C.N. Phys. Rev. 117 22 (1960b)

Lee, T.D. & Yang, C.N. Phys. Rev. 117 897 (1960c)

Lesensky, L. & Boorse, H.A. Phys. Rev. 87 1135 (1952)

Liebenberg, D.H. Phys. Rev. Lett. 26 744 (1971a)

Liebenberg, D.H. Jnl. L.T. Phys. 5 267 (1971b)

London, F. Nature 141 643 (1938a)

London, F. Phys. Rev. 54 947 (1938b)

London, F. J. Phys. Chem. 43 49 (1939)

London, H. Proc. Roy. Soc. A171 484 (1939)

McClintock, P.V.E. Phys. Lett. 46A 145 (1973)

McMillan, W.L. Phys. Rev. 138A 442 (1965)

Manchester, F.D. Canad. J. Phys. 33 146 (1955)

Manchester, F.D. & Brown, J.B. Canad. J. Phys. 35 483 (1957)

Matheson, C.C. & Tilley, J. Proc. Int. Conf. LT9A 210 (1964)

Mendelssohn, K. & White, G.K. Proc. Roy. Soc. A63 1328 (1950)

Milbrodt, T.O. & Pollack, E.L. Phys. Rev. A8 930 (1963)

Notarys, H.A. Phys. Rev. Lett. 22 1240 (1969)

Olijhoek, J.F., van Beelen, H., de Bruyn Ouboter, R., Taconis, K.W. & Koops, W. Physica 72 355 (1974)

Olijhoek, J.F., van Beelen, H., de Bruyn Ouboter, R., Taconis, K.W. & Koops, W. Physica 72 381 (1974)

Onsager, L. Nuov. Cim. 6 Suppl. 2 249 (1949)

Penrose, O. Onsager, L. Phys. Rev. 104 576 (1956)

Peshkov, V.P. J. Phys. (USSR) 8 381 (1944)

Peshkov, V.P. J. Phys. (USSR) 10 389 (1946)

Peshkov, V.P. Prog. L.T. Phys. (ed. Gorter, C.J.) 4 1 (1966)

Phillips, A. & McClintock, P.V.E. Phys. Rev. Lett. 33 1468 (1974)

Picus, G.S. Phys. Rev. 90 719 (1953)

Picus, G.S. Phys, Rev. 94 1459 (1954)

Pippard, A.B. "Elements of Classical Thermodynamics" (Cambridge Univ.Press 1960)

Pitaevski, L.P. J.E.T.P. 13 451 (1961)

Putterman, S.J. & Rudnick, I. Phys. Today 24 39 (1971)

Raja Gopal, E.S. Ann. Phys. 25 196 (1963)

Rayfield, G.W. & Reif, F. Phys. Rev. Lett. 11 305 (1963)

Rayfield, G.W. & Reif, F. Phys. Rev. 136A 1194 (1964)

Robinson, J1E. Phys. Rev. 82 440 (1951)

Rolin, B.V. Proc. 7th Int. Conf. Refrig. I.I.R. (Paris) 1 187 (1936)

Rolin, B.V. & Simon, F. Physica 6 219 (1939)

Sabisky, E.S. & Anderson, C.H. Phys. Rev. Lett. 24 1049 (1970)

Sabisky, E.S. & Anderson, C.H. Phys. Rev. A7 790 (1973)

Schiff, L. Phys. Rev. 59 839 (1941)

Schwartz, K.W. Phys. Rev. B12 3658 (1975)

Seki, H. Phys. Rev. 128 502 (1962)

Selden, R.W. & Dillinger, J.R. Phys. Rev. 138A 1371 (1965)

Selden, R.W., Werntz, J.H. Jnr., Fleming, R.J. & Dillinger, J.R. Phys. Rev. 138A 1363 (1965)

Silton, D.M. & Moss, F. Phys. Rev. Lett. 29 542 (1972)

Smith, B. & Boorse, H.A. Phys. Rev. 90 156 (1953a)

Smith, B. & Boorse, H.A. Phys. Rev. 92 505 (1953b)

Smith, B. & Boorse, H.A. Phys. Rev. 98 328 (1955a)

Smith, B. & Boorse, H.A. Phys. Rev. 99 358 (1955b)

van Spronsen, E., Verbeck, H.J., de Bruyn Ouboter, R., Taconis, K.W. & van Beelen, H. Physica 61 129 (1972)

van Spronsen, E., Verbeck, H.J., de Bruyn Ouboter, R., Taconis, K.W. & van Beelen, H. Phys. Lett. 45A 49 (1973)

van Spronsen, E., Verbeck, H.J., de Bruyn Ouboter, R. Taconis, K.W. & van Beelen, H. Physica 77 570 (1974)

van Spronsen, E., Verbeck, H.J. van Beelen, H. Bruyn Ouboter, R. & Taconis, K.W. Physica 81B 91 (1975)

Telschow, K., Rudnick, I. & Wang, T.G. Jnl. L.T. Phys. 18 43 (1975)

Telschow, K., Rudnick, I. & Wang, T.G. Phys. Rev. Lett. 32 1292 (1974)

Tisza, L. Nature 141 913 (1938)

Tisza, L. J. Phys. Radium 1 165 (1940a)

Tisza, L. J. Phys. Radium 1 350 (1940b)

Tisza, L. Phys. Rev. 72 838 (1947)

Tisza, L. Phys. Rev. 75 885 (1949)

Turkington, R.R. & Edwards, M.H. Phys. Rev. 168 169 (1967)

Turkington, R.R. & Harris-Lowe, R.F. Jnl. L.T. Phys. 10 369 (1973);Jnl. L.T. Phys 28 513 (1977)

Verberck, H.J., van Spronsen, E., Mars, H., van Beelen, H., de Bruyn Ouboter, R. & Taconis, K.W. Physica 73 621 (1974)

Vinen, W.F. Proc. Roy. Soc. A242 493 (1957)

Vinen, W.F. Proc. Roy. Soc. A243 400 (1958)

Vinen, W.F. Prog. in L.T. Phys. (ed. Gorter, C.J.) 3 1 (1961a)

Vinen, W.F. Proc. Roy. Soc., A260 218 (1961b)

Vinen, W.F. "Liquid Helium" (ed. Careri) 336 (Academic Press 1963)

Vinen, W.F. "Quantum Fluids" (ed. Brewer) 74 (North-Holland 1966)

Wagner, F. Phys. Lett. 44A 489 (1973a)

Wagner, F. Jnl. T. Phys. 13 185 (1973)

Wang, T.G. & Petrac, D. Phys. Rev. B11 4221 (1975)

Waring, R.K. Phys. Rev. 99 1704 (1955)

Weaver, J.C. Phys. Rev. A6 378 (1972)

Weaver, J.C. Phys. Rev. A6 378 (1972)

Weaver, J.C. Phys. Lett. 43A 397 (1973)

Weaver, J.C. Phys. Lett. 47A 379 (1974)

Webber, R.T., Fairbank, H.A. & Lane,C.T. Phys. Rev. 76 609 (1949)

Wilks, J. "Properties of Liquid and Solid Helium" Chapter 11 (Clarendon Press 1967)

Williams, G.A. & Packard, R.E. Phys. Rev. Lett. 32 587 (1974a)

Williams, G.A. & Packard, R.E. Phys. Rev. Lett. 33 280 (1974b)

Wolfke, M. & Keesom, W.H. Proc. Acad. Sci. Amst. 31 81 (1928a)

Wolfke, M. & Keesom, W.H. Proc. Acad. Sci. Amst. 31 800 (1928b)

Woods, A.D.B. & Hollis Hallet, A.C. Can. J. Phys. 41 596 (1963)